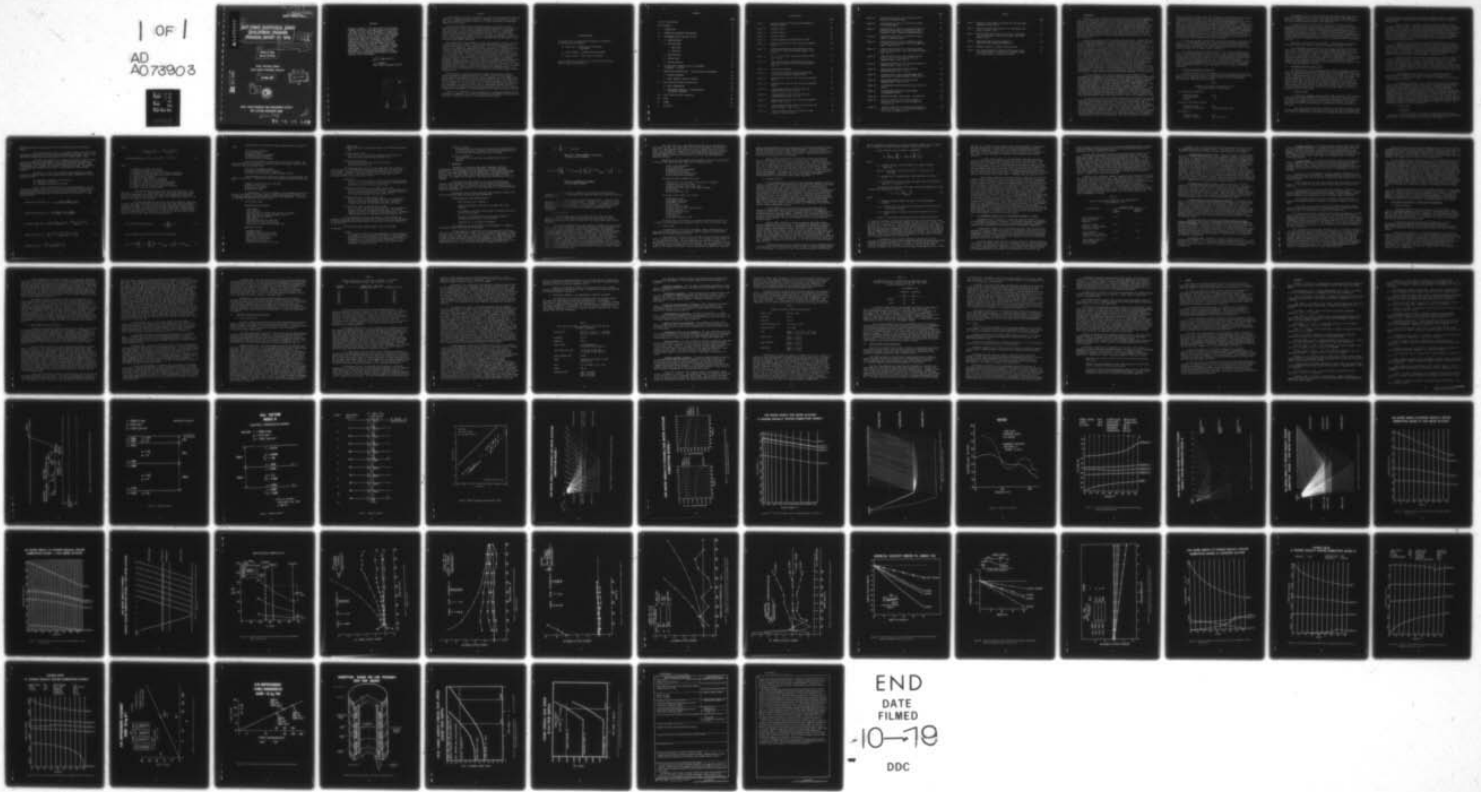AD-A073 903   NAVAL OCEAN RESEARCH AND DEVELOPMENT ACTIVITY NSTL S--ETC F/G 17/1
DEEP-TOWED GEOPHYSICAL ARRAY DEVELOPMENT PROGRAM PROGRESS REPOR--ETC(U)
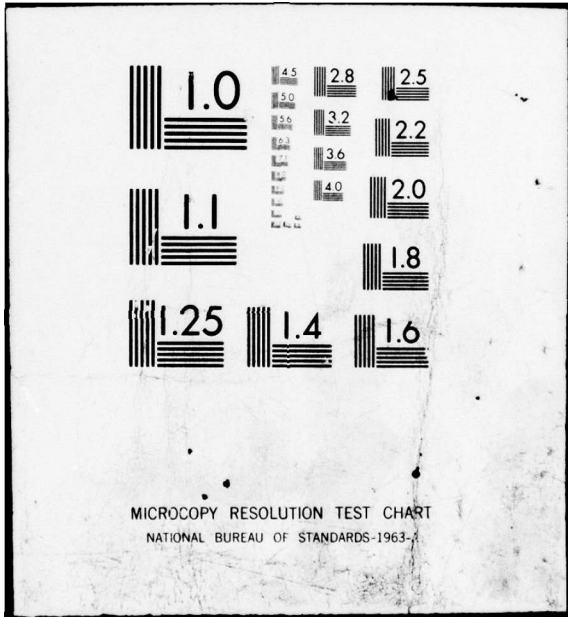FEB 79 M G FAGOT, B E ECKSTEIN

UNCLASSIFIED   NORDA-TN-41   NL

1 OF 1
AD
A073903

END
DATE
FILMED
-10-79
DDC

MICROCOPY RESOLUTION TEST CHART
NATIONAL BUREAU OF STANDARDS-1963-A

AD A073903

DEEP-TOWED GEOPHYSICAL ARRAY DEVELOPMENT PROGRAM PROGRESS REPORT (FY 1978)

LEVEL

Technical note

Martin G. Fagot
Bruce E. Eckstein

Ocean Technology Division
Ocean Science Technology Laboratory

February 1979

D D C
RECEIVED
SEP 18 1979
A

76 p.

NAVAL OCEAN RESEARCH AND DEVELOPMENT ACTIVITY
NSTL STATION, MISSISSIPPI 39529

79 09 17 069

FOREWORD

The Navy's interest in the lower region of the acoustic
frequency domain has increased the need for more defini-
tive models of the ocean's subbottom as a transmission
media that refracts, diffracts, diffuses and dissipates,
as well as reflects, acoustic energy. A multi-channel
array system towed near the bottom in the deep ocean
provides the capability to determine the detailed
geophysical character of the subbottom structure and
thus provides the high resolution geoacoustic input
parameters required for modeling. This report presents
the progress during FY78 on the development of a deep-
towed system. The report reviews progress on the
development of a system performance prediction model,
interval velocity measurement considerations, and deep
tow sound source requirements.

R. C. Swenson
Head, Ocean Technology Division

ABSTRACT

A multi-channel array system towed near the bottom in the deep ocean provides the capability to determine detailed geophysical character of the subbottom structure. This report presents the progress during FY 78 on the development of a deep-towed geophysical array system.

The identified system's design measurement goals are accurate sound speed determination ($\leq 1\%$), quantitative reflection strength measurements, high-resolution layer definition (4 m), and subbottom penetration up to 500 m. The development approach employs a quantitative performance prediction model for a deep-towed source/multi-channel array configuration which includes: a subbottom multilayer acoustic model, a ray trace capability, and a sonar equation and spatial model. The status of the performance prediction model is reviewed, with the deficiencies noted and planned improvements identified.

The subbottom model input parameters include layer thickness, density, interval velocity, and velocity gradient. The performance prediction effort employed a subbottom model typical of the Venezuelan Basin. The ray trace capability focused primarily on a deep-towed, wide-angle reflection application. A refracted ray trace routine for head and diving waves has been initiated for future assessment of refraction spread requirements and reflection data processing complications arising from refracted arrivals. A sonar equation analysis provided an initial estimate for defining the basic sonar requirements of a deep-towed sound source. These analysis results were used to review the state-of-the-art in high power, low-frequency, deep-towed, acoustic sources. The review identified a candidate approach employing a Helmholtz resonator-type source with the following characteristics: source level, 204 dB/μpam; frequency, 400 Hz; bandwidth, 200 Hz; size, 0.5 m diameter x 0.9 m long; and weight (water), 380 kg. A static tow analysis established the initial tow system characteristics for placing the source/array system at a preselected depth. Tow speeds up to 3 kn at tow depths of 4 km are predicted for projected system component characteristics.

The sensitivity of system configuration parameters on extracting interval velocity has been initiated employing the Dix (1955) interval velocity equation. Plotted results are presented for varied critical parameters of array length, offset, and altitude. Within the constraints of noise-free data and the limits imposed by the Dix equation, the initially identified configuration parameters are array length = 500 m, offset = 50 m, and altitude = 200 m. A preliminary sensitivity analysis of array deformation on interval velocity accuracy measurement indicates that for a fixed 1^0 array tilt angle (kiting) errors can be in excess of 4%. Plans to identify implementation requirements and towing configurations to reduce this error are given.

A review of oil exploration industry techniques for extracting subbottom velocity information is presented. The review considered basic environmental and operational constraints; these were compared to the deep-towed configuration.

ACKNOWLEDGEMENTS

CONTENTS

ILLUSTRATIONS

TABLES

I. INTRODUCTION

With the U.S. Navy's interest in the lower regions of the acoustic frequency domain (less than 500 Hz), concern has increased over the modeling of the deep ocean floor and its accompanying subbottom layers as transmission media that refract, diffract, diffuse and dissipate, as well as reflect, sound waves that eventually reach a receiving hydrophone in the water column. Geoacoustic and geophysical models of ocean floor acoustic interaction, which take all energy paths into account, are needed as inputs to acoustic propagation loss calculations. Such detailed models have substantially greater potential accuracy than traditional models that treat the bottom as an acoustic baffle, especially when data are extrapolated to different geophysical locations and/or different source-target depths than used in the input data acquisition.

The Naval Ocean Research and Development Activity (NORDA), develops the models and technology bases supporting Navy system design tradeoffs through the coordinated efforts of the Ocean Technology, Sea Floor, Oceanography, Ocean Acoustics, and Numerical Modeling Divisions. In regard to ocean floor acoustic interactions, the process consists of: (1) the acquisition and recording of appropriate types and the quality of geophysical/geoacoustic data acquired at sea; (2) the formatting, processing, and display of these data in a form which optimizes further analysis; (3) the interpretation of the displayed data in terms of geophysical models of the ocean floor, described in acoustic terminology; (4) the integration of these models with other models and data pertaining to the water column, surface, and noise sources; (5) data bank input, storage, maintenance, and retrieval; (6) the further interpretation of geophysical models of the ocean floor in terms of sediments and structures to provide an understanding of the geomorphology responsible for the observed acoustic properties of the ocean floor; (7) the use of the general body of knowledge comprising geology, geophysics, and geomorphology to estimate sedimentary structure and composition in areas where field measurements are scarce or nonexistent; (8) the interpretation of the resulting estimated/extrapolated geophysical models in acoustic terms; and (9) further acoustic analysis and data bank management as described above.

A critical factor in the successful operation of this process is the development of instrumentation and field measurement systems capable of acquiring the necessary types of geophysical/geoacoustic data with sufficient accuracy, resolution, and frequency response, plus the development of the capability to format, process, and display this data in an optimum manner which meets the requirements of the above-described analysis. The papers referenced by Urick (1974) and Hamilton (1974) comment on the detailed role of the ocean floor in acoustic propagation, and summarize the ocean floor geophysical parameters required by acousticians. In order to improve the accuracy of and confidence in geophysical models required by Navy acousticians for the purposes previously discussed, it is necessary to improve the data collection, analysis, and presentation capabilities of seismic reflection and refraction measurements, which constitute the basic input to said geophysical models.

The resolution, which, near subbottom parameters, can be measured in the deep ocean, must be improved over existing capabilities to meet the Navy's requirement to understand acoustic bottom interaction. In addition, the confidence level of interpretation must be increased (Ballard, 1977; Fagot, 1978). These requirements can, in turn, be partially met by extending the use of multi-channel, true amplitude, seismic technology to deep-ocean areas. This technology, as developed by the petroleum exploration industry (Sheriff, 1977; Savit, 1977; Schneider, 1971) over the past two decades, allows the collection on a continuous basis: (1) high-resolution layered structure within the constraints of sound source bandwidth, (2) interface reflectivity as a function of grazing angle, (3) sound velocity and attenuation as a

function of depth, (4) migration of side reflections to true position, and (5) direct interpretation of lithology. These data are presently collected utilizing near-surface sources and receivers with optimized measurement geometries for shallow water. Use of shallow-water systems in deep water has demonstrated a limited capability to extract geoacoustical parameters with high precision. If a near-bottom source and receiver array could be utilized in the deep ocean, the geometries would be identical to shallow-water techniques and a wealth of proven processing technology would become applicable. Specifically, if the outputs of a sequence of hydrophones spaced over a distance which is long in relation to receiver-bottom distance can be individually recorded, along with an acoustic source keyed from the surface and in line with the hydrophones, and if such a device could be towed near the sea floor in the deep ocean, such a geometry would have been achieved.

The near-bottom towed source/receiver array system employed in deep water will provide: (1) multi-channel data, which allows processing to extract geoacoustic properties over long traversed spatial distances; (2) self-calibration due to no surface-reflected interference, (3) reduced ray distortion prior to acoustic energy bottom encounter, and (4) reduced acoustic footprint.

This progress report will present the results of the initial phase in the design of a deep-towed geophysical array system. Figure 1 depicts the conceptual configuration of the system. Presented will be a general review of the development program objectives with identification of the design considerations for the system. Included as major discussion topics will be: (1) geoacoustic measurement requirements, (2) performance prediction model design, (3) oil exploration industry velocity measurement techniques, (4) array design considerations, (5) deep-towed sound source design status, (6) static tow analysis, and (7) plans for continued development.

II.   GEOACOUSTIC MEASUREMENT REQUIREMENTS

The prime objective of this development program is to provide the researcher with data that will allow defining the geoacoustic and stratigraphic character of the ocean floor and subbottom structure. Table 1 presents the basic measurement requirements as identified by the researcher.

TABLE 1

GEOACOUSTIC MEASUREMENTS REQUIREMENTS FOR THE
DEEP-TOWED GEOPHYSICAL ARRAY SYSTEM

● COMPRESSIONAL SOUND SPEED

Penetration Depth	200 m
Layer Resolution	4 m
Accuracy	1%

● RELATIVE REFLECTION STRENGTH

Penetration Depth	500 m
Quantitative Requirement	True Amplitude and Phase

● ABSORPTION

Penetration Depth	200 m
Frequency (Acoustic)	500 Hz and lower

The highest priority is given to extracting the compressional sound speed in the near subbottom region with high precision and resolution. Sound speed as a function of frequency is not critical. The operating frequency must be compatible with layer resolution and penetration depth requirement.

Of second priority is the ability to extract the reflection strength of acoustic energy with true relative amplitude and phase. This ability is primarily a requirement to measure the complex impedence of each reflecting horizon. Layer resolution of 4 m is still required, but penetration depth increases to 500 m. This measurement requirement will result in a quantitative high-resolution subsurface picture of the reflecting interfaces. The seismic trace, a basic interpretative tool of the geophysicist, provides reflection strength data that can be used to provide the geologist with a lithographic description of the subbottom through stratigraphic modeling.

Absorption is a lower priority requirement. Data acquired at an acoustic frequency of 500 Hz and lower are desired with a penetration depth of 200 m.

These measurement requirements focus on obtaining a detailed quantitative description of the near subbottom, less than 500 m penetration depth. This can be contrasted to oil exploration industry requirements where deep penetration on the order of 3000 m and greater is desired. In addition, higher subbottom layer resolution is desired over the present oil exploration requirement. The measurement requirement being addressed by this development will supplement the oil exploration capability as drilling moves into deeper water, as well as the Navy's need for placement of bottom-mounted structures by providing high-resolution engineering data on near subbottom geophysical character.

III. PERFORMANCE PREDICTION MODEL DESIGN

The approach taken in this development was to design a performance prediction model that can be used to determine the sensitivity of design parameters through an iterative trade-off analysis. The performance model will include: (1) a multi-layer acoustic model employing structural characteristics typical of the deep ocean, (2) a ray trace capability for both reflection and refraction ray paths, (3) a sonar equation model which can address signal amplitude variables, and (4) a static and dynamic spatial model for the deep-towed system configuration. In addition, the capability has been incorporated into the prediction model to compute the interval velocity based on inputs from the ray trace model (arrival times). A discussion giving the status and identifying deficiencies and planned future efforts will be presented on each of these areas.

A. SUBBOTTOM MODEL

Identifying a typical subbottom acoustic model containing layer thickness, sound speed, sound speed gradient, and density has proven and is proving to be a formidable task. Data with sufficient resolution and acoustic detail for the first 200 - 500 m of subbottom structure, not suprisingly, are minimal. The varying measurement requirements this development is addressing identifies why there is a deficiency.

The initial approach has been to select available data that generally meet the measurement requirement. These data have primarily been used in developing the basic suite of software required to predict the geophysical array system performance.

The future effort will concentrate on refining the subbottom models and includes general subbottom classes that define anticipated operating areas on a geophysical province basis.

Figure 2 presents a subbottom geoacoustic model with the basic data provided by Hamilton (1974). This model is designated Subbottom Model 1 throughout the report. The abyssal hill model presented by Hamilton was modified by increasing layer thickness to provide at least 200 m of subbottom structure. Although the question of realizability of this modified model to actual subbottom structure may be raised, the prime objective in its use has been to exercise the ray trace model during its development. As an example, Subbottom Model 1 and the array geometries used resulted in achieving a critical angle and angle of intromission, which is evident from the ray trace data.

Subbottom Model B is typical of the central Venezuelan Basin (Fig. 3). The horizon located at a subbottom depth of 230 m is known as horizon A" and that located at a subbottom depth of 450 m is known as horizon B". The interval velocity data were primarily derived from Deep Sea Drilling Project data gathered at drill holes 146/149. A discussion on the geological/geophysical characteristics of the Venezuelan Basin is presented by Matthews (1976). The density values for each subbottom layer were derived from data presented by Hamilton (1978).

In addition, Model B was modified by stratifying it with 50 m layers; this resulted in Subbottom Model C (Fig. 4). The stratification retained the linear velocity gradient across each interface as established in Model B. In addition, horizon A" was translated to a subbottom depth of 250 m, and horizon B" was translated to a subbottom depth of 500 m. The density at each 50 m layer was changed to provide an impedence contrast, and therefore, a reflecting horizon. Model C has been used primarily to compute interval velocity for more closely spaced layers than available with Model B.

The performance prediction analysis also required using acoustic attenuation of the subbottom travel path in assessing signal amplitude considerations. The attenuation values as a function of frequency are presented in Figure 5 (Hamilton, 1976).

As discussed by Hamilton (1976), it must be noted that the attenuation values refer to the energy lost upon transmission of a compressional wave from all causes: spherical spreading, reflection, refraction, scattering phenomena, and intrinsic attenuation in the material. The values are therefore effective attenuation. Stoll (1977) presents attenuation values as a function of depth for dilatational waves of the first kind based on a theoretical approach which considered effective stress and not spreading/interface loss. These values are less than presented in Figure 5, but are not significant in the 100 - 500 Hz region. The use of Hamilton's data implies a conservative approach and may force a re-evaluation of attenuation values as the deep-tow system design is refined and a specific hardware approach is selected; but for the initial performance prediction analysis, the conservative values of Figure 5 are employed.

B. RAY TRACE MODEL

1. Reflection

The initial effort in developing a performance prediction model concentrated on a ray trace capability focused on a deep-towed, wide-angle reflection application. The output available at this stage of model design is

4

spreading/interface loss and travel time for horizontally stratified subbottom layers.

The transmission loss, which is calculated by adding absorption to the spreading/interface loss, allows assessing system amplitude variables. This includes such areas as determining the required source level and system dynamic range.

The travel time computation is a measure of the ray's travel time from the source to each of the hydrophones. These values have primarily been used in computing the root-mean-square (RMS) and interval velocities for different system configurations, i.e., variable array lengths, offsets, and altitude. The capability to perturbate array parameters that result in array deformation has also been included.

The design of the ray trace reflection model assumes the following conditions in order to derive a set of equations that predict transmission time and transmission loss:

- Continuity of vertical particle velocity
- Continuity of pressure
- A non-zero linear velocity gradient

Snell's Law can be derived from the first two assumptions. The law states that the ratio of the sine of a ray's angle of incidence to the sound speed is a constant along the ray path (Officer, 1958). Using this result and the linear velocity gradient assumption, the following equations can be derived for a single reflecting layer.

$$\text{Transmission Coefficient} \quad (R_t) = \frac{2 \, P_1 \, C_2 \, \cos \theta_1}{P_2 \, C_2 \, \cos \theta_1 + P_1 \, C_1 \, \cos \theta_2} \tag{1}$$

$$\text{Reflection Coefficient} \quad (R_r) = \frac{P_2 \, C_2 \, \cos \theta_1 - P_1 \, C_1 \, \cos \theta_2}{P_2 \, C_2 \, \cos \theta_1 + P_1 \, C_1 \, \cos \theta_2} \tag{2}$$

$$\text{Horizontal Range} \quad (Rge) = \frac{C_0}{g} \left[\frac{2 \, (\cos \theta_0 - \cos \theta_1)}{\sin \theta_0} - \frac{(\cos \theta_r + \cos \theta_0)}{\sin \theta_0} \right] \tag{3}$$

$$\text{Transmission Time} \quad (T_t) = \frac{1}{g} \left\{ \ln \left[\frac{\text{TAN}^2 \, (\theta_1/2) \, * \, \text{TAN} \, (\theta_r/2)}{\text{TAN} \, (\theta_0/2)} \right] \right\} \tag{4}$$

$$\text{Spreading Loss} \quad (S_L) = \left| \frac{Rge \, * \, C_0 \, * \, \cos \theta_r \, * \, Z}{g \, * \, \sin^3 \theta_0} \right| \tag{5}$$

5

where

$$Z = \frac{2 \ (COS \ \theta_0 - COS \ \theta_1)}{COS \ \theta_1} + \frac{(COS \ \theta_0 + COS \ \theta_r)}{COS \ \theta_r}$$

Spreading/Interface Loss (T_L) = 10 LOG (R_r^2) + 10 LOG (S_L) (6)

where:

       C_0 (Velocity of sound at the source)
       C_r (Velocity of sound at the receiver)
       C_1 (Velocity of sound just above the reflecting interface)
       C_2 (Velocity of sound just below the reflecting interface)
       g (Sound velocity gradient)
       P_1 (Density of layer above the interface)
       P_2 (Density of layer below the interface)
       θ_0 (Angle of incidence of a ray leaving the source)
       θ_1 (Angle of the ray at the reflecting interface)
       θ_2 (Angle of the ray refracted through the interface)
       θ_r (Angle of the ray at the receiver)

        Note that the angles θ_1, θ_2, and θ_r can be derived by Snell's Law given θ_0, C_0, C_1, C_2, or C_r. The computation for range (Rge) assumes θ_0 is given, but for the deep-towed configuration, the range to the hydrophone is specified; therefore, an iterative loop is used to converge the incidence angle (θ_0) for a ray *path from the* source to the hydrophone.

        The above equations are derived for the single reflecting layer case. The multi-layer case treats each layer as a single layer case, adding the results in an appropriate manner. The source incidence angle is determined in the iterative loop where the ranges (Rge) from each of the single layer cases are added together in the process of converging to the angle for the multi-layer case. After the proper source incidence angle (θ_0) is determined, T_{LM} and T_{tM} for the multi-layer case are computed from the single layer case equations as follows:

Total Time for Multilayer Case $T_{tM} = \sum_{LAY=1}^{n} (T_t)$ (7)

Total Spreading and Interface Losses for Multilayer Case

$$T_{LM} = 10 \ LOG \ (\sum_{LAY=1}^{n} S_L) - \sum_{LAY=1}^{n-1} \left[10 \ LOG \ (R_{t_{DOWN}}^2 * R_{t_{UP}}^2) \right] - 10 \ LOG \ R_{r_{LAY=n}}^2 \qquad (8)$$

6

The operation of the reflection model program requires five types of input:

- Plot scaling parameters
- Title information
- Hydrophone location parameters
- Subbottom model parameters
- Array perturbation parameters

The scaling parameters determine the size of the plots drawn. The title is written on the computer listing and on each of the plots. There are three hydrophone location parameter types:

- Number of hydrophone locations
- Altitude of each hydrophone location
- Distance from the source to each hydrophone location

These parameters uniquely define the location of each hydrophone with respect to the source. Furthermore, the four layer parameters defined for each layer are:

- Speed of sound at the top of the layer
- Density of the medium
- Sound velocity gradient
- Thickness of layer

If perturbations of the array (changes of the hydrophone location with respect to the source) are desired, special controls are keyed to deform the array. All necessary constants can be determined from these input parameters. Given a set of input data, the program lists the following:

- Title (from input)

- Subbottom model parameters

    Layer number
    Layer thickness
    Layer dip angle (at present only zero dip is allowed)
    Layer sound velocity (top and bottom of layer)
    Layer sound velocity gradient
    Layer density
    Source grazing angle for each layer
    Source critical angle for each layer
    Source angle of intromission for each layer

- Ray data for model

    Hydrophone number
    Hydrophone range (Rge) from source
    Hydrophone altitude (above bottom)
    Layer number of reflection
    Ray's source incidence angle
    Transmission time of ray
    Spreading and Interface loss of ray

Dynamic range
Transmission time and spreading/interface loss differences between
layers

- Array's dynamic range
  Based on T_L and is the maximum spreading and interface loss
  minus the minimum spreading and interface loss

- Array's receiving time
  Based on T_t and is the last return's time minus
  the previous return's time

The following outputs are color plots where each color indicates a
different layer. If more than four subbottom layers are used in the model, the
colors repeat. Although one color may indicate more than one layer, it always
indicates the same layers. The output examples given in the report are in
black/white, whereas the originals are in color.

- Ray trace
  Plots, in color, each ray path from the source to each hydrophone
  (see Fig. 6). Also included in this plot are the subbottom model
  parameters and the title from the input data.

- Spreading and Interface Loss vs. Range (T_{LM} vs. Rge)
  Plots in color, T_{LM} for the range from the first hydrophone of the
  array to the last hydrophone of the array. Hydrophone locations
  and scales are indicated on the plot (see Fig. 7).

- Transmission Time vs. Range (T_{tM} vs. Rge)
  Plots, in color, T_{tM} for the range from the first hydrophone of
  the array to the last hydrophone of the array. Hydrophone
  locations and scales are indicated on the plot (see Fig. 7).

- Transmission Time^2 vs. Range^2 (T_{tM}^2 vs. Rge^2)
  Plots, in color, T_{tM}^2 for the range from the first hydrophone of
  the array to the last hydrophone of the array. This plot is
  generally used with the interval velocity computation. Hydrophone
  locations and scales are indicated on the plot (see Fig. 8).

If the perturbation controls were keyed in, similar outputs are
generated, except that the array and source could be moved vertically from the bottom
or the array rotated counterclockwise about the source, or a new array substituted
for the old one.

The reflection model program operates under the following
requirements:

- Rge>0
  This limitation implies that the hydrophones can have any physical
  arrangement in a plane intersecting the source. The hydrophones
  may be above or below the source's altitude or on the bottom. The
  hydrophones may be arranged vertically, horizontally or in any
  configuration, as long as the horizontal range (Rge) to each
  hydrophone is greater than zero.

- Source Altitude>0

  This states that the source for this program may not physically be placed on the bottom. A practical limit for this program would be 1 m, although the program may allow lower altitudes.

- Velocity gradient>0

  This model will not work when the gradient equals zero or is negative.

2. Refraction

In addition to assessing a deep-towed, wide-angle reflection configuration, consideration is also being given to a wide-angle refraction configuration. This arrangement could be implemented by either extending the array length or increasing the offset of the reflection array. To assess the refraction configuration, a ray trace capability for both head and diving waves is being developed. This capability is primarily a modification of the reflection ray trace software.

A refraction ray trace capability will also allow identifying subbottom conditions where refracted arrival will be present during reflection profiling. This complication, a real-world situation, must be considered in data processing techniques. The refraction ray trace capability will allow assessing data processing considerations.

The design of the ray trace refraction model as noted is based on the ray trace reflection model with the additional assumptions:

- Head waves have these characteristics:

  Travel parallel to an interface

  Travel at the medium's velocity at the lower side of the interface

  Are produced by rays with source angles of incidence equivalent to the "Critical Angle"

  Return to the hydrophones via rays with source angles of incidence equivalent to the "Critical Angle"

  Spreading loss is via spherical spreading

Diving waves are rays which return to the hydrophone via subbottom curved paths without reflecting off an interface.

The head wave ray is computed using the characteristics of the head waves and the ray trace reflection model. The ray's source incident angle is assumed as equal to the "Critical Angle." Furthermore, the ray path is modified by forcing the ray to travel a Range (Rge Head) along the interface. This Range (Rge Head) has a length such that the return ray path to the hydrophone occurs along a Critical Angle Ray (see Fig. 9). The reflection model equations for transmission time (T_{tM}) and transmission loss (T_{LM}) are modified as shown in equations (9) and (10).

$$T_{t_M} = \left(\sum_{LAY=1}^{n} T_t \right) + T_{HEADWAVES}{}^a \qquad (9)$$

^{a}VELOCITY OF SOUND ASSUMED AS THE VELOCITY
AT LOWER SIDE OF INTERFACE

$$T_{L_M} = 10 \text{ LOG} \left[\left(\sum_{LAY=1}^{n} S_L \right) + T_{L_{HEADWAVE}}{}^b \right] - \sum_{LAY=1}^{n} \left[10 \text{ LOG} \left(R_{t_{DOWN}}^2 * R_{t_{UP}}^2 \right) \right] \qquad (10)$$

^{b}SPHERICAL SPREADING FOR HEADWAVE
PATH IN LOWEST INTERFACE

The Diving wave is computed by the reflection model assuming an imaginary interface at the depth where the curved ray path turns toward the receiving hydrophone ($\theta_1 = 0°$).

The operation of the ray trace refraction model is identical to the operation of the ray trace reflection model. An example of a ray trace plot which contains both head and diving waves is given in Figure 9. This program at present generates listings and ray trace plots. The capability to generate the plots of transmission loss, transmission time, and transmission time^2 has not been implemented.

C. SONAR EQUATION

The active sonar equation as presented by Urick (1975) has been implemented to allow determining either the required source level for a given detection threshold or the signal-to-noise ratio for a given source level at each hydrophone.

The spreading/interface loss input variable is derived from the ray trace model. This variable constitutes the spreading and layer reflection/transmission loss from the source via subbottom paths to each hydrophone. The subbottom absorption component of propagation loss is computed by multiplying the path length by the attenuation factor per unit length. The absorption loss is added to the spreading/interface loss to obtain the transmission loss. The water column absorption is not included due to its relative low magnitude for the near-bottom towed configuration. The subbottom attenuation values are given in Figure 5 (Hamilton, 1976). Using these values is a conservative approach, as noted, since these are effective attenuations that include spreading/interface loss. It is felt that the actual subbottom component of the transmission loss will be between the two cases: (1) Figure 5 values, plus spreading/interface loss; and (2) Figure 5 values without spreading/interface loss.

The noise levels for a deep-towed array present one of the major data deficiencies to date. The values used in the initial assessments are presented in Figure 10. These represent the radiated noise for a typical tow ship at a 4 km range. Also presented for comparison is the deep-sea ambient noise for moderately rough sea-state conditions. Present plans are to make noise measurements on a deep-towed ambient noise array to refine the noise levels for the performance prediction analysis.

Operation of the sonar equation model program is similar to the operation of the ray trace reflection model except for the following inputs:

- Plot scaling parameters
- Title information
- Hydrophone location parameters
- Bottom model parameters
- Array and medium characteristics
- Array perturbation parameters

The array and medium characteristics are:

- Source level (if the signal to noise ratio is computed)
- Bandwidth of the source signal
- Center frequency of the source signal
- Attenuation coefficient at the center frequency
- Noise level
- Receive detection level

The output listing format is as follows:

- Hydrophone number
- Hydrophone Range (Rge)
- Hydrophone altitude
- Layer number
- Source incidence angle
- Source level or signal-to-noise ratio
- Center frequency
- Attenuation coefficient
- Ray path length
- Noise level
- Hydrophone detection level

An output plot of source level vs. Range or signal-to-noise (S/N) ratio vs. Range to each hydrophone can be generated (see Fig. 11 for an S/N level plot).

D. SPATIAL MODEL

An understanding of the static and dynamic spatial characteristics of a deep-towed profiling system must be gained to predict adequately the measurement capability for the deep-towed configuration.

Static spatial characteristics are defined as those influences placing the system at preselected depth. Typical inputs are: (1) tow speed, (2) tow cable drag, (3) tow body weight and drag, (4) array weight and drag, and (5) tow depth. The above parameter can be varied to assess such areas as: (1) the required cable length to obtain the desired tow depth with fixed fish weight, drag characteristics, and tow speed; (2) the required fish weight to obtain the desired tow depth with fixed cable

11

length, drag characteristics, and tow speed; and (3) the maximum tow speed to obtain the desired tow depth fixing the other system parameters. The initial spatial modeling focused on the static spatial characteristics of the system and resulted in generating the basic software to address this problem. Some typical results for a projected tow configuration will be presented.

Dynamic spatial characteristics are defined as those resulting from dynamic forces which perturb towing in a horizontal mode at a constant forward velocity. The dynamic model will address such questions as: How is the tow ship heave motion translated to the tow body and the array? Basically, the dynamic model will look at those system tow parameters that affect array deformation. These results will then be used to alter hydrophone positions in the ray trace model, thereby altering transmission times that affect the precision of determining interval velocity measurements. The dynamic model will allow looking at the sensitivity of system tow parameters in performing the required geoacoustic measurements. Concentrated effort on the dynamic spatial model is planned.

E. INTERVAL VELOCITY

The prime measurement requirement for the deep-towed geophysical profiling system is to determine the compressional sound speed (interval velocity) for the near subbottom (200 m) strata. This requirement has resulted in focusing effort on reviewing existing techniques, primarily those utilized in the oil exploration industry for horizontal towed seismic streamer systems. This review is providing the basic background required to assess the advantages, limitations, and implementation considerations in utilizing a deep-towed system for extracting interval velocities. Although the review is not complete in the sense of identifying the optimum system configuration or the data processing approach, a basic interval velocity computation model employing the Dix technique has been implemented. This has provided the capability to initiate assessing system configuration parameters (array length, offset, array altitude), and to a limited extent, array deformation, which affects interval velocity measurement accuracy.

A brief summary of the existing techniques and approaches thus far reviewed for determining interval velocity will be presented. The theoretical mathematical derivation of the computation procedures will not be repeated, but can be obtained from the referenced papers. Rutherford (1976) presented a detailed review of analytical techniques for determining velocity profiles, and also included refracted arrival methods. The following review will focus on using wide-angle reflection data.

The Dix (1955) technique is the basic reference found when interval velocity determinations are to be made. Dix presented two approaches to determine interval velocity for non-dipping layers. One method, the reduced time-reduced distance method, solves depth and velocity for the first layer characteristics. It employs the Green (1938) method, and then subsequently reduces the deep layers to a single layer case, which is again solved for layer characteristics employing Green's method. The second method is termed the interval velocity equation method. This method employs an approximation based on the sine angle substitution for a tangent of the ray incidence angle. This requires that (1) the source to receiver offset (X) be small compared to the depth of the reflector, and (2) the velocity contrast between layers be small.

As previously stated, the Dix equation method has been implemented and the requirement that the velocity contrast be small in order to maintain accurate results will be illustrated. In addition, it will be shown that even with incident angles

12

near $30°$, certainly a case where $\sin \theta \neq \tan \theta$, accurate interval velocity results can be obtained if the layer velocity contrast is less than 300 m/sec.

The Dix interval velocity equation is presented:

$$V_n^2 = \left[V_{RMS(n)}^2 \sum_{i=1}^{n} T_i - V_{RMS(n-1)}^2 \sum_{1}^{n-1} T_i \right] / T_n \tag{11}$$

where:

V_n = interval velocity of the nth layer for a normal incidence travel path

$V_{RMS}(n)$ = reciprocal of the slope of the $T^2 - X^2$ plot for the nth layer

T_i = two-way normal incidence travel time through the ith layer at $X = 0$

T_n = the difference in two-way normal incidence travel time between the nth and n − 1 layer at $X = 0$

The familiar relationship for the least distance path between the source, reflector, and hydrophone is given by:

$$T_{x,n}^2 = T_{0,n}^2 + \left[\frac{1}{V_{RMS(n)}^2} \right] X^2 \tag{12}$$

where:

X = horizontal distance between the sound source and hydrophone (offset)

$T_{x,n}$ = arrival time of a reflection from the base of the nth layer at X horizontal distance

$T_{0,n}$ = two-way normal incidence travel time to the base of the nth layer

$V_{rms}(n)$ = time-weighted, mean-square velocity through the nth layer

This equation represents an approximate hyperbolic travel path for reflection time vs. range on a $T - X$ plot and a nearly straight line plot on the $T^2 - X^2$ plot. Since the actual ray travel path is a least-time path, equation (12) only approximates a straight line on a $T^2 - X^2$ plot. Higher order terms have been used (Clay, 1965) to describe more accurately the hyperbolic path, but as pointed out by Taner (1969) for the X distances generally encountered in practice, at least for the oil exploration industry, equation (12) gives an accuracy of about 2% for V_{RMS}. Due to the recent interest in such areas as stratigraphic interpretation and wave equation migration, this 2% accuracy may prove to be insufficient.

A comprehensive review of both theoretical approach and practical implementation of the wide-angle reflection method employing the sonobuoy measurement technique is presented by Maynard et al. (1974). He reviews interval velocity solutions presented by such pioneers in the area as Dix, Durham, and Green. According to Maynard, most reflection data have been analyzed employing Dix's (1955;

13

equation (11)) interval velocity equation than by any other method. He points out that when employing $T^2 - X^2$ type analysis with an airgun/sonobuoy measurement technique in deep water (2 km or more), the interval velocities can only be determined to about the nearest 0.1 km/sec at best for vertical layer intervals of 200 m, and also that the precision decreases as the subbottom layer interval decreases.

Le Pichon (1968) presented a modified reduced time-reduced distance technique for sonobuoys to compute interval velocities in the deep water. These velocity results, as stated, had an average error of less than 0.1 km/sec. As pointed out by Bryan (1974), this technique assumes straight-line paths, which can lead to significant errors under certain cases. Errors resulting from determining the sound speed in the water column can be negligible for that layer, but can contribute significant error to the thinner subbottom layer when the water column data are reduced from the subbottom data. This approach produces generally favorable results with thickness ratios (water depth ÷ subbottom layer thickness) up to 15.

Bryan (1974) presented an alternate approach to determining velocity and subbottom layer thickness for thickness ratios up to 100, termed the ray parameter method. Bryan also presented a thin layer approximation to this basic method for thickness ratios up to 500. Although this method focused on 3.5 kHz data where high range resolutions (large bandwidth) are compatable with the high thickness ratios, the basic method is applicable to seismic array data. This method does not require knowledge of the structure above the subbottom layer of interest, and, as contrasted to the Dix interval velocity equation, does not require small angles of incidence. This method does assume, as does Dix's, that the velocity structure above the subbottom layer be a function of depth only. The ray parameter (p) is basically the slope of the T-X curve. It is also pointed out that the method does not depend on an accurate determination of the origin of the T - X curves, only that the record (T - X plot) span a sufficiently large range of p values to define a straight line (tangent) will be adequate. This latter feature has additional possible application where T_0 is not precisely known, such as with explosive sources. The ray parameter method has some appealing features for basic application to the deep-towed geophysical system: (1) its usefulness for high thickness ratios and therefore high layer resolution, (2) the potential increased interval velocity measurement accuracy by not requiring small incidence angles, and (3) the solution does not require detailed knowledge of the structure above the layer.

IV.   OIL EXPLORATION INDUSTRY VELOCITY MEASUREMENT TECHNIQUES - A REVIEW

Undoubtedly, the oil exploration industry has made the greatest strides in extracting and using velocity information. The projected deep-towed system geometry is a translation of the marine oil exploration near-surface geometry; therefore, a review of their techniques for extracting velocity information is appropriate.

A comprehensive summary of the measurement techniques, data processing, and application of velocity information by the oil exploration industries up to 1970 is presented by Schneider (1971). As pointed out by Schneider, the original and still predominant use of velocity information is for moveout correction and common depth point (CDP) stacking. The newer image-forming technique, migration, also requires extensive use of velocity information.

The normal moveout (NMO) velocity or stacking velocity is measured directly from seismic field data, and for parallel non-dipping layers is equal to V_{RMS} (slope of $T^2 - X^2$ plot) as defined by equation (12). A cosine of the dip angle correction is required for dipping horizons. Applying a normal moveout (NMO) correction allows each hydrophone channel to be brought into time registration relative to the

normal-incidence, two-way travel time for a particular reflecting horizon. The time registered channels are then summed, resulting in attenuated random noise and the reduction of multiple entrapped reflections.

Although other data gathering schemes are employed (such as common source point (CSP), common receiver point (CRP), and common offset plane (COP)), the predominant scheme is CDP. Most data processing focuses on CDP data. A CDP data gather is also less sensitive to dipping horizon than, say, CSP gathers. A CSP gather is basically the field data obtained from a single shot-receive sequence. A CDP data gather is based on coincidence hydrophone position from shot to shot, and therefore requires accurate knowledge of over-the-ground source/reciever velocity, a requirement that may be difficult to achieve with a deep-towed configuration. If shots occur at distance intervals equal to one-half hydrophone spacing, a full fold stack can be generated; if they occur at distance intervals equal to hydrophone spacing, a one-half fold stack can be generated.

Schneider (1971) presented a summary of acceptable error for RMS and interval velocity as a function of velocity use. The summary is given in Table 2. As stated, the interval velocity accuracy in the presence of random noise is based on an interval/RMS velocity error ratio equal to approximately 1.4 times the ratio of bed depth to bed thickness. Maintaining the interval/RMS velocity ratio for stratigraphic detailing, and applying it to the measurement requirement being addressed by this development, equals a 19 m layer interval at 400 m depth. This is certainly below the measurement goal and may be a questionable comparison without a detailed assessment of the noise environment (S/N) for the deep-towed system This type of assessment is planned.

TABLE 2

VELOCITY ACCURACY REQUIREMENTS FOR OIL EXPLORATION USE
(AFTER SCHNEIDER, 1971)

USE OF VELOCITY	ACCEPTABLE ERROR	
	RMS VELOCITY	INTERVAL VELOCITY
NMO Corrections for CDP Stack as Currently Practiced	2-10 %	____
Structural Anomaly Detection: 100 ft Anomaly at 10,000 ft Depth	0.5 %	____
Gross Lithologic Identification: 1000 ft Interval at 10,000 ft Depth	0.7 %	10 %
Stratigraphic Detailing: 400 ft Interval at 10,000 ft Depth	0.1 %	3 %

15

Schneider (1971) also identified the major factors which affect the accuracy of moveout-based velocity estimates (V_{RMS}). These factors will also affect the deep-towed configuration, therefore, the more critical factors are presented:

● Random Moveout Estimation Error: This error results from the presence of noise in the data which generates a jitter component on moveout correction and V_{RMS} curves. The magnitude of statistical fluctuation increases with depth (record time) due to the combined effects of generally decreasing S/N ratio, bandwidth, and normal moveout with depth. The greatest precision is available at a record time where the maximum spread length (array length) is first used. At both earlier and later times, the maximum moveout available for estimating velocity decreases, resulting in an increased percent error for a fixed moveout error. Also, the precision of the velocity estimate can be improved by averaging a series of velocity estimates. It was stated that for an S/N ratio of 4:1 and a 20 Hz center frequency, the minimum expected error is 1.5% for a single velocity estimate and improves to about 0.25% for an average of 25 velocity estimates consecutively spaced within a 3/4 mile lateral distance. Although it appears that statistical error can be reduced and velocity measurement precision improved by increasing array length and/or averaging, a limit is reached due to some non-statistical source of error.

● Random Static Correction Error: Statics are arrival time delays resulting from factors other than normal incidence time and moveout. The result of statics are traces within gathers which do not align in time on a predescribed trajectory. One type of static error is a non-horizontal array (deformation). Static errors are considered large if the time delay (advance) is greater than half the period of the dominant reflection energy. There are automatic static correction techniques primarily used on land seismics that generally work well for high S/N ratio conditions and static errors less than those defined as large.

● Near-Surface and Distributed-Velocity Anomalies: This problem occurs when lateral-velocity anomalies have dimensions on the order of a CDP spread (array length). As the array (spread) moves over an anomaly, differential travel time variations are introduced at different offsets within the CDP set, causing the moveout curve to become non-hyperbolic. This problem results from violation of the basic premise for reflection surveying that the subsurface must be homogeneous over the insonified area. Test examples were given which showed that while the movement anomaly decreases, with decreasing spread length, the absolute movement also decreases but at a faster rate; thus, but the fractional velocity error is largest for the small offset.

● Multiple Reflection Interference and Offset-Dependent Wave Shape (Complex Reflection): This type of interference and other non-random interference (such as offset-dependent wave shape interference) can bias velocity estimates made on primary reflections. Reflections from a series of closely spaced beds of differing velocity are a non-random interference. The reflection wavelet will change its shape with offset with a resulting velocity error and bias, since moveout-based velocity estimates assume the wavelet to be independent of offset. The thin layer interference is therefore frequency dependent, a consideration to be evaluated for the deep-towed configuration.

● Curved Ray Path: The effects of curved ray paths result from non-hyperbolic moveouts. It was stated that neglecting high-order terms in the T^2-X^2 analysis causes little error in either RMS or interval velocity for offsets less than or equal to reflection depth, a fact that may not be true for the deep-towed configuration.

16

• <u>Complex Structure:</u> For uniformly dipping structure, the cosine of the dip angle correction noted earlier is appropriate; but for more complex structure, such as arbitrarily dipping and curved structure, the simple correction is not adequate. One approach has been to employ a local two-dimensional layered model whose depths, dips, and interval velocities are adjusted iteratively to give a best fit to observed travel times (inverse modeling), an approach that is becoming increasingly employed.

• <u>Survey Geometry:</u> This problem was related to marine survey where the seismic streamer was at an angle to the line of traverse caused by cross currents. In steep cross dip areas, a linear moveout error will be superimposed on the hyperbolic moveout. Since a mechanical means of assuring a straight tow may not be achievable, this problem must be taken into account in interpretation of velocity estimates.

Taner et al. (1970) presented a review of the basic limitations of the seismic reflection method, with emphasis on determining RMS and interval velocities. The following conclusions reflect the basic considerations when employing the seismic reflection method.

• The method requires subsurface linearity over the distance of the array length. If this condition is not met, velocities and depth cannot be accurately determined.

• Due to geometric effects and non-linear subsurface, RMS velocity analysis interpretation involves more complexity than initially thought. In complex geology areas, more velocity determinations are needed. Lateral distances on the order of one-half mile are required in order to get good stacking velocities.

• The stacked section itself may be misleading owing to the velocity structure and geometry resulting in apparent dip reversals, phantom structure, and faults.

• In areas of dip, using RMS velocities derived from velocity spectral analysis or even velocities from well log surveys can result in erroneous interval velocities unless dip information is included in the calculations.

This latter point has been recognized and has placed more emphasis on inverse modeling, which takes dip structure into account. Stratigraphic and lithologic analyses depend on accurate interval velocity values. A discussion of computational procedures for interval velocity determination, which takes into account the complex subsurface structure, is presented by Sattlegger (1965), Cook et al. (1969), Sherwood et al. (1972), and Gerritsma (1977). This certainly is not a complete reference of the work being done in this area, but does review some of the major considerations in this type of analysis.

Also reviewed were the techniques employed by the oil exploration industry to obtain RMS velocities (moveout velocities) on a routine basis. The paper by Taner et al. (1969) discusses extracting velocity spectra (velocity versus two-way normal incidence travel time) employing a semblance coherency measure. This technique basically determines the best hyperbolic trajectory for a wave travel path and generally employs CDP-gathered data. How well a specific trajectory, based on different RMS velocities, correlates from trace to trace is the semblanced measure. As pointed out by Neidell et al. (1971), other coherency measures can be employed. Semblance, as defined by Neidell, is a time domain coherence measure relating directly to an appropriately defined output/input energy ratio.

17

The resulting velocity spectra from a semblance velocity analysis are used to: (1) determine the velocity function needed for optimum stacking; (2) check the final stacked section against any procedural, interpretational, or computational error; (3) determine the effect of multiple interference; and (4) determine two-way normal incidence travel time and RMS (apparent) velocities for estimating interval velocites employing, for example, the Dix interval velocity equation (11).

Dr. Paul Stoffa (personal communication, 1978) has implemented what he terms a high-resolution semblance velocity analysis technique. This technique basically eliminates a windowing operation which improves the temporal and velocity resolution of the semblance technique. He basically uses the semblance statistic as a phase velocity discriminant. The two-way depth interval uses the basic sampling interval of 4 msec and the velocity scan steps are 25 m/sec. The results from this technique are in good agreement when compared to velocity well log data in shallow water. This technique will be reviewed in more detail as applied to deep-towed data where high layer and velocity resolution are required. It should be noted again that this technique was applied to CDP-gathered data and the application to deep-towed data where the CDP gather scheme in question must be investigated. The semblance measure is independent of the gather scheme, but the accuracy of the results ties directly to the basic advantages of CDP data over CSP data. It is worth pointing out that Dr. Stoffa has also applied his semblance technique to wide-angle reflection sonobuoy data.

This review has identified factors that influence performance of a deep-towed geophysical profiling system which must be considered in its design. The fundamental capability to determine interval velocities employing the Dix interval velocity equation is an initial step in evaluation of system parameters. A more detailed approach is planned containing system operation and environmental parameters that reflect more realistic in situ conditions. The planned effort will be reviewed.

V.   ARRAY DESIGN CONSIDERATION - INTERVAL VELOCITY MEASUREMENT

A. GENERAL BACKGROUND

The previous section identified many factors to be considered in the design of a deep-towed geophysical profiling system. The progress made to date has been to review measurement techniques and implement a basic performance prediction analysis capability. Although this basic capability is only an initial step toward a more descriptive prediction analysis, it has provided an insight into the factors that must be considered in an array design.

A series of ray traces and the resulting transmission loss and transmission time values have been generated while varying such array/environmental related parameters as array length, offset, altitude and subbottom model. The transmission time data have been used primarily for interval velocity analysis.

The ray trace presentation in itself does not provide a great deal of quantitative data, but does provide a check that the software has executed properly. Typical displays were presented in Figure 6, and, in addition, Figures 12 and 13 show a set of ray traces for different environmental and array parameter conditions. Close observation shows curved ray paths resulting from sound speed gradients. As pointed out earlier, a straight ray path is generally assumed when solving for interval velocity, a source of error when long subbottom travel paths are encountered. The transmission time plots for Figures 12 and 13 are presented in Figures 14 and 15, respectively.

18

For the computations of interval velocities to be presented, determining the value of V_{RMS} from the slope of the $T^2 - X^2$ plot was obtained with essentially ideal data in the sense that practical complications in picking arrival through noise and refracted arrival superimposed on the reflection data did not exist. Generating synthetic seismograms with these types of complications is planned. An initial step in this direction has been taken by implementing a head wave and diving wave ray trace capability. For example, the array and environmental conditions that resulted in the reflection ray trace of Figure 6 also are the conditions that generate head waves that are received starting at hydrophone 6. This is clearly shown by the head wave ray trace presented in Figure 16.

As pointed out earlier by Schneider (1971), the greatest precision in making velocity (V_{RMS}) measurement occurs at a record time (To) where the maximum array length is first used. An intuitive feel for this can be obtained by observing Figure 17. This is a normal moveout (NMO) correction plot for the array and environmental condition presented in Figure 6. The precision is proportional to the ratio of the difference in NMO (ΔNMO) to record time To for a specified array length (offset). For comparison at To = 55 msec with an offset=186 m, the ΔNMO = 15 msec and with an offset = 550 m, the ΔNMO = 82 msec. It can be seen that for a fixed moveout measurement error, Δt, determining RMS velocity based on NMO trajectory is more sensitive for the small offsets. This would imply that greater offsets (longer arrays) should be employed to increase measurement precision; but other factors, such as decreased S/N ratio and ray bending, can and do limit precision (see Schneider, 1971).

B. ARRAY PARAMETER TRADE-OFF ANALYSIS

A series of plots showing interval velocity error in percent as a function of different array/environmental parameters will be presented. The reference, or true, interval velocity was the mean velocity at the center (layer thickness/2) of the layer taken from the input subbottom model. The measured interval velocity was obtained by employing the Dix interval velocity equation method (see equation (11). A positive (+) interval velocity error indicates that the measured velocity is greater than the reference interval velocity, and a negative (-) interval velocity error indicates that the measured velocity is less than the reference interval velocity.

A set of interval velocity error data was generated employing subbottom model C (see Fig. 4). This data set consisted of varying a single major array parameter. Figures 18, 19, and 20 present the results for varying array length, array altitude and offset, respectively. The initial observation shows large errors associated with determining the interval velocity for layer 6, just below horizon A", for most practical array configuration parameters. Also by viewing Figure 18, for an array length of 500 m, the error becomes less progressive with deeper subbottom layers below layer 6. Layer 6 is the transition from the low velocity structure of horizon A" and the high velocity structure between horizons A" and B". The velocity difference for model C equalled 968 m/sec. This large error results from violating at least one, or under certain array configurations, two of the basic assumptions for use of the Dix equation; namely, (1) the incidence angle for a ray from the source to the receiver must be small (where sin=tan) and (2) the velocity contrast with the layer above must be small.

A test case was generated primarily to determine the value of the velocity difference that caused the large errors. The results are presented in Figure 21. The subbottom model was basically Model C, but with a single layer down to horizon A" (250 m thickness), and then a deeper 50 m layer in which the interval velocity was

19

varied to produce a velocity difference between the two layers from 100 m/sec to 1000 m/sec. The plotted results presented are for the interval velocity error of the 50 m layer. Three different array configurations were used. For the 50 m array and 50 m offset, the error was less than $\pm 1\%$ for the maximum velocity difference; assuming straight ray path, the incidence angle was less than 6°. For a 50 m offset and a 500 m array length, the maximum velocity difference that could be tolerated and still not exceed 1% error was 480 m/sec. The incidence angle for this condition equalled 29°, certainly a case where $\sin \neq \tan$. The last case was for a 300 m offset and 500 m array length, and, to maintain an error less than 1%, the maximum velocity difference could not be greater than 285 m/sec. The incidence angle for this case equalled 39°. Although this test case did not precisely define the limits of the Dix analysis technique, it did show that the small incidence angle requirement can be violated within tolerable error limits if the layer velocity difference is small. On the other hand, if a large velocity contrast exists (968 m/sec for Model C), but a small incidence angle is maintained, then the error can be kept to less than 1%. This latter point can be shown from the data presented in Figure 19. For an interval velocity error of 1% or less for high-velocity layer 6, the altitude must be 715 m or greater for the array parameters employed. Again assuming straight ray paths (source to subbottom layer to far phone), the incidence angle for these conditions equals 15°, a case where $\sin \cong \tan$. It might be noted that a generally accepted rule of thumb for using the Dix interval velocity equation is that the incidence angle should be equal to or less than 15°.

As noted earlier (Fig. 18, 500 m array length), the error became progressively less for each subbottom layer below the high velocity contrast for fixed array parameters. This results because the large error, layer 6 in our case, biases the velocity determination of the next deeper layer, but the bias decreases with the deeper layers. The case presented for layer 8 (the interval velocity error), 100 m below the high velocity contrast of layer 6, is less than 1%.

A second set of velocity error analyses was performed using subbottom model 1. Typical results for varying array lengths are presented in Figure 22. These results are typical (error <1%) for array parameter conditions selected. It should be noted that the velocity contrasts between interfaces for subbottom model 1 do not exceed 118 m/sec.

Subbottom model 1 was used in the initial effort to assess the effects of array deformation on interval velocity measurement accuracy. An array configuration with array length = 500 m, offset = 50 m, and altitude = 200 m was subjected to fixed tilt angles (kiting). The interval velocity error for tilt angles from 0° to 5° was computed and the results are presented in Figure 23. The error for 0° tilt (horizontal array) was less than 0.1% for this configuration, but increased rapidly with increased tilt angle. Even for a 1° tilt angle, the interval velocity error for layer 4 approached -4%. These large errors far exceed the basic measurement requirement and identify a critical technical risk area (array deformation) that must be assessed in detail during future efforts.

The same array parameters as used above were also employed in assessing array droop. The array was deformed, as simply represented by the arc of a circle. The amount of droop was the distance measured from a cord joining both ends of the array and a tangent to the array in the horizontal plane. This configuration and the error results are presented in Figure 24. Although the practical realization of this configuration may be questioned, the 2% error for a displacement of 20 m over a 500 m array length emphasizes the criticality of array deformation knowledge on measuring interval velocity.

20

Subbottom model 1 was also used to review velocity errors associated with fixed system timing errors. By using the same array configuration that was employed on the deformation analysis, the transmission time to each phone was increased in fixed steps up to 10 msec over the transmission time that would be obtained directly from the ray trace routine for a horizontal array. This increase in time is designated as picking error. The interval velocity errors resulting from these picking errors are presented in Figure 25. Note that the error decreases with increasing layer depth. With a 10 msec timing error, the maximum interval velocity error associated with layer 1 (water) is less than 1.25%.

The analysis to date on array design considerations for extracting subbottom interval velocity information has been a rather simplistic approach, but it has identified areas that require more detailed study. This includes: (1) defining a more realistic subbottom and ray trace model, (2) identifying a processing technique optimized for the deep-towed configuration, (3) defining the operating noise environment for more realistic performance prediction, and (4) identifying more precisely anticipated array deformation characteristics. Studies into these areas are planned.

VI.   DEEP-TOWED SOUND SOURCE DESIGN STATUS

A.   BASIC CONSIDERATION

The basic concept being explored for the deep-towed geophysical profiling system, as noted, is to place the array and sound source at depth. The profiling penetration depth requirement of 500 m dictates that a relatively low frequency sound source be employed. Defining the operating frequency is one of the major difficulties in sound source design.

The sonar equation was solved for the source level required when employing different source and environmental parameters. The transmission loss noted earlier consisted of the spreading/interface reflection loss derived from the ray trace routine and the absorption loss derived by multiplying the subbottom ray path length by the Hamilton (1976) attenuation value as a function of frequency (Fig. 5). Also, as noted earlier, the noise levels employed the values presented in Figure 10.

Subbottom model B was initially employed to determine the required source level as a function of frequency. Fixed array parameters for a typical configuration were used: array length=500 m, array altitude=200 m, and offset=50 m. The spreading/interface loss for these parameters and subbottom model B are presented in Figure 26. Near hydrophone 10, a critical angle condition existed for the interface between layers 3 and 4 and a critical angle was approached between layers 2 and 3; therefore, the spreading/interface loss decreased with range due to the reflection coefficient approaching 1.0. Figure 27 is a typical plot of required source level as a function of hydrophone position for an operating frequency of 400 Hz. Table 3 presents a summary of required source levels to the far hydrophone (number 12 at offset=550 m) over a 100-1000 Hz operating frequency range for energy reflected off interface 2-3 (A") and interface 3-4 (B"). These results indicate that with a source level of 202 db//μpam penetrating to the deeper interface 3-4 (450 m total subbottom thickness), an operating frequency of 500 Hz and lower is required. This operating frequency can be increased to 900 Hz for the shallower interface 2-3 (230 m subbottom thickness) with about the same source level. It should be noted that the source levels presented in Table 3 would result in S/N=0 for a return received at hydrophone 12 from the respective interfaces. The S/N plot is presented in Figure 28 for these fixed array parameters, subbottom model B, source level of 204 db//μpam, and the noise spectra of Figure 10.

TABLE 3

REQUIRED SOURCE LEVEL AS A FUNCTION OF FREQUENCY FOR SUBBOTTOM
MODEL B AND ARRAY ALTITUDE = 200 M AND OFFSET = 550 M

FREQUENCY	SOURCE LEVEL (db//μpam)	
(HZ)	INTERFACE 2-3 (A")	INTERFACE 3-4 (B")
100	163	168
200	165	173
400	177	193
500	183	202
700	193	221
900	203	239
1000	210	253

A similar analysis was performed employing subbottom model 1. The spreading/interface loss values (presented in Fig. 7) were combined with absorption and noise levels at a frequency of 400 Hz, and the required source level was computed. The results are presented in Figure 29. A source level of 200 db//μpam would provide excess signal except for reflection off the interface between layer 2 and layer 3. This interface is a weak reflector and also has an angle of intromission that is readily apparent from the required source level associated with hydrophone 12. Figure 11 presented S/N level and a source level equal to 204 db//μpam for this subbottom model.

The required source levels are very sensitive to the subbottom model and environmental parameters employed. The results obtained for subbottom model 1 are more suspect for the reason already noted than those obtained for subbottom model B. The latter subbottom model is felt to be typical for the Venezuelan Basin area. A large contributor to the high required source levels is the attenuation. The analysis employed a conservative approach in that attenuation included absorption plus spreading and interface reflection losses. The noise level employed in these analyses probably represents the minimum level to be encountered for a deep-towed configuration. The source level results, primarily those presented in Table 3, represent an optimistic design goal for the sound source development, and if they can be achieved, should provide excess signal-to-noise ratio. Additional analyses employing other subbottom/environmental parameters is planned.

It is interesting to translate source levels generated at depth to an equivalent source level generated at the near surface. As an example, translating a 202 db//μpam (Table 3, 500 Hz, interface 3-4) source level located at an altitude of 200 m to the near surface in 4000 m of water would result in a peak source level of 228 db//μpam, a high source level for a system operating at a center frequency of 500 Hz (see Mero et al., 1974, and Kramer et al., 1968). This illustrates the implied optimistic peak source levels thus computed for the deep-towed configuration.

An alternative to the "big bang/brute force" approach in achieving penetration is to employ some type of data processing technique to gain an effective higher source level. One of the simpler techniques is to employ stacking of individual traces, which provides a gain=10 log N for random noise where N=number of traces to be stacked. The oil exploration industry employs this technique (as noted earlier), generally with CDP data. The traces are brought into time registration by

22

applying a normal moveout correction and then stacked, resulting in a single composite trace with processing gain improvement. These traces also sum a series of hydrophone outputs (known as groups) within each channel.

A variation of this technique can be employed to achieve processing gain for the signals received at each hydrophone with the basic assumption that (1) the noise is random and (2) there is subbottom spatial coherence over the array length. This technique requires summing (vertical stacking) the traces at each hydrophone from a consecutive series of shots. Figure 30 presents the S/N gain as a function of the number of stacked traces N. For example, an array 1000 m long towed at a speed of 2 kn with a shot repetition rate of one per 30 sec will allow 32 traces to be stacked within a lateral tow distance of 1000 m. This would result in a 15 db S/N ratio improvement. These results are also applicable for an array 500 m long being towed at 1 kn. Other combinations of array length and tow speeds are tabulated on Figure 30.

This technique can result in distorted waveforms when the subbottom reflectors are dipping. As pointed out by Levin (1977), the vertical stacking under these conditions acts as a filter. The filter response is a function of operating frequency, sound speed between the source and reflector, lateral distance between shot points, depth of reflector, offset from source to hydrophone, and the horizon dip angle. The signal amplitude reduction (filter response) as a function of N for the following typical parameters was computed: (1) tow speed=1 kn, (2) shot repetition rate=1 per 15 sec, (3) offset=550 m, (4) reflector depth=horizon A" from subbottom model B, (5) sound speed=1540 m/sec (RMS) from subbottom model B, (6) operating frequency 400 Hz and (7) dip angle=2°. The amplitude reduction of the stacked traces equals 0.90, 0.85, 0.50, and for N=4, 6 and 12, respectively. If the tow speed is doubled (2 kn), but the other parameters remain constant, the amplitude reduction equals 0.52 and 0.45 for N=4 and 6, respectively. Under these conditions for N=12, a null in the filter response is passed through and the amplitude is determined by a side-lobe of the filter, a condition which should be avoided for practical use of this stacking technique. As shown, vertical stacking is sensitive to dipping interfaces, and under many practical operating conditions, this techique will provide minimal gain and even a reduction in the S/N ratio. A more detailed analysis will be performed on this technique when an updated dipping subbottom model and a more definitive array deformation configuration are available.

Another approach to effectively increasing source level is to transmit a signal with a time-bandwidth product greater than unity, and then to rely on matched filtering (cross-correlation) to provide the increased gain. This can be accomplished by transmitting a long duration pulse with modulation (bandwidth) compatible with the layer resolution requirement. A pulsed FM waveform is one candidate. Careful consideration must be given to this approach since bottom returns must be coherent with the transmitted signal. This may be true for near-normal incidence, but degradation may occur for noncoincidence source-receiver configuration. The degree of potential degradation for the deep towed source-receiver configuration needs to be addressed prior to implementation of a system capable of generating and processing the required waveshapes. The potential gain that could be obtained with time-bandwidth products up to 200 is presented in Figure 31. For example, with a 0.25 sec pulse length (compatible with an altitude of 200 m to assure no reception during transmit) and a bandwidth of 200 Hz (compatible with a resolving ability of 4 m), the signal processing gain is 17 db. With a source capable of transmitting a source level of 190 db//µpam for 0.25 sec duration, the effective source level would be 207 db//µpam. Stated another way, two systems having the same resolving ability (200 Hz bandwidth) and equal peak source levels, but with one transmitting a short pulse (5 msec) and the other transmitting a long pulse

23

(0.25 sec) having phase encoded information, the long pulse system can effectively provide an additional 17 db source energy. But again, the lack of coherence between transmit and receive signals can negate this gain.

Employing the semblance coherency technique noted earlier is another processing scheme which improves the S/N ratio. Employing this processing technique will also be examined in the future.

B. SOUND SOURCE APPROACH - ELECTROMECHANICAL TECHNOLOGY ASSESSMENT

The Underwater Sound Reference Detachment (USRD) of the Naval Research Laboratory (NRL) was tasked to assess the state-of-the-art in high power, low-frequency acoustic sources for deep-towed application. This assessment (Groves, 1978) will be summarized and some practical considerations for implementation of the recommended approach will be presented. NRL/USRD was tasked to address the source requirements summarized in Table 4 and recommend a technical approach that is within present state-of-the-art technology.

TABLE 4

DEEP-TOWED SOUND SOURCE REQUIREMENTS FOR STATE-OF-THE-ART
TECHNOLOGY ASSESSMENT

SOURCE LEVEL:	220 db re 1 µpa at 1 m (maximum)
	204 db re 1 µpa at 1 m (minimum)
FREQUENCY:	<500 Hz
BANDWIDTH:	>200 Hz
PULSE LENGTH:	5 msec (pulsed CW)
	125/250/500 msec (pulsed FM)
PULSE REPETITION RATE:	1 pulse per 15 sec (max)
	1 pulse per 30 sec (desired)
PHASE RESPONSE (FM):	Linear
POWER:	Compatible with 5700 m of RG8/U
	coaxial cable
SIZE:	0.6 m diameter X 1.8 m long
WEIGHT:	460 kg
OPERATING DEPTH:	3000 m (minimum)
	4000 m (desired)
	6000 m (maximum)

The assessment reviewed transducer types and defined their applicability to the deep-tow requirement. Critical factors extracted from the assessment are presented.

Bender Bar Transducer: For high power, low-frequency applications, these types of transducers become very heavy, far beyond the size and weight limits of the deep-tow application.

Flextensional Transducers: These transducers can be made relatively small and light, but require a method to compensate for hydrostatic pressure. Most commonly, the interior of the transducer is either air filled or oil filled with compliant tubes inserted; neither approach is considered feasible for this application.

Moving Coil (Electrodynamic) Transducer: These transducers are capable of generating moderately high source levels at relatively low frequencies, but unfortunately require an air or gas compensation system (again not considered feasible for the deep-tow application).

Electromechanical Transducers: The general configuration is a large electric motor driving two opposing pistons through eccentrics on a crank shaft. In this configuration, they are inherently narrow bandwidth devices and also use air as a pressure compensation/pressure release mechanism.

Ceramic Flexural Disc Transducers: This transducer can offer a good power-to-weight ratio and a potentially high efficiency for some applications, but the design suffers from the same pressure compensation and pressure release problem as do most others.

Hydroacoustic Flexural Disc Transducers: This type represents one of the few feasible alternatives. For the specified deep-towed application, the advantages are a relatively high overall efficiency and broad attainable bandwidth, while the disadvantages are a low power-to-weight ratio and a limited depth capability.

Impulse Sources: This type includes such sources as explosives, spark gap devices, and air guns. These were ruled out due to the severe handling problems associated with their operation. One type that does present a possible alternative is the cocked piston. With this approach, a piston is cocked against ambient pressure and then suddenly released, resulting in an implosion generating a large negative acoustic pulse. This approach was not considered due to a low time-bandwidth product (TW) and lack of control of the acoustic waveform in the water.

Helmholtz Resonator Transducer: The Helmoltz boosted ceramic driver can be configured within the size and weight constraints specified and provide the minimum source level with the required bandwidth. The Helmholtz cavity may be free-flooded with seawater, and the ceramic transducer requires no pressure compensation/pressure release mechanism. The assessment concluded that within the present state-of-the-art, the Helmholtz booster ceramic projector is best suited to meet the overall requirements for the deep-towed application.

A pictorial cut-away of the conceptual design of the Helmholtz sound source is presented in Figure 32. The transducer consists of a Helmholtz cavity and orifice driven by a stack of segmented ceramic rings. One surface of the ceramic drives the Helmholtz cavity, while the other surface radiates directly into the medium; at the Helmholtz frequency, the radiation from the orifice and the exposed

surface are in phase, thus resulting in a boost of the low-frequency response of the ceramic driver. The Helmholtz resonance is placed at the low end of the frequency band to be covered and provides a significant increase in the response over the desired band. The ceramic driver has a 12 db per octave slope; therefore, to maintain a flat frequency response of the propagating energy over the band of interest requires pre-shaping of the signal to the ceramic driver.

The specifications for the Helmholtz resonator transducer are presented in Table 5. The operating center frequency was 400 Hz, the bandwidth equalled 200 Hz, and the Helmholtz resonance was placed near 300 Hz. The 204 db//μpam source level can be achieved, but the efficiency in generating this level is proportional to the size of the transducer. Two models differing in length were recommended. These models were 0.9 m and 1.8 m long and required 38 kva and 19 kva peak volt-amperes, respectively, for an untuned configuration to achieve the 204 db//μpam source level.

TABLE 5

HELMHOLTZ RESONATOR TRANDUCER SPECIFICATIONS

SOURCE LEVEL:	204 db// μpam
FREQUENCY:	400 Hz
BANDWIDTH:	200 Hz
PULSE REPETITION RATE:	1 pulse per 15 sec
OPERATING DEPTH:	Full Ocean
SIZE:	Model 1 - 0.5 m dia x 0.9 m long Model 2 - 0.5 m dia x 1.8 m long
WEIGHT (AIR):	Model 1 - 500 kg Model 2 - 1020 kg
WEIGHT (WATER):	Model 1 - 380 kg Model 2 - 775 kg
PEAK POWER:	Model 1 - 34 kva Model 2 - 17 kva

The assessment reviewed the electrical compatability of 5700 m of RG8/U to provide the required input power for generating the desired source level. The power required to drive each model in a tuned and untuned configuration through the 5700 m of cable was computed. The results are presented in Table 6. It is apparent that the high volt-amperes required to drive the transducers through the long tow cable can pose practical implementation problems. An alternate approach would be to store energy in capacitors or batteries at the deep-towed source to provide the high peak power for each shot and then trickle charge the stored energy between shots. At 400 Hz, the real peak power required for the tuned source equals 5.1 kw and 2.8 kw for the 0.9 m and 1.8 m length transducers, respectively. Since the transducer will be a reactive load at other frequencies within the frequency band of interest, even in a tuned configuration, the power amplifier will be required to furnish increased volt-amperes over the tuned condition. At 300 Hz, the volt-amperes required equal 19 kva and 11 kva for the 0.9 m and 1.8 m length transducers, respectively.

TABLE 6

VOLT-AMPERES REQUIRED TO GENERATE 204 DB//μPAM SOURCE LEVEL
THROUGH 5700 M OF RG8/U COAXIAL CABLE FOR TUNED AND UNTUNED
HELMHOLTZ TRANSDUCER AT 400 HZ

Volt-Amperes (kva)

	Transducer Length (m)	
	0.9	1.8
UNTUNED	339	189
TUNED	112	108

It should be noted that the average power requirement for the system is low. The duty cycle for even a long pulse (0.25 sec) that may be used in transmitting phase-encoded information at a repetition rate of 1 pulse per 15 sec only equals 1.7%. At the tuned frequency, this represents an average power requirement to the transducer of 85 watts and 47 watts, respectively, for the 0.9 m and 1.8 m length units. With a short-pulsed cw signal (5 msec) at the same repetition rate, these average power requirements reduce to 1.7 watts and 0.9 watts, respectively, for the 0.9 m and 1.8 m transducer lengths.

Plans include expanding this initial assessment to refine the specific characteristics of the sound source before selecting the approach to be implemented. This includes evaluating the practical bandwidth achievable with the Helmholtz transducer from preshading the drive signal to obtain a flat transmitting response. Also, a more detailed assessment of the impulse type source (specifically, the cocked piston) is planned. The lack of source signature control for this type source may be overcome through data processing employing one of the techniques described earlier. This is true especially if the data can be processed based on a single shot-receiver sequence (CSP). If sufficient peak acoustic power can be achieved with the cocked piston approach, the low TW product would not pose a problem.

VII. STATIC SPATIAL SYSTEM TOW ANALYSIS

The initial tow analysis has focused on the static characteristics of placing and towing the system, array, and sound source package at a preselected depth. A comprehensive review of the steady-state tow analysis and a description of the analytical techniques employed is given by Milburn (1978).

This effort was based on specifying the system characteristics typical of those anticipated for the final configuration. Although the results are only an initial projection, they have provided an insight into the basic operational considerations imposed on deep towing the geophysical array system.

The first area addressed was determining the tow speed as a function of tow cable length at a specified tow depth and system characteristics. The steel tow cable employed for the analysis had the following characteristics: diameter 17.5 mm (0.69 in) and break strength 9300 kg (20,400 lb). The instrument fish and sound source/telemetry electronics had a weight in water of 545 kg (1200 lb); and the array tethered to the fish was 550 m (1804 ft) long, with a drogue chute attached to the tail. The results of this analysis are plotted in Figure 33 for desired tow depths

of 4 km and 6 km. Specifying a practical tow cable length limit of 9.15 km (30,000 ft), tow speeds of 0.77 m/sec (1.5 kn) and 1.26 m/sec (2.45 kn) at tow depths of 6 km and 4 km, respectively, are projected.

An option for increasing tow speed and maintaining the desired tow depth with a fixed tow cable length was explored through increasing the weight of the fish. A safety factor of 1.5 and a maximum tow cable length of 9.15 km (30,000 ft) was specified for the analysis. The analysis results for a desired tow depth of 6 km is presented in Figure 34. These results indicate that up to a tow speed of 0.77 m/sec (1.5 kn), additional cable is payed out to a maximum cable length of 9.15 km to maintain the desired tow depth. Above this speed the cable length is fixed at 9.15 km and the weight of the fish is increased up to a maximum tension at the ship equal to the 1.5 safety factor, with a resulting tow speed of 1.0 m/sec (1.95 kn). Although the weight of the fish, 3000 kg (6600 lb), may be excessive from a practical handling viewpoint and the safety factor may be low considering dynamic loads, this analysis does show an available option for increasing tow speed. A similar analysis for a tow depth of 4 km results in a tow speed of 1.54 m/sec (3 kn).

These types of analyses will be refined when more definitive characteristics of the deep-towed system are known. In addition, a dynamic analysis is planned to define the array spatial characteristics resulting from the dynamic forces acting on the fish/array/tow cable. This analysis will look at those system tow parameters which affect array deformation and will allow optimizing the tow configuration to minimize deformation.

VIII. PLANS

The plans for future development of the deep-towed geophysical array system are tabulated. These plans primarily reflect the effort for the next fiscal year (FY 1979) with a brief summary for the proposed completion of the total development.

● Compile more definitive subbottom models depicting ranges of anticipated subbottom characteristics on a major geophysical province basis to improve the performance prediction model.

● Refine the selected values of subbottom attenuation for a less conservative estimate through a more detailed review of available data.

● Generate synthetic seismic data for both reflection and refraction spreads - includes typical subbottom models, anticipated source wavelets, and environmental noise.

● Implement automatic velocity analysis (semblance routine) employing synthetic seismic data. Very deep tow configuration parameters and noise levels will be used to assess system parameter sensitivity for making interval velocity measurements. This effort will also be used to scope data acquisition hardware requirements for such areas as measuring array deformation.

● Review and recommend an optimum measurement/processing technique for extracting interval velocity and for generating high resolution depth sections with a deep-towed source/array system configuration. Includes: (1) accuracy tradeoffs to be considered for a CSP and CDP shooting configuration, (2) criticality of knowing array spatial position for each shot with CSP data and for each series of shots with CDP data, (3) array configuration consideration to assure spatial aliasing does not degrade data, and (4) defining improvements or degradation in meeting the measurement requirements that would result by including both a reflection and refraction spread.

• Recommend an automatic data processing (ADP) approach and estimate cost to process and display data obtained from the deep-towed geophysical array system. Includes: (1) a review of NORDA's present and planned ADP capability to meet the seismic processing requirement, (2) a review of advantages, limitations and cost to perform data processing by an outside commercial/government contractor, and (3) identifying processing (pre-processing) that could be performed practically at sea under the constraints of employing a micro-processor/minicomputer.

• Expand static tow analysis to predict array deformation for lumped buoyancy flotation distributed along the array aperture. Assess impact on meeting the system's measurement goals.

• Implement a dynamic spatial model to predict array deformation resulting from dynamic tow forces. Recommend an optimum tow configuration based on static and dynamic models to minimize array deformation.

• Perform a field measurement experiment with an existing horizontally towed array (365 m) capable of being towed at a depth of 2000 m to validate the performance prediction analysis. Although this array is not optimized for the geophysical application, basic array performance characteristics can be measured. These data, combined with multi-channel subbottom data, will allow more accurate prediction of the geoacoustic measurement accuracy and the deep-towed sound source acoustic requirements. The experimental objectives will be: (1) measurements of array noise levels as a function of array configuration, array tow depth, and array tow speed; (2) measurement of array deformation as a function of array configuration, array tow cable length, and array tow speed, (3) simultaneous collection of ship/array motion and cable tension data to allow dynamic performance prediction, and (4) collection of seismic profiling data employing the deep-towed array and different sound source types, such as near-surface towed sparker, near surface towed air gun, mid-water (244 m) SUS explosives, and deep-water (2440 m) SUS explosives.

• Define the operational and performance characteristics of the major system components based on the performance prediction analysis and field experimental results. The major components include: deep-towed sound source, hydrophones/preamplifiers, engineering sensors, telemetry system, power distribution system, data conditioning, system interfaces, pre-processing hardware, and data recording system.

• Generate a study report to management at the end of FY 1979 which will recommend to a total system implementation program. The report will review projected measurement capability, identify technical risk areas, recommend hardware configuration, recommend an ADP approach, define program schedule, and estimate program cost. Based on this report, a proposed completion could be as follows:

Fabricate sound source system and field test with existing horizontal towed array.

Fabricate optimized geophysical array, data acquisition, and recording system. Interface with sound source system.

Field tests complete deep-towed geophysical array system in well-defined geoacoustical area and assess measurement performance. Generate final development program report reviewing the performance capability.

IX. SUMMARY

This report has reviewed the progress during Fiscal Year 1978 on the Deep-Towed Geophysical Array Development Program. Included was a review of the identified geoacoustic measurement requirement that this development is addressing.

The design approach being pursued has been through the development of a performance prediction model for a deep-towed source/multichannel array configuration. The model includes: a subbottom multi-layer acoustic model, a ray trace capability for reflected and refracted arrivals, and a sonar equation and spatial model to address amplitude and arrival time variables. The capability to compute interval velocities employing the Dix interval velocity equation has been incorporated into the model. The status of the performance model was reviewed for deficiencies and planned improvements were identified.

Since the deep-towed configuration is a translation of the marine oil exploration industry's near-surface geometry, a review of their techniques for extracting velocity information was performed. The review included basic environmental and operational considerations for extracting velocity data and contrasted these considerations to the deep-towed configuration.

An initial sensitivity analysis of system configuration parameters (array length, offset, and altitude) on extracting interval velocity within the constraints of the existing performance prediction model was performed. The resulting identified parameters were: array length, 500 m; offset, 50 m; and altitude, 200 m. The analysis also showed the criticality of array deformation in performing interval velocity measurements and identified the requirement to perform field measurements with an existing array to better define array deformation.

The results of a sonar equation analysis provided an initial estimate for defining the basic sonar requirements of a deep-towed sound source. Although the noise levels for a deep-towed configuration need refinement, the analysis results did provide the basic input for performing an assessment of available technology for a high-power, low-frequency, deep-towed acoustic source. The assessment resulted in defining a candidate approach employing a Helmholtz resonator type source with the following characteristics: source level, 204db//μpam; frequency, 400 Hz; bandwidth, 200 Hz; size, 0.5 m diameter x 0.9 m long; and weight (air), 500 kg.

A static tow analysis was performed to establish the tow system characteristics for placing the source/array system at a preselected depth. The analysis results indicate that for projected system component characteristics, tow speeds up to 3 kn at a tow depth of 4 km can be achieved. The requirement to perform a dynamic tow analysis was identified to predict array deformation characteristics resulting from the dynamic tow forces.

Finally, the plans for continued development of the deep-towed system were reviewed. The effort during FY 1979 will be a combination of performance prediction modeling and experiment validation. The results of this effort will be a report recommending to management a complete system implementation program with the projected measurement capability identified. The report will also recommend the at-sea data acquisition hardware requirements and the data processing requirements to extract desired geoacoustic parameters.

X.   REFERENCES

Ballard, J. Alan (1977). Interpretation of Single-Channel Seismic Reflection Records. Naval Ocean Research and Development Activity, NSTL Station, MS, NORDA Report 1.

Bryan, George M. (1974). Sonobuoy Measurements in Thin Layers. In: Physics of Sound in Marine Sediments, Lloyd Hampton (ed.), New York, Plenum Press.

Clay, C.S. and Peter A. Rona (1965). Studies of Seismic Reflections from Thin Layers on the Ocean Bottom in the Western North Atlantic. Geophysics, v. 70, n. 4, p. 855-869.

Cook, Ernest E. and Turhan M. Taner (1969). Velocity Spectra and Their Use in Stratigraphic and Lithologic Differentation. Geophysical Prospecting, v. 17, p. 433-448.

Dix, Hewitt C. (1955). Seismic Velocities from Surface Measurements. Geophysics, v. 20, n. 1, p. 68-86.

Fagot, Martin G. (1978). Marine Seismic Display Enhancement Program, Final Report, Volume 1: Results. Naval Ocean Research and Development Activity, NSTL Station, MS, NORDA Technical Note 13.

Gerritsma, P. H. A. (1977). Time-to-Depth Conversion in the Presence of Structure. Geophysics, v. 42, n. 4, p. 760-772.

Green, C. H. (1938). Velocity Determination by Means of Reflection Profiles. Geophysics, v. 3, p. 295-305.

Groves, E.D. (1978). Deep Tow Low Frequency Sound Source Technology Assessment. NRL/USRD Ref. 8277:AMY:dab, 16 June (unpublished).

Hamilton, Edwin L. (1974). Geoacoustic Model of the Sea Floor. In: Physics of Sound in Marine Sediments, Lloyd Hampton (ed.), New York, Plenum Press.

Hamilton, Edwin L. (1976). Sound Attenuation as a Function of Depth in the Sea Floor. J. Acoust. Soc. Am., v. 59, n. 3, p. 528-535.

Hamilton, Edwin L. (1978). Sound Velocity-Density Relations in Sea Floor Sediments and Rocks. J. Acoust. Soc. Am., v. 63, n. 2, p. 366-377.

Kramer, F.S., R.A. Peterson, and W.C. Walter (eds.) (1968). Seismic Energy Sources Handbook. Presented at the 38th Annual Meeting of the Society of Exploration Geophysicists, Denver, Colorado, October.

Le Pichon, Xavier, John Ewing and Robert E. Houtz (1968). Deep-Sea Sediment Velocity Determinations Made While Reflection Profiling. J. Geophys. Res., v. 73, n. 8, p. 2597-2614.

Levin, Franklyn K. (1977). Vertical Stacking as a Reflection Filter. Geophysics, v. 42, n. 5, p. 1045-1047.

Matthews, James E. and Troy L. Holcombe (1976). Regional Geological/ Geophysical Study of the Caribbean Sea (Navy Ocean Area NA-9). Naval Oceanographic Office, Publication NOO-RP3.

Maynard, G. L., G.H. Sutton, D.M. Hussong, and L.W. Kroenke (1974). The Seismic Wide Angle Reflection Method in the Study of Ocean Sediment Velocity Structure. In: Physics of Sound in Marine Sediments, Lloyd Hampton (ed.), New York, Plenum Press.

Mero, Thomas N. and John Freitag (1974). Seismic Source Signature Analysis. U.S. Naval Oceanographic Office, Technical Note 6222-5-74, 29 p. (unpublished).

Milburn, Darrell and Martin Fagot (1979). Steady-State Analysis of Candidate Tow Cables for a Deep Tow Geophysical Array System. Naval Ocean Research and Development Activity, NSTL Station, MS, NORDA Technical Note 40 (in press).

Neidell, N.S. and Turhan M. Taner (1971). Semblance and Other Coherency Measures for Multi-Channel Data. Geophysics, v. 36, n. 3, p. 482-497.

Officer, C.B. (1958). Introduction to the Theory of Sound Transmission. New York, McGraw-Hill Book Co., 284 p.

Rutherford, Steven R. (1976). Analytical Techniques for Determining Sub-Bottom Velocity Profiles in Unconsolidated Sediments. Applied Research Laboratory, Univ. of Texas at Austin, Report No. ARL-TR-76-68, 95 p.

Sattlegger, Johann (1965). A Method of Computing True Interval Velocities from Expanding Spread Data in the Case of Arbitrary, Long Spreads, and Arbitrary Dipping Plane Interfaces. Geophysical Prospecting, v. 13, p. 306-318.

Savit, Carl H. and Lee E. Siems (1977). A 500-Channel Streamer System. Presented at the 1977 Offshore Technology Conference, Houston, TX, Preprint No. OTC 2833.

Schneider, William A. (1971). Developments in Seismic Data Processing and Analysis (1968-1970). Geophysics, v. 36, n. 6, p. 1043-1073.

Sheriff, Robert E. and Tona A. Lauhoff (1977). Marine Geophysical Exploration: The State of the Art. IEEE Transactions on Geoscience Electronics, v. GE-15, no. 2.

Sherwood, J.W.C. and P.H. Poe (1972). Continuous Velocity Estimates and Seismic Wavelet Processing. Geophysics, v. 37, No. 5, p. 769-787.

Stoll, Robert D. (1977). Acoustic Waves in Ocean Sediments. Geophysics, v. 42, n. 4.

Taner, Turhan M., Ernest E. Cook, and Norman S. Neidell (1970). Limitations of the Reflection Seismic Method; Lessons from Computer Simulation. Geophysics, v. 35, n. 4, p. 551-573.

Taner, Turhan M. and Fulton Koehler (1969). Velocity Spectra - Digital Computer Derivation and Applications of Velocity Functions. Geophysics, v. 34, n. 6, p. 859-881.

Urick, R.J. (1974). Underwater Sound Transmission through the Ocean Floor. In: Physics of Sound in Marine Sediments, Lloyd Hampton (ed.), New York, Plenum Press.

Urick, R.J. (1975). Principles of Underwater Sound, Second Edition. New York, McGraw-Hill Book Co.
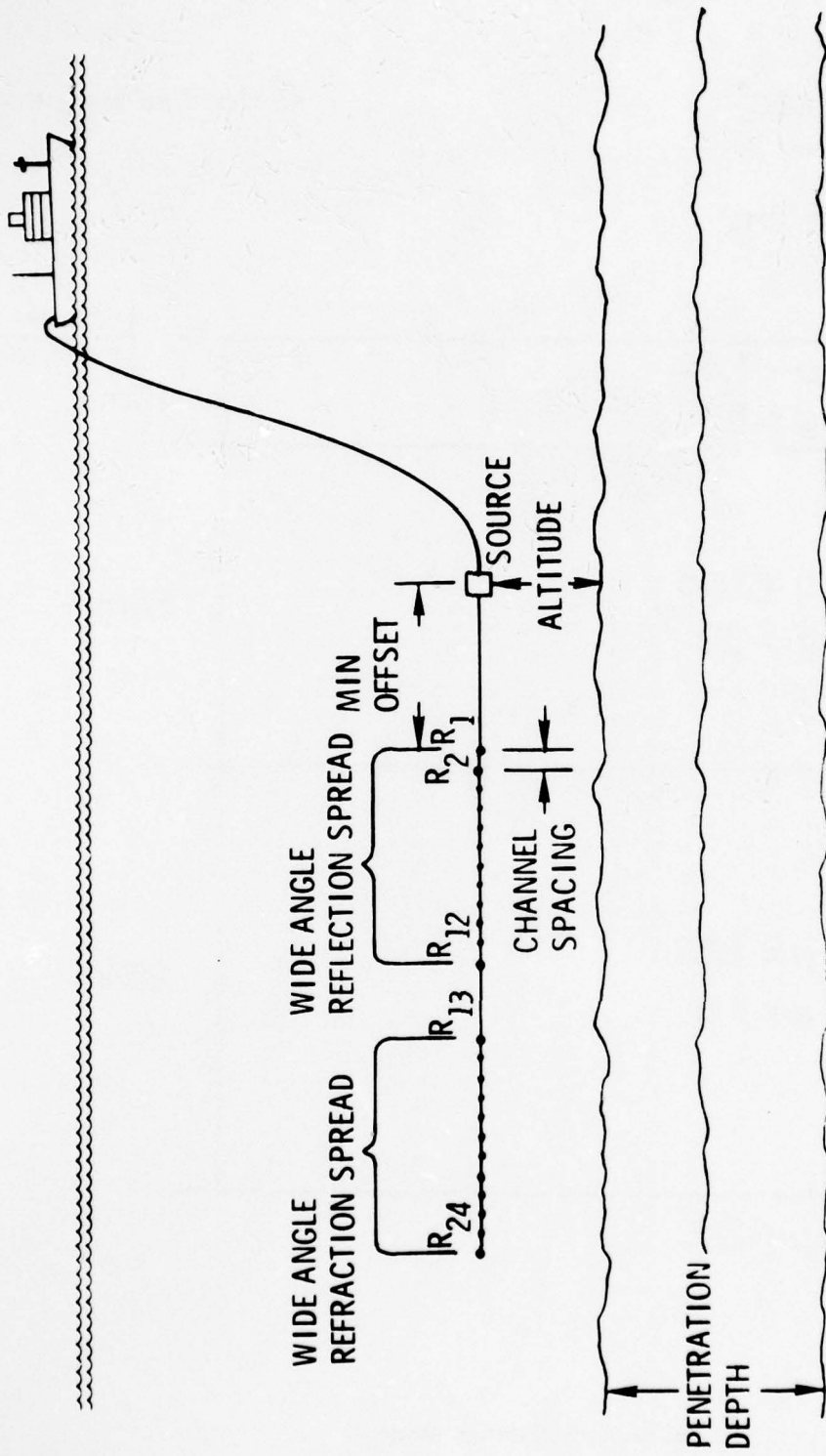
Figure 1. Concept configuration for deep-towed geophysical profiling system

c = 1546.6 m/sec

g = 0.017 sec^{-1}

p = 1.0517 gm/cm^3

$*$ *Modified Hamilton*

WATER

SUB-BOTTOM

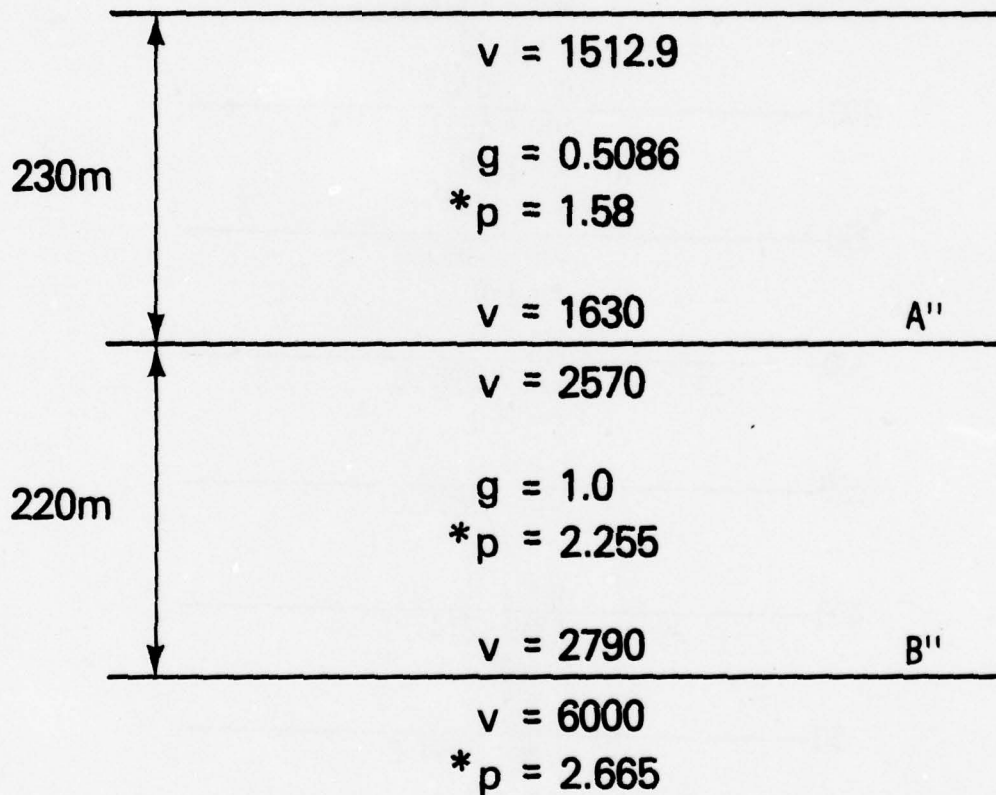c = 1539   p = 1.44

c = 1549   g = 1.0

10m

c = 1545

p = 1.45

g = 1.0

50m

c = 1595

c = 1598

p = 1.63

g = 1.0

180m

c = 1778

c = 5700   p = 2.6
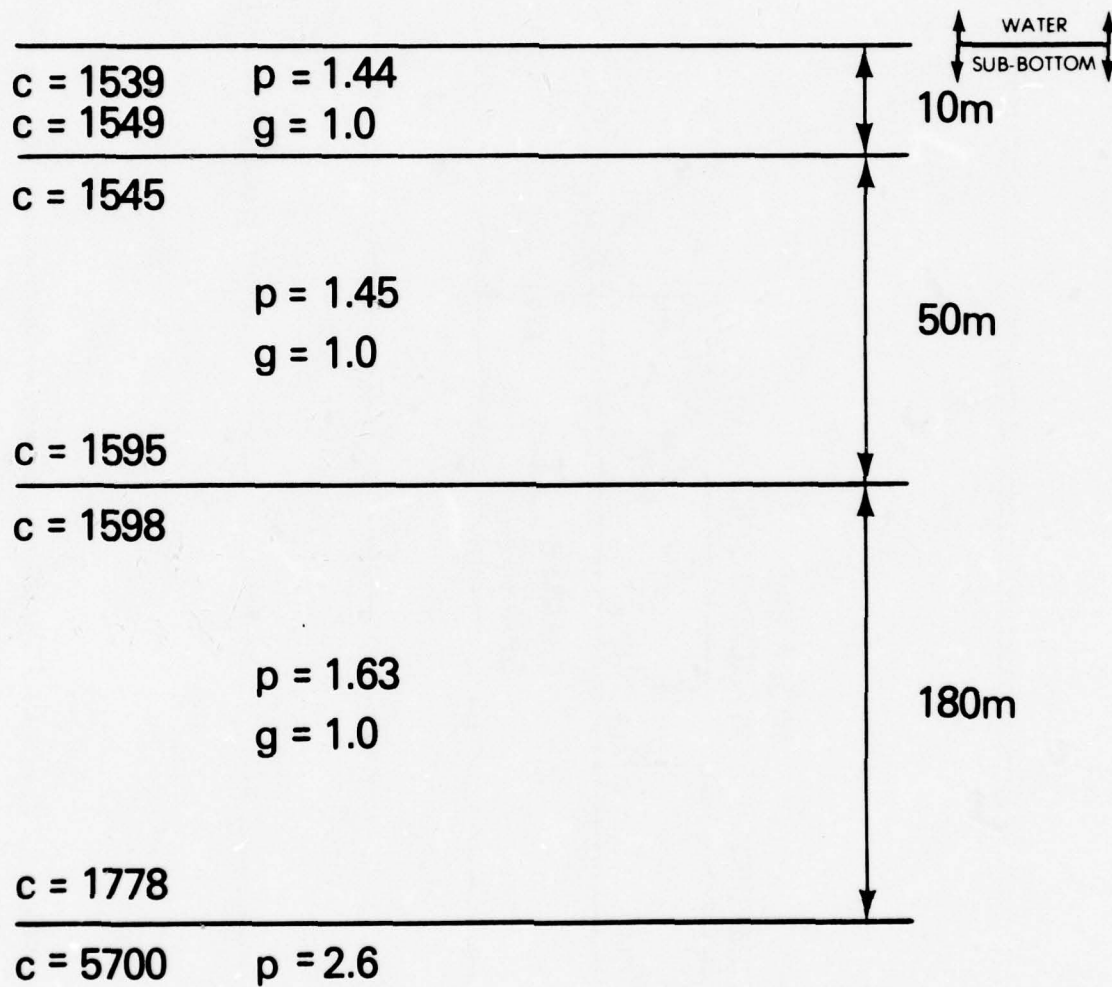
Figure 2. Subbottom Model 1

SUB - BOTTOM
MODEL B

(CENTRAL VENEZUELAN BASIN)

WATER: v = 1536 m/sec

g = 0.017 sec^{-1}

p = 1.0517 gm/cm^3

230m
v = 1512.9

g = 0.5086

*p = 1.58

v = 1630   A''

v = 2570

220m
g = 1.0

*p = 2.255

v = 2790   B''

v = 6000

*p = 2.665

*From: E. Hamilton
JASA 63(2), Feb. 1978
p. 366-377

Figure 3. Subbottom Model B
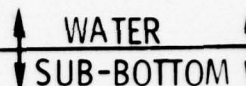
LAYER SUB-BOTTOM DEPTH (m)

$V_m = 1498.3$ m/sec
$\rho = 1.0517$ gm/cm^3
$g = 0.017$ sec^{-1} ↕ WATER
0 ——————————————————————————————— ↕ SUB-BOTTOM
$V_m = 1525.6$
1            $\rho = 1.18$
            $g = .5086$
50 ——————————————————————————————
            $V_m = 1551.0$
2            $\rho = 1.28$
            $g = .5086$
100 ——————————————————————————————
            $V_m = 1576.4$
3            $\rho = 1.38$
            $g = .5086$
150 ——————————————————————————————
            $V_m = 1601.9$
4            $\rho = 1.48$
            $g = .5086$
200 ——————————————————————————————
            $V_m = 1627.3$
5            $\rho = 1.58$
            $g = .5086$ A''
250 ——————————————————————————————
            $V_m = 2595.0$
6            $\rho = 1.9$
            $g = 1.0$
300 ——————————————————————————————
            $V_m = 2645.0$
7            $\rho = 2.0$
            $g = 1.0$
350 ——————————————————————————————
            $V_m = 2695.0$
8            $\rho = 2.1$
            $g = 1.0$
400 ——————————————————————————————
            $V_m = 2745.0$
9            $\rho = 2.2$
            $g = 1.0$
450 ——————————————————————————————
            $V_m = 2795.0$
10            $\rho = 2.3$
            $g = 1.0$ B''
500 ——————————————————————————————
            $V = 6000$
11            $\rho = 2.665$

Figure 4. Subbottom Model C
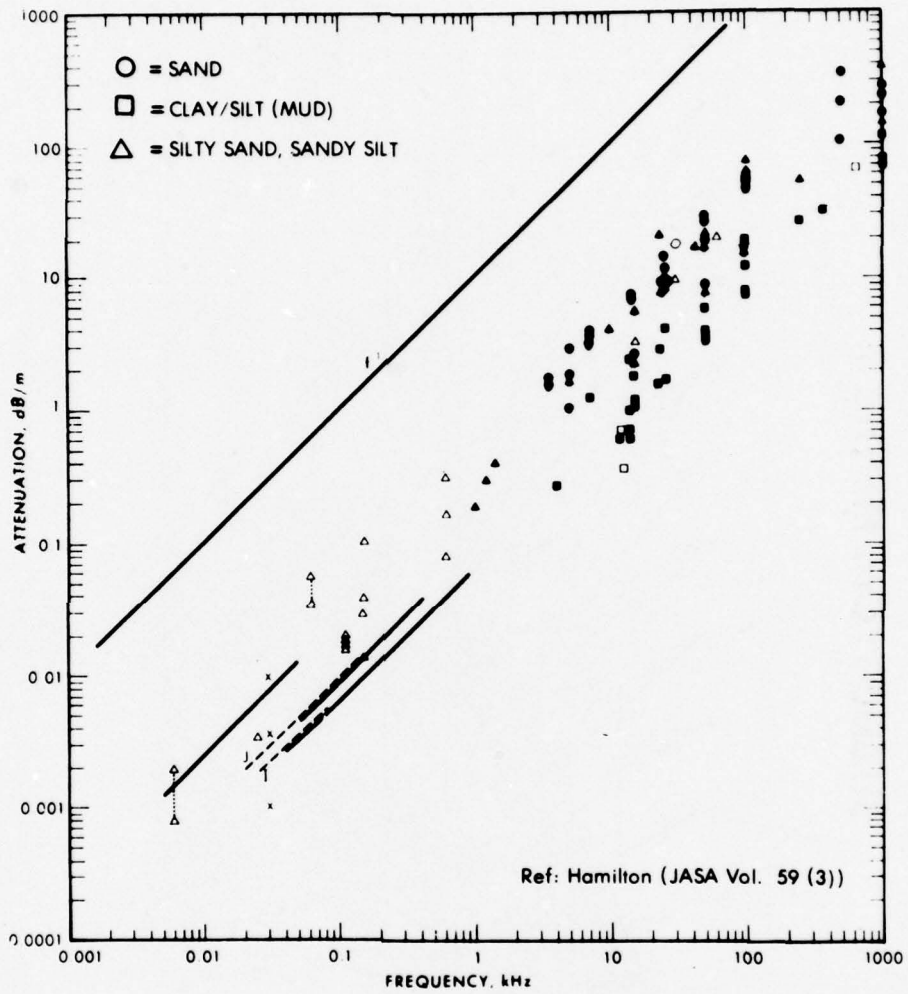
Figure 5. Effective absorption (after Hamilton, 1976)

500 METER ARRAY/12 PHONES/200 METER ALTITUDE
SUBBOTTOM MODEL 1
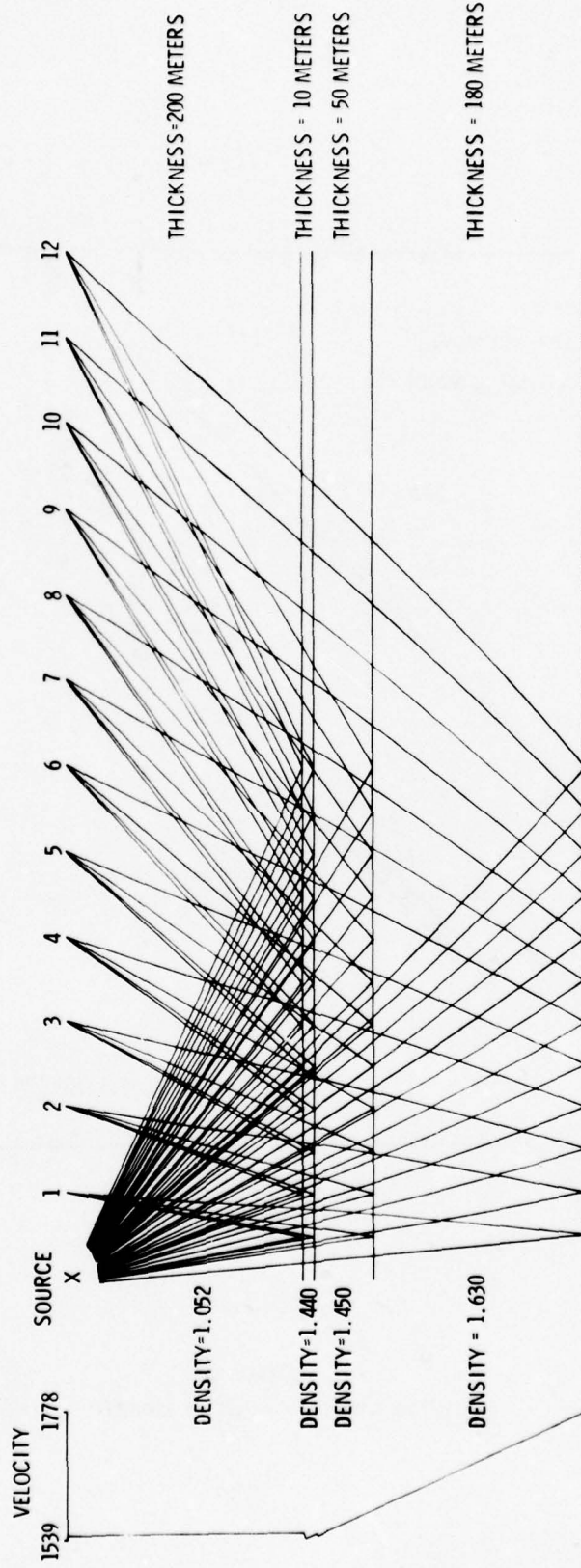
Figure 6.   Reflection ray trace for 500 m array and subbottom model 1

500 METER ARRAY/12 PHONES/200 METER ALTITUDE
SUBBOTTOM MODEL 1
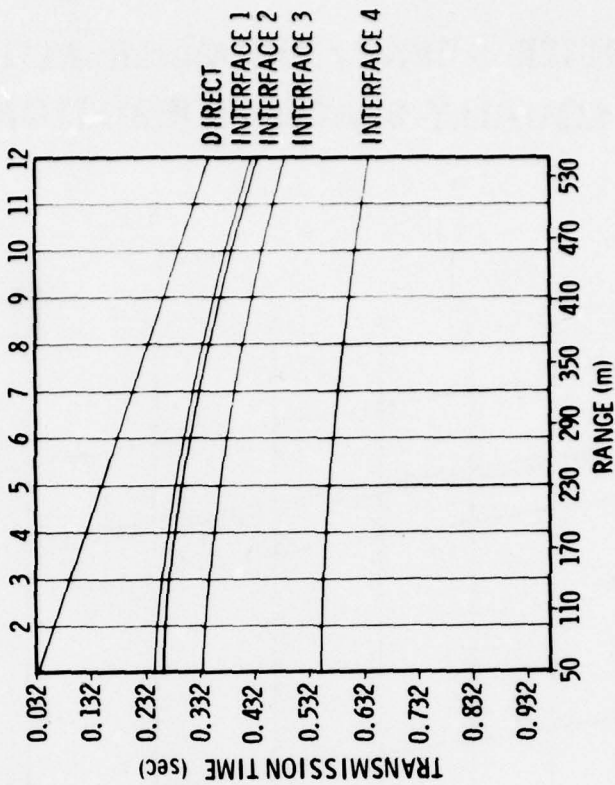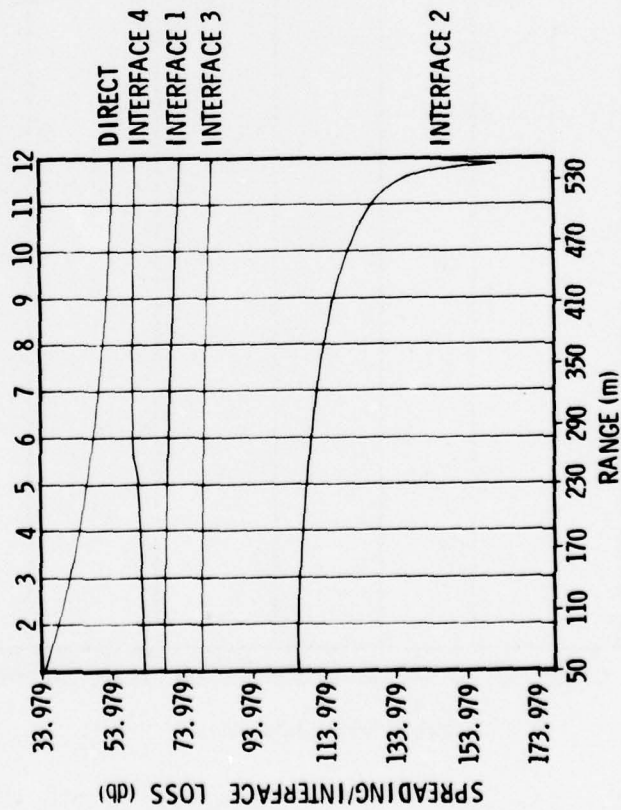
Figure 7. Spreading/interface loss and transmission time plot for 500 m array and subbottom model 1 (ref. Fig. 6)

500 METER ARRAY/200 METER ALTITUDE
12 PHONES EQUALLY SPACED/SUBBOTTOM MODEL 1
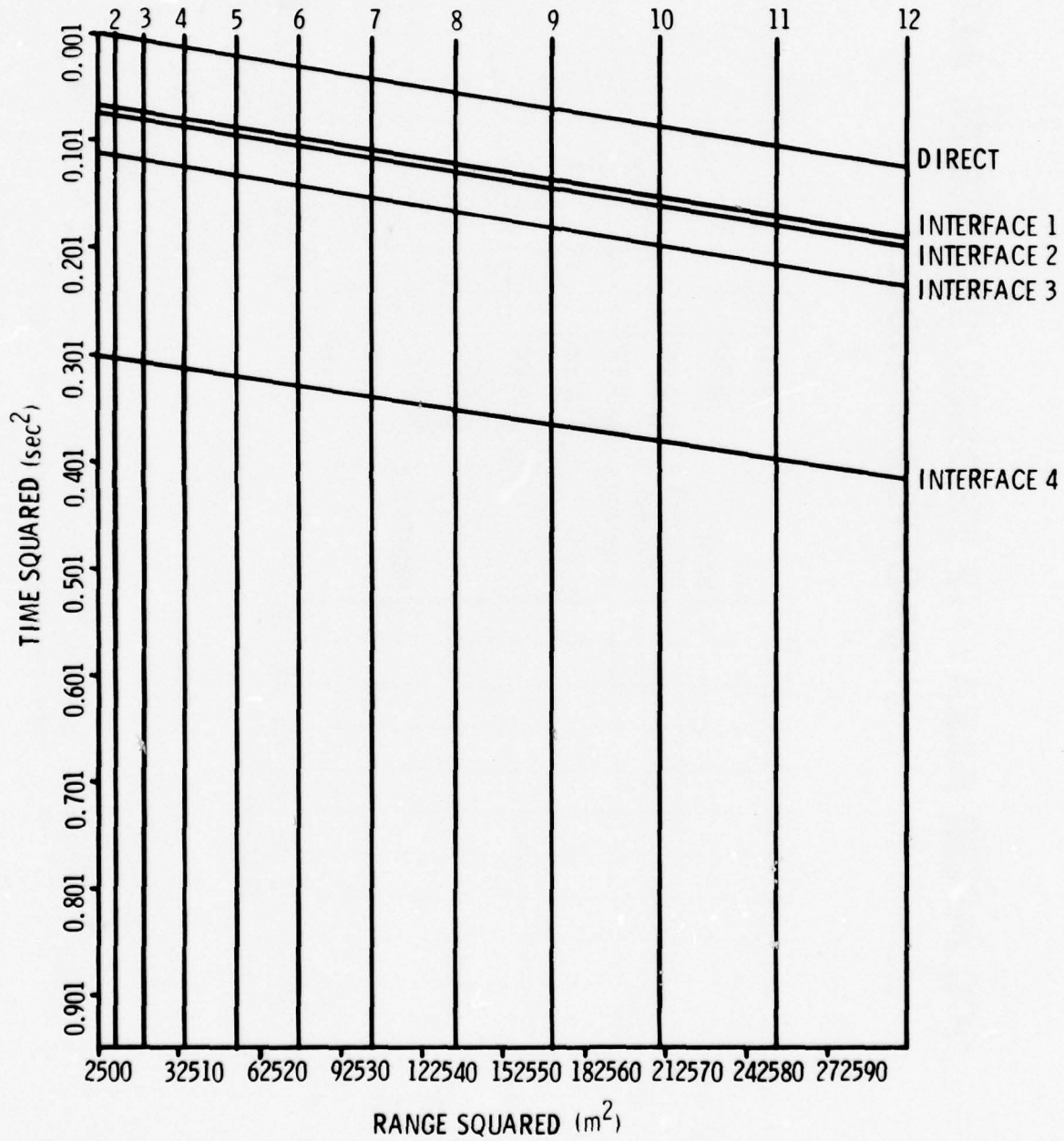
Figure 8. $T^2 - X^2$ plot for 500 m array and subbottom model 1 (ref. Fig. 6)
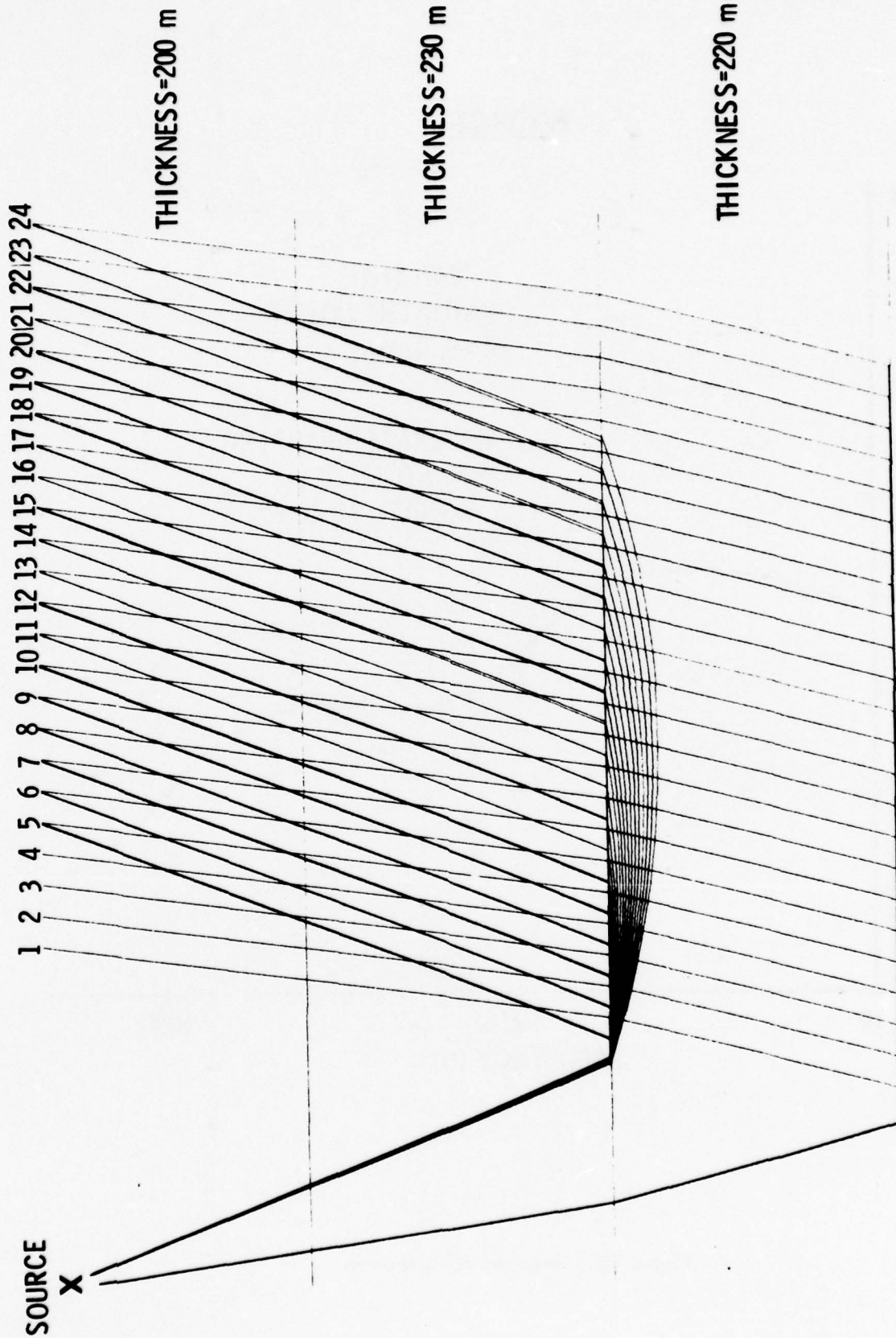
Figure 9. Head wave/diving wave refraction ray trace for 1045 m array and 500 m offset employing subbottom model B

41
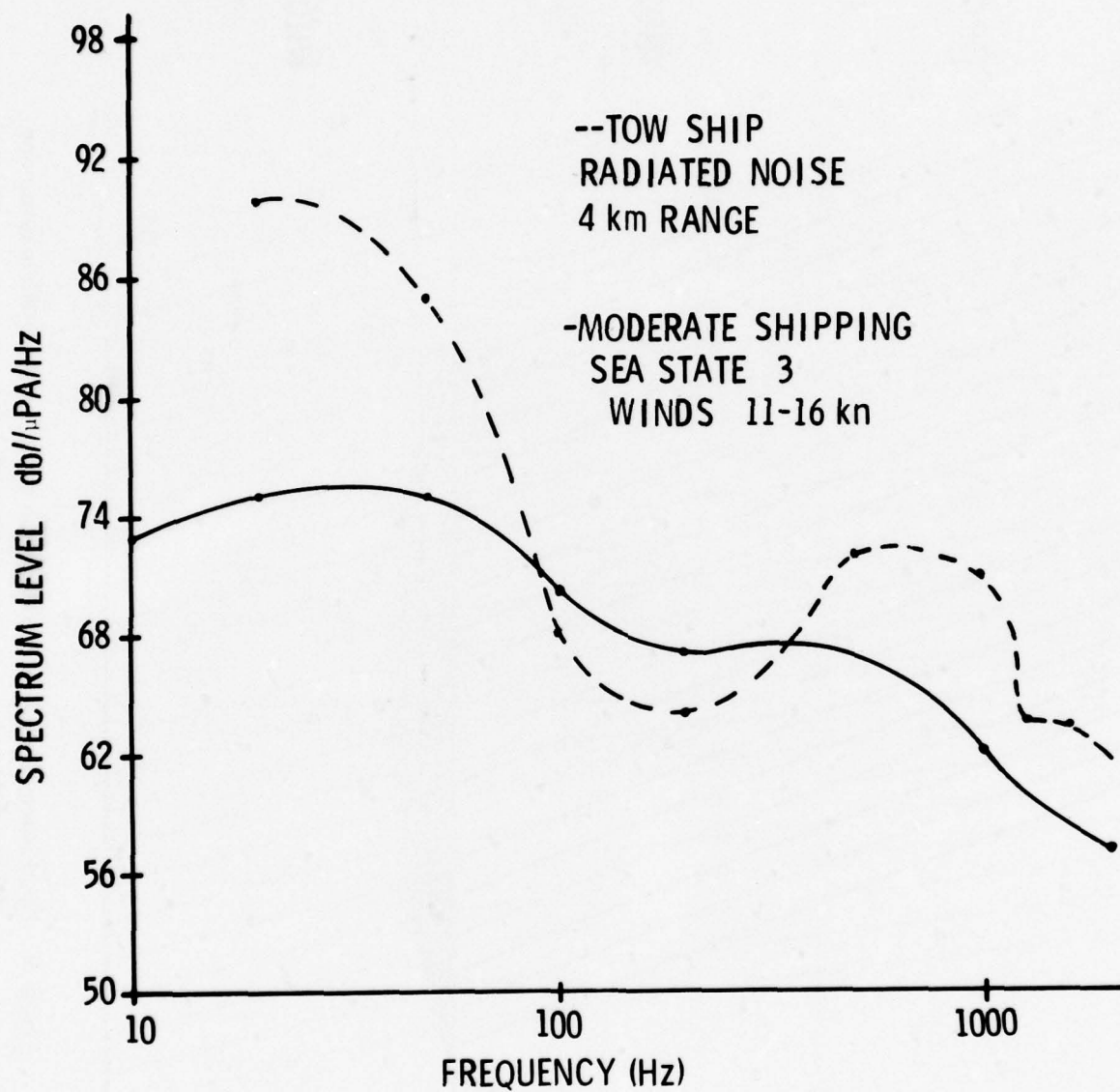
NOISE

Figure 10. Deep sea noise spectra

42

ARRAY LENGTH	500 m	SOURCE LEVEL	204 db//μPAM
OFFSET	50 m	NOISE LEVEL	70 db//μPA/Hz
ALTITUDE	200 m	BANDWIDTH	200 Hz
		FREQUENCY	400 Hz
		ABSORPTION	.033 db/m
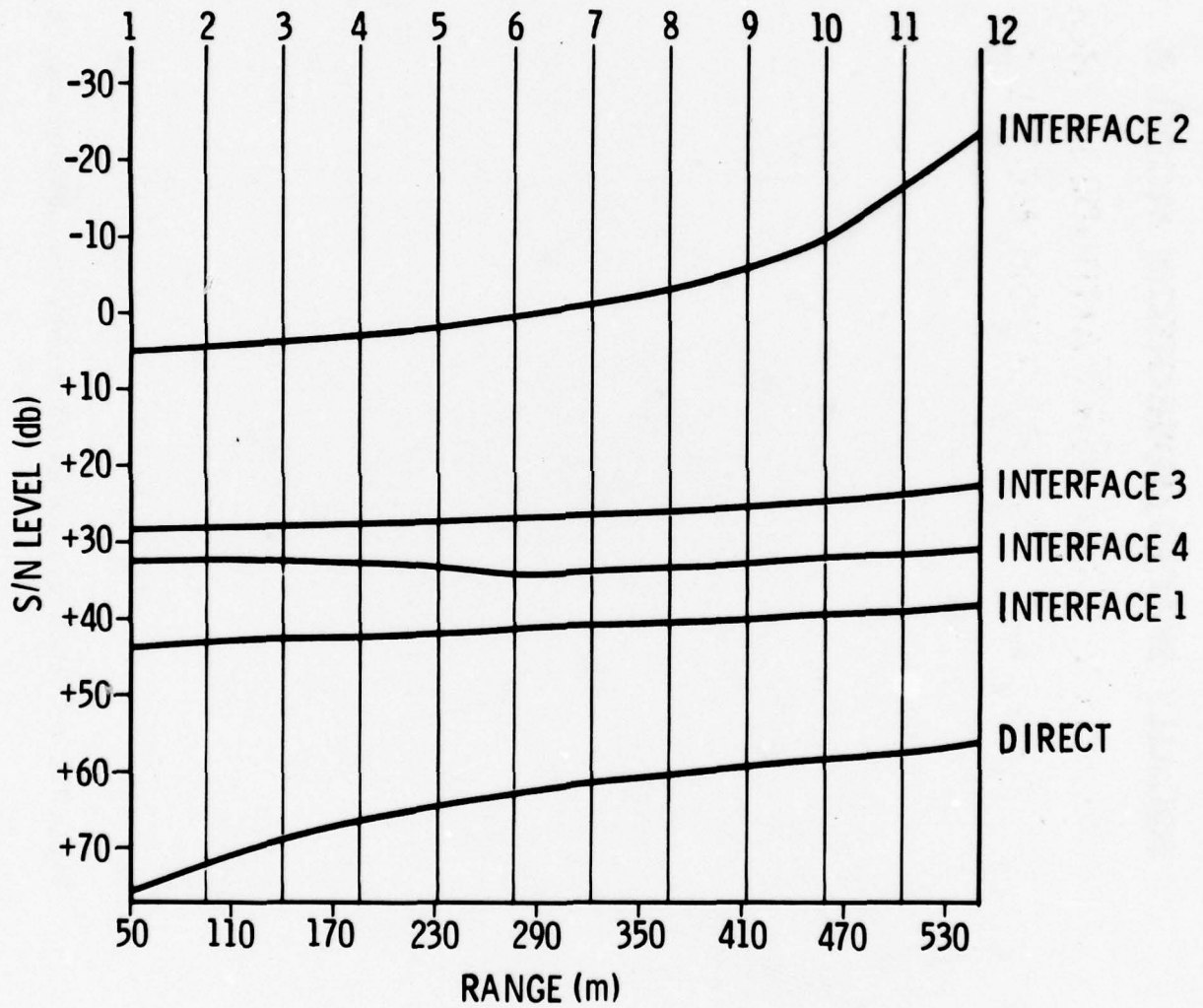
Figure 11. S/N level plot for 500 m array and deep towed sound source employing subbottom model 1

43

500 METER ARRAY/200 METER ALTITUDE 12 PHONES
EQUALLY SPACED/SUBBOTTOM MODEL B

THICKNESS=200 m
METERS

THICKNESS=230 m
METERS

THICKNESS=220 m
METERS

SOURCE
X

1 2 3 4 5 6 7 8 9 10 11 12
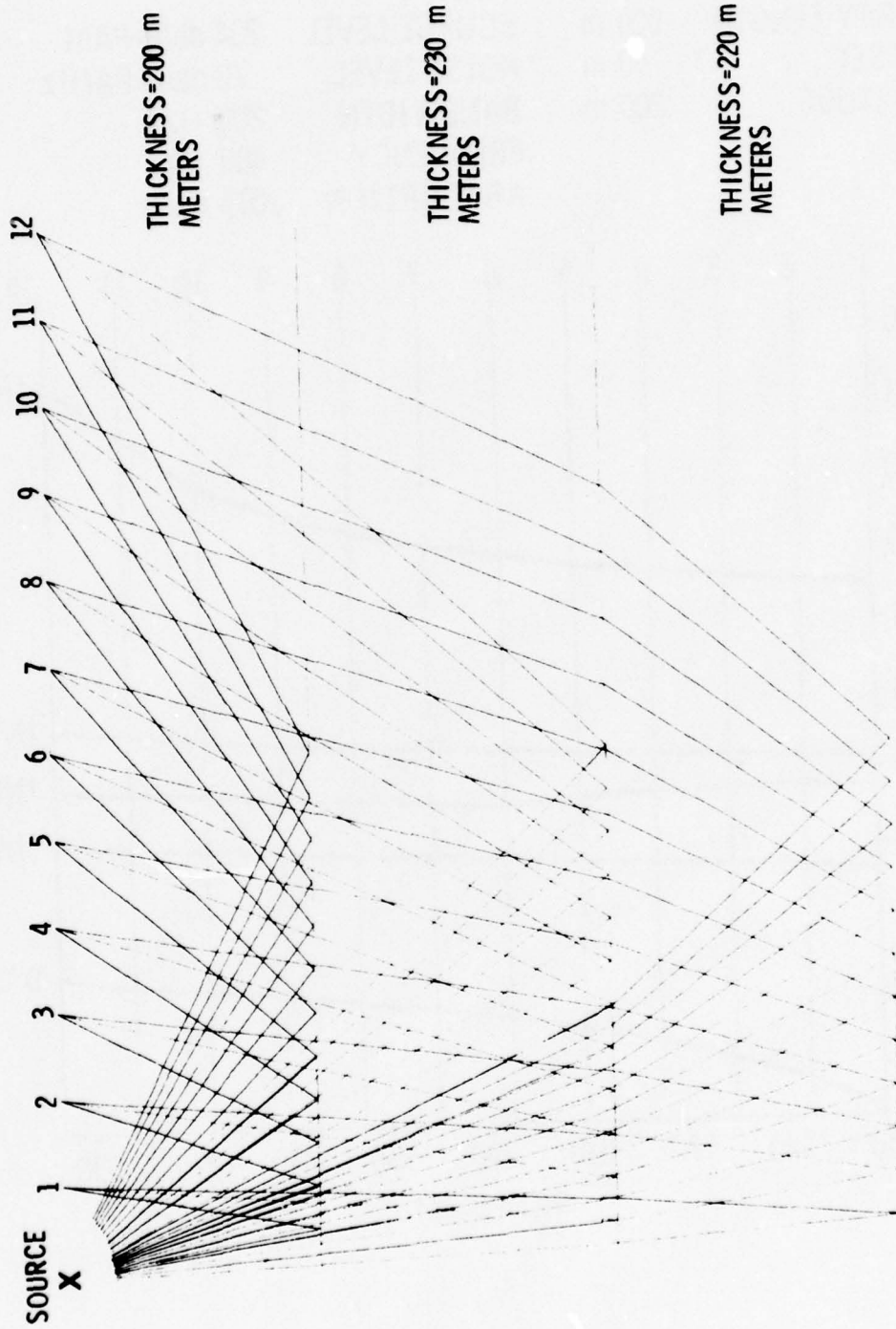
Figure 12. Reflection ray trace for 500 m array and subbottom model B

310 METER ARRAY/32 PHONES EQUALLY SPACED
SUBBOTTOM MODEL 1 /200 METER ALTITUDE
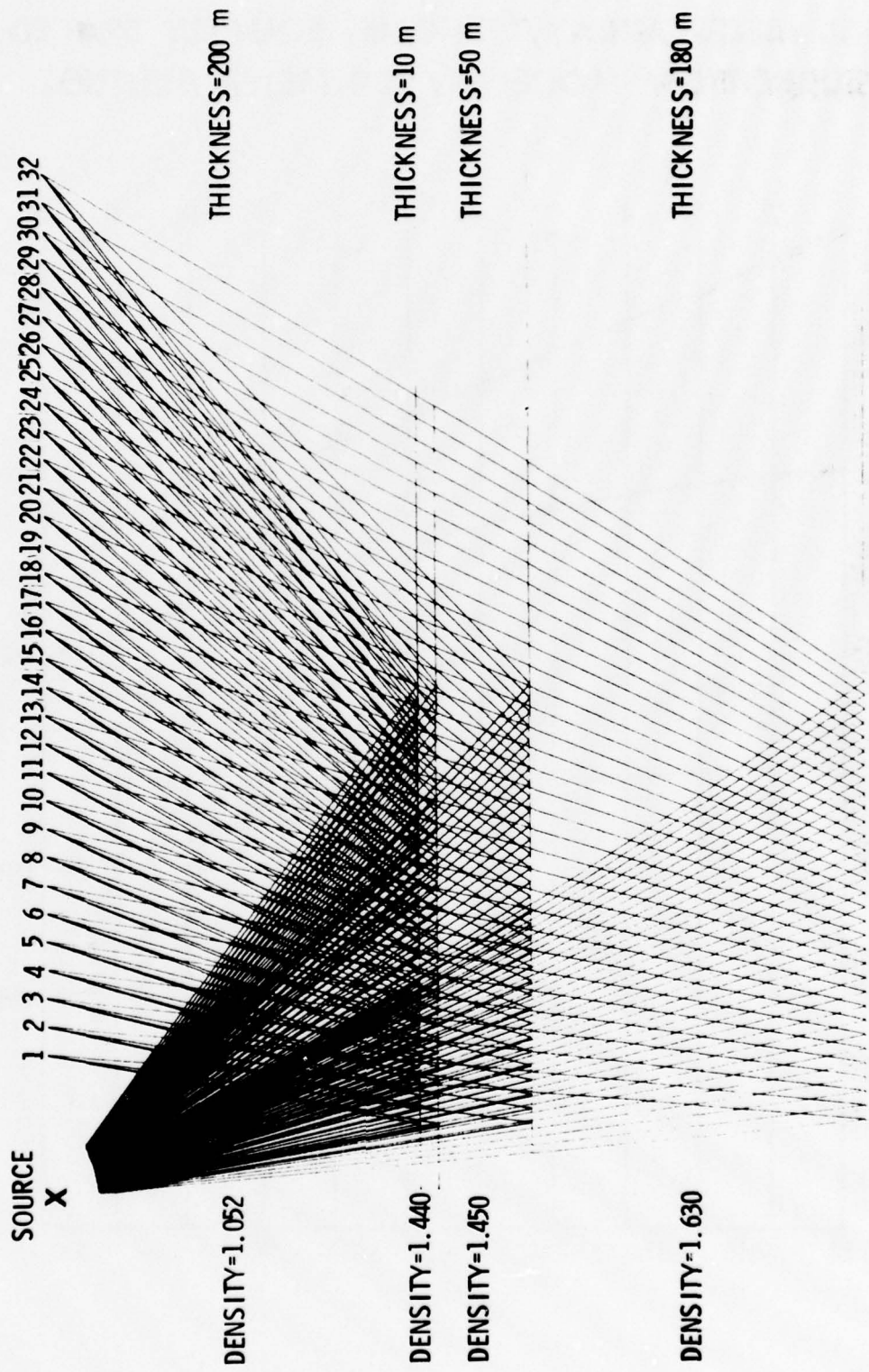
Figure 13. Reflection ray trace for 310 m array and subbottom model 1

500 METER ARRAY/12PHONES EQUALLY SPACED
SUBBOTTOM MODEL B / 200 METER ALTITUDE
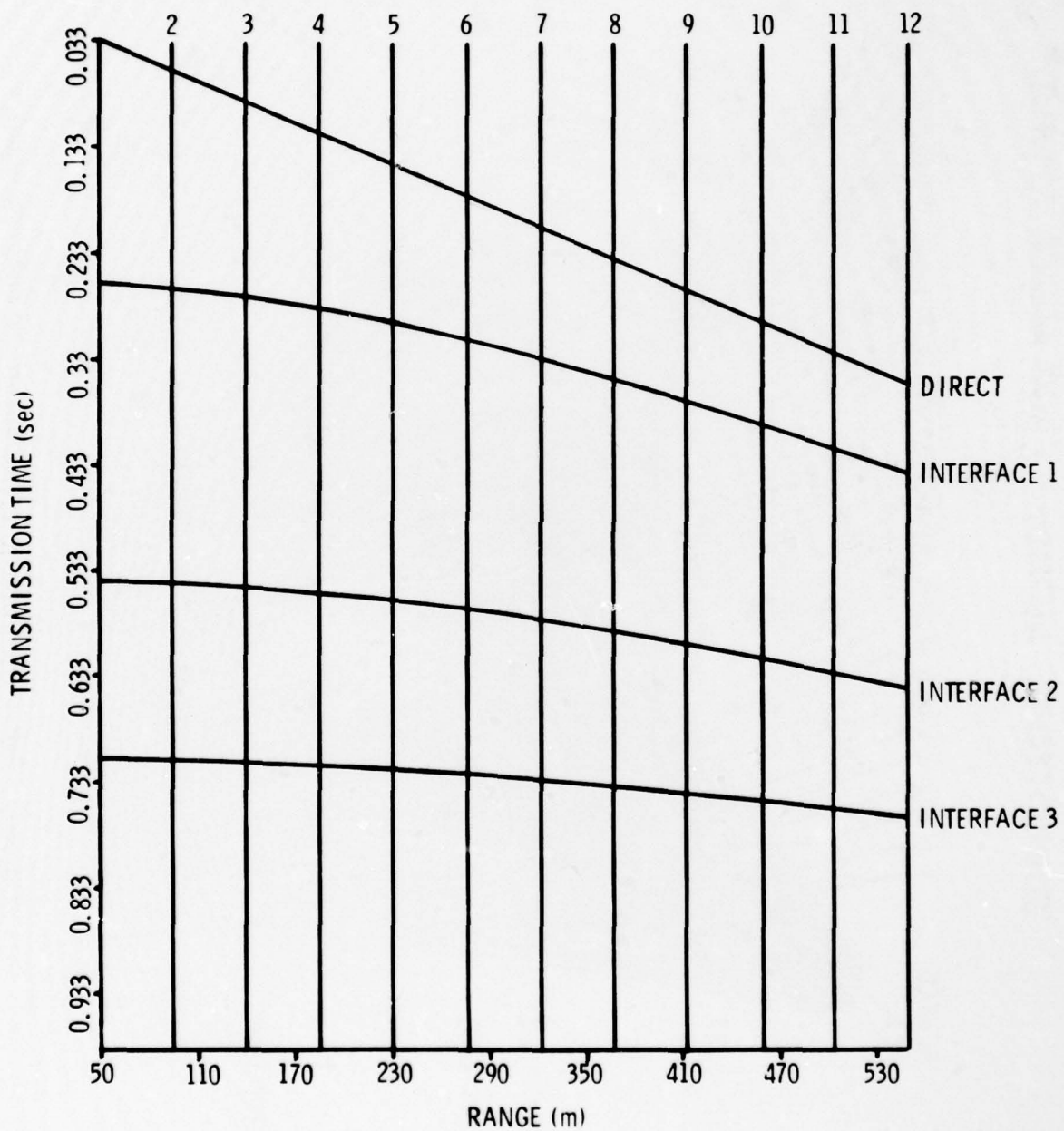
Figure 14. Transmission time plot for 500 m array and subbottom model B
(ref. Fig. 12)

310 METER ARRAY/32 PHONES EQUALLY SPACED
SUBBOTTOM MODEL 1 /200 METER ALTITUDE
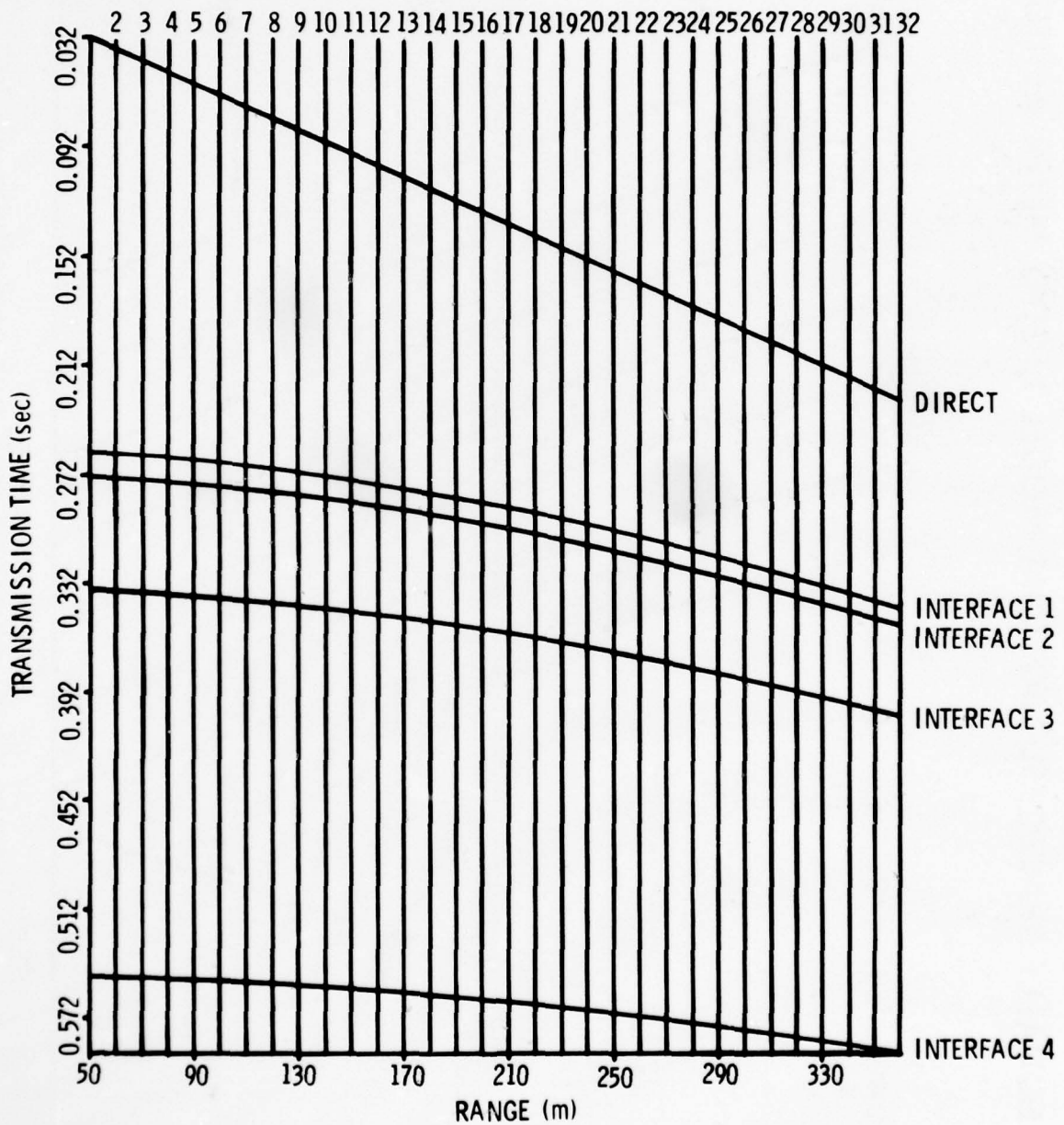
Figure 15. Transmission time plot for 310 m array and subbottom model 1 (ref. Fig. 13).

500 METER ARRAY/12 PHONES

EQUALLY SPACED/SUBBOTTOM MODEL 1/200 METER ALTITUDE

THICKNESS=200 m

THICKNESS=10 m

THICKNESS=50

THICKNESS=180 m

SOURCE 1 2 3 4 5 6 7 8 9 10 11 12
X
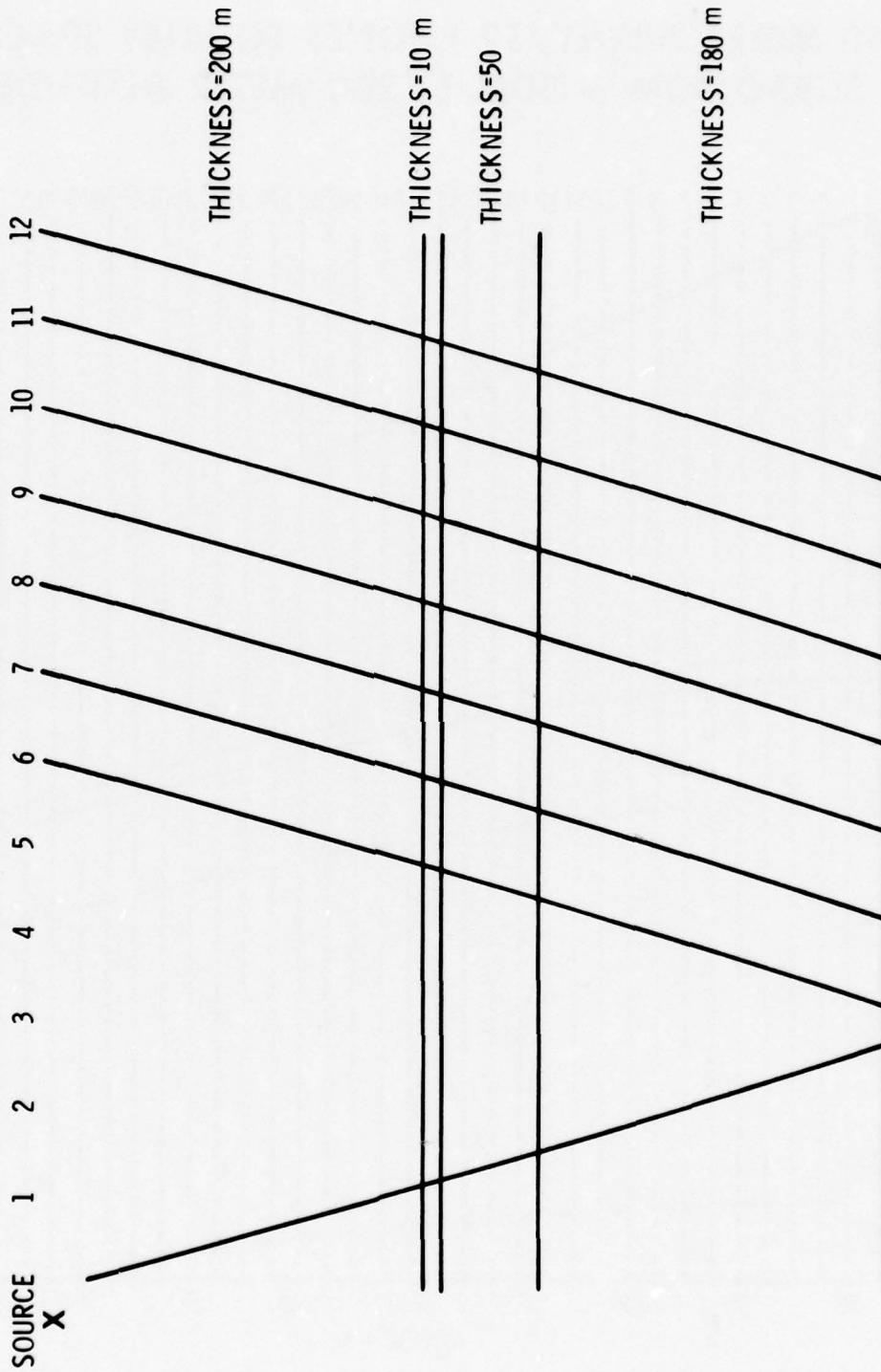
Figure 16. Head wave ray trace for 500 m array and subbottom model 1
(ref. Fig. 6)

NORMAL MOVEOUT CORRECTION PLOT
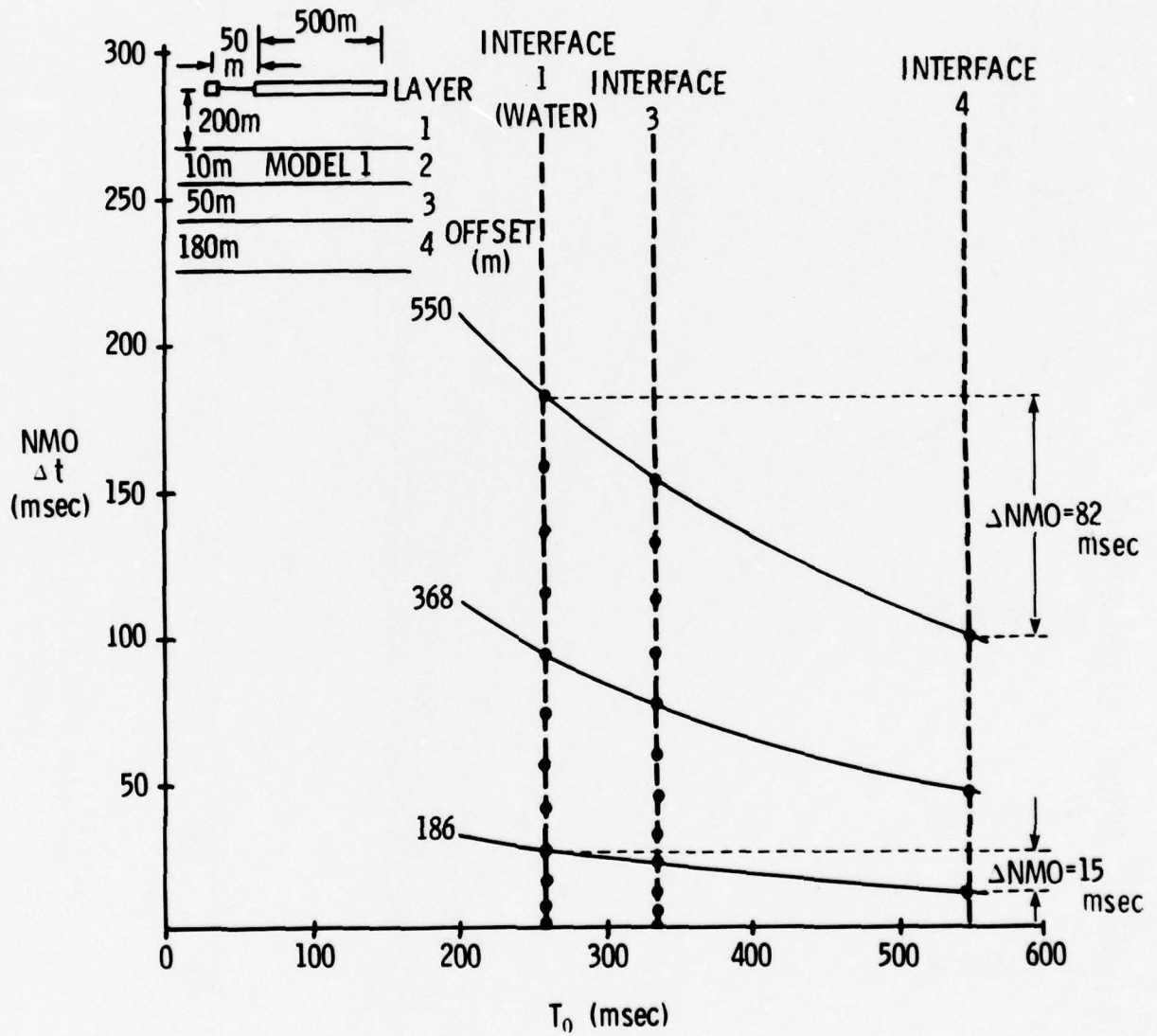
Figure 17. Normal moveout correction plot for 500 m array and subbottom model 1 (ref. Fig. 6)
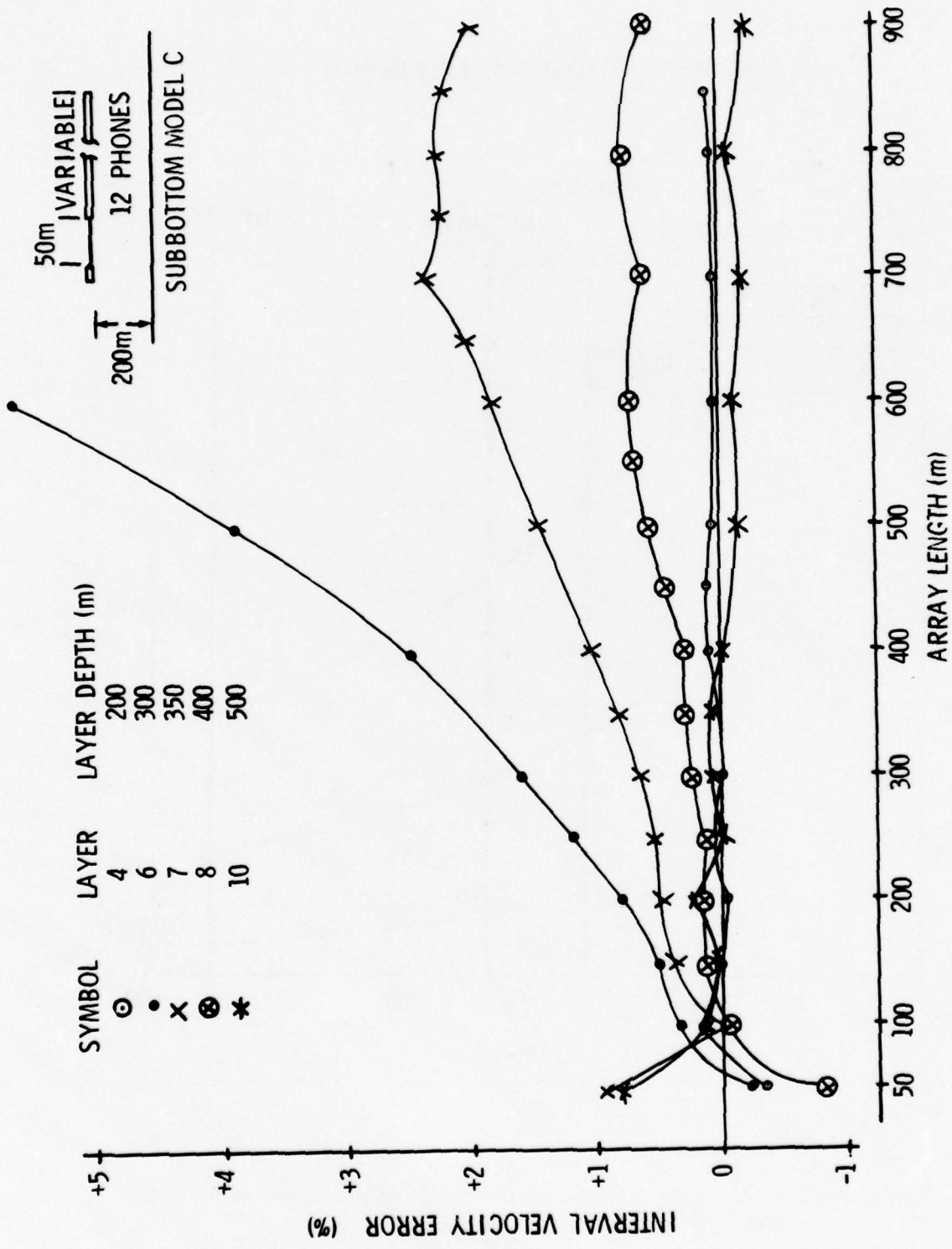
Figure 18. Interval velocity error as a function of array length for subbottom model C
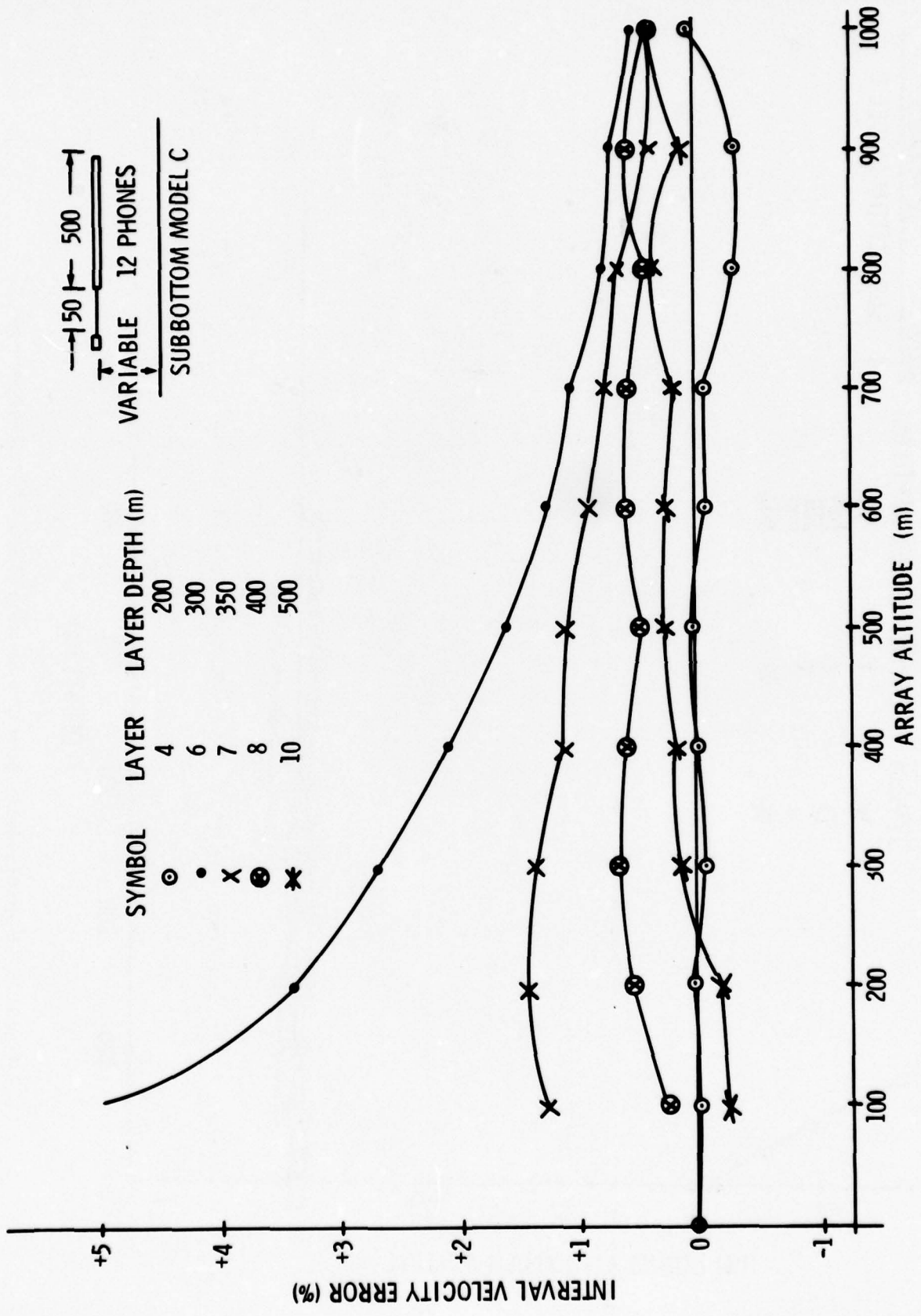
Figure 19. Interval velocity error as a function of array altitude for subbottom model C
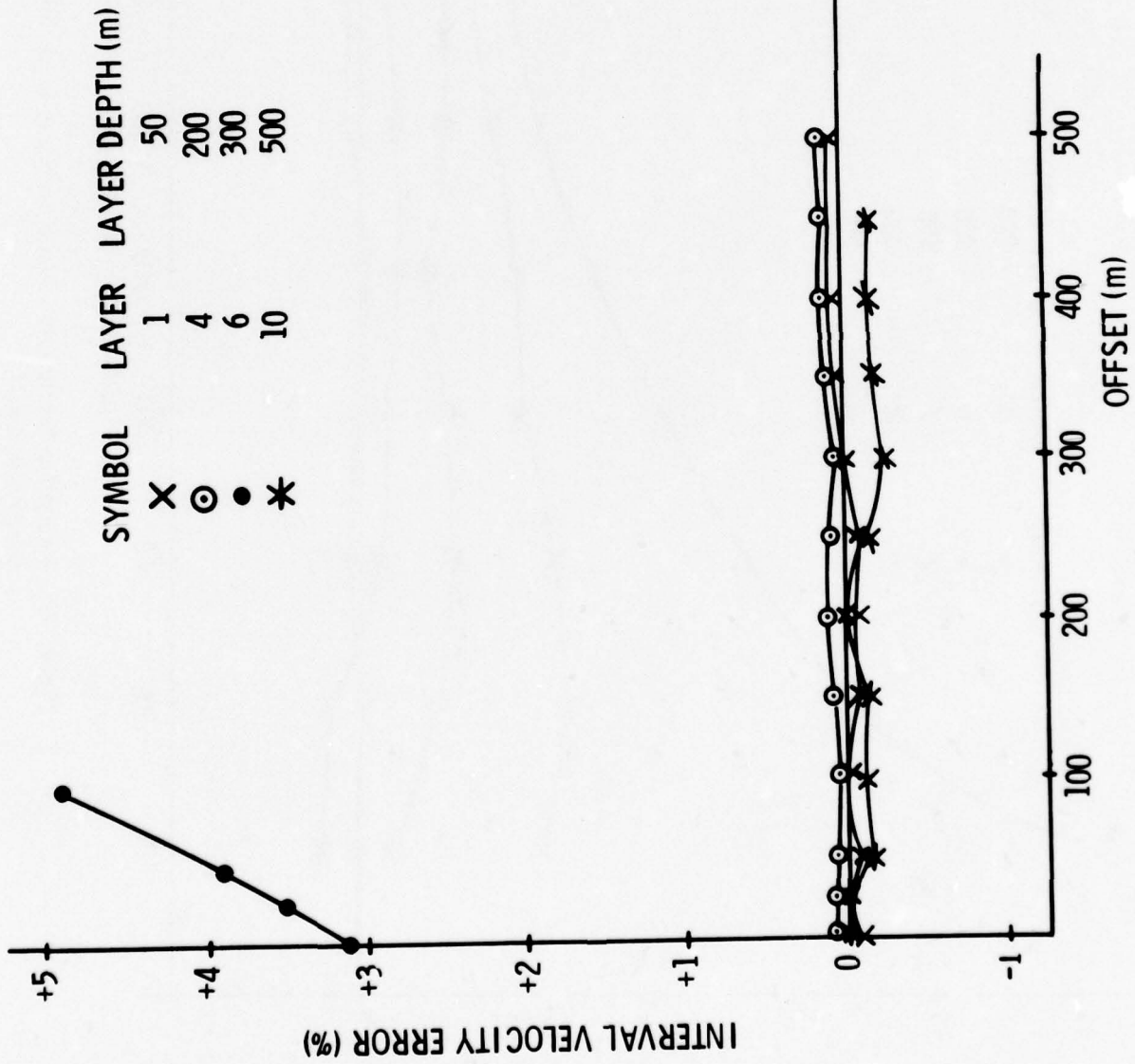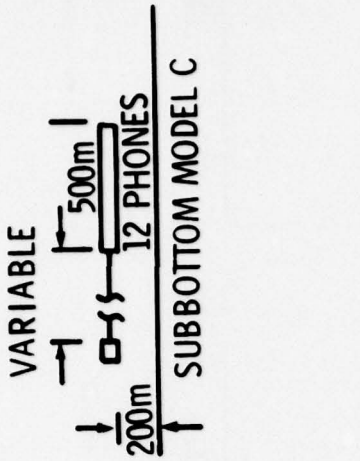
Figure 20. Interval velocity error as a function of offset for subbottom model C
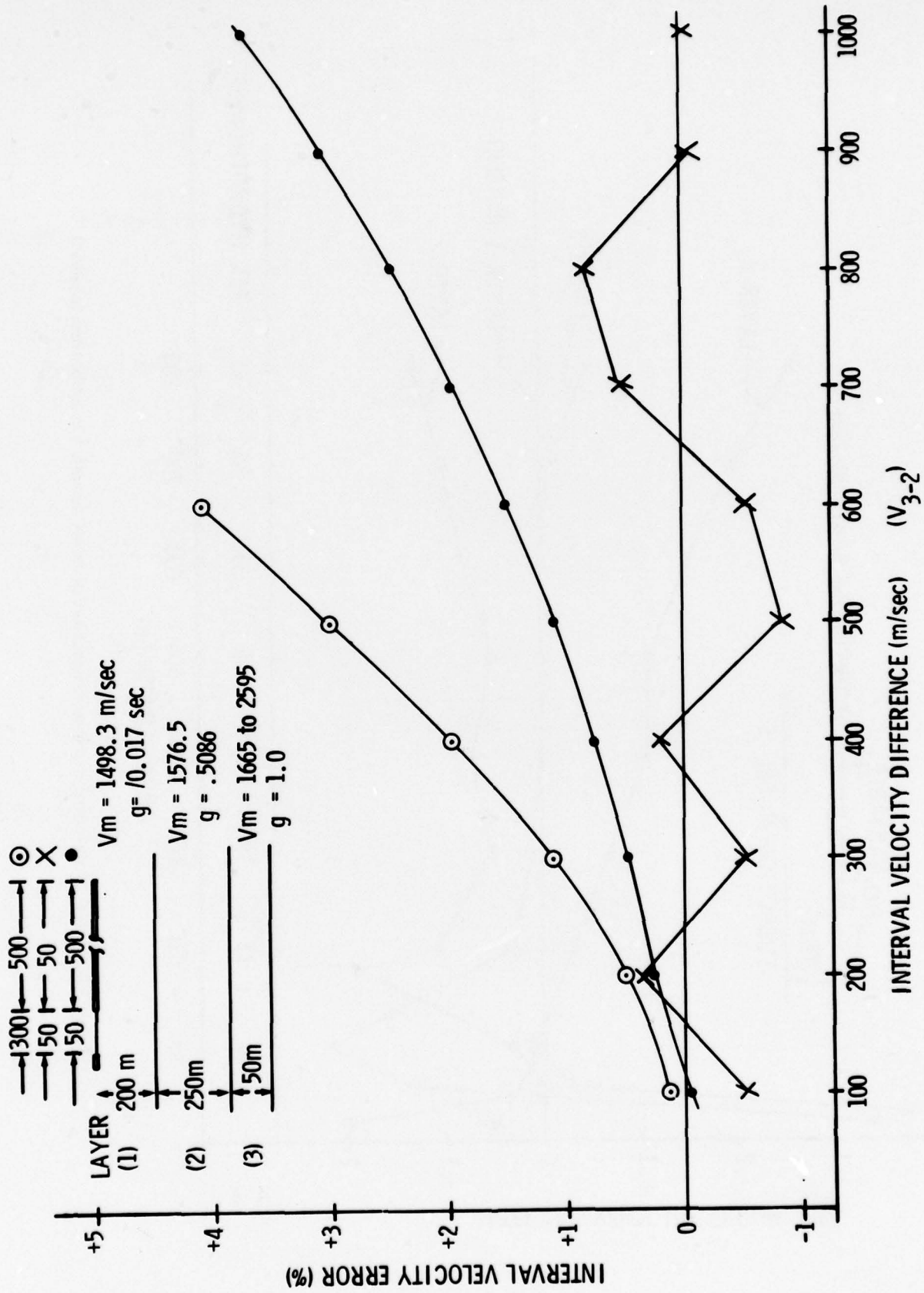
Figure 21. Interval velocity error for a layer mean velocity difference of 100 m/sec to 1000 m/sec. Error plotted for layer 3 (modified subbottom model C).
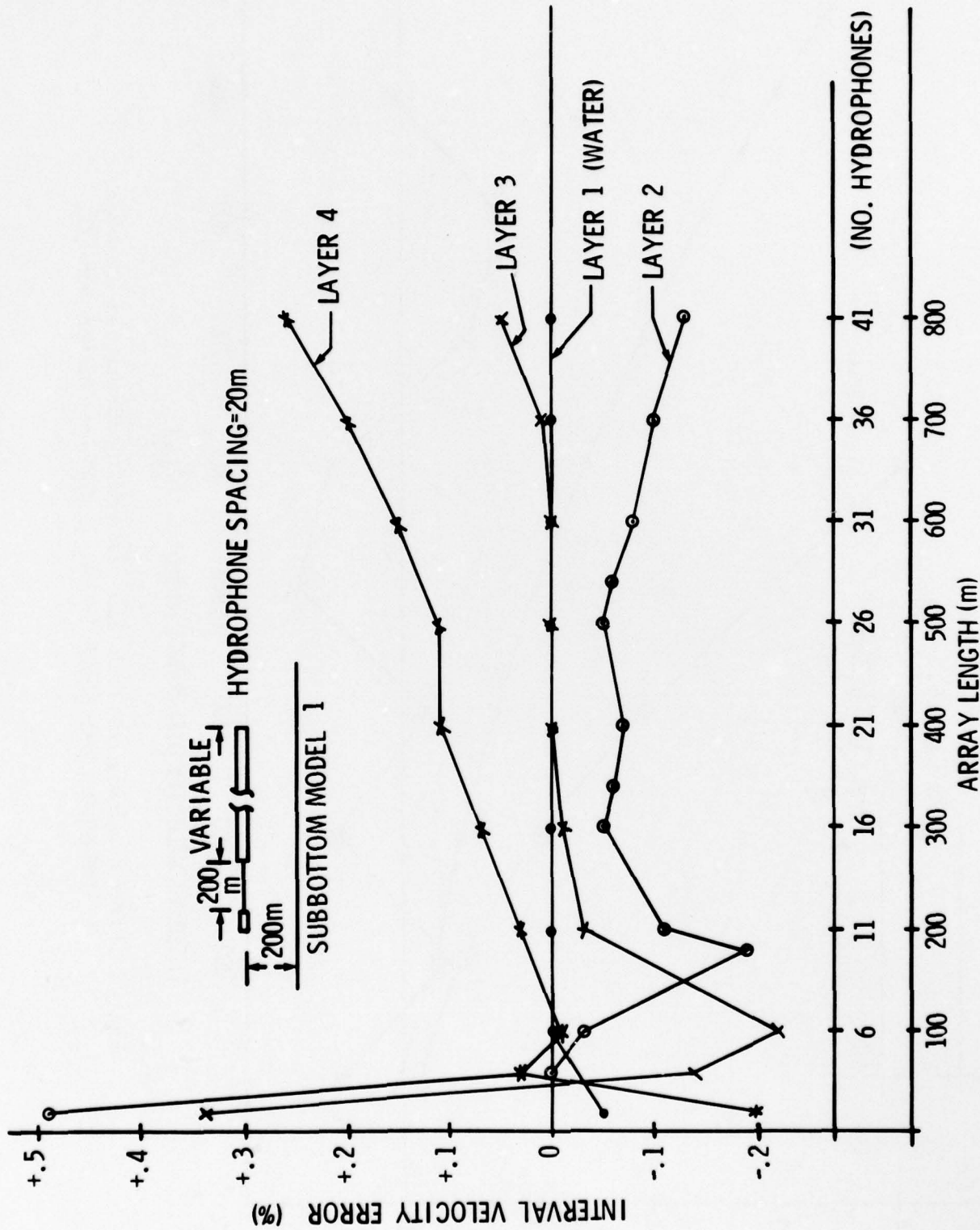
Figure 22. Interval velocity error as a function of array length for subbottom model 1

INTERVAL VELOCITY ERROR VS. ARRAY TILT
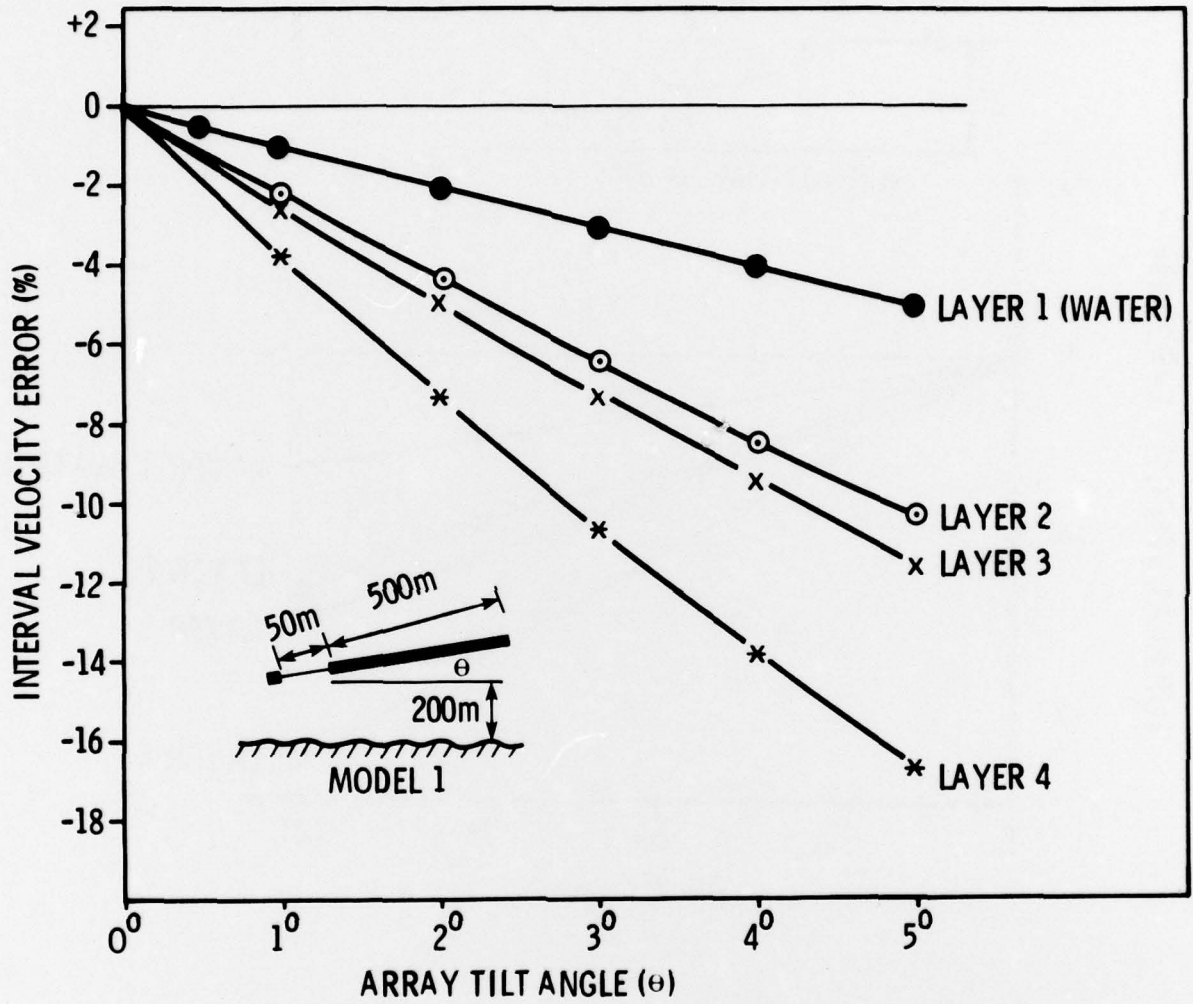
Figure 23. Interval velocity error as a function of array tilt angle for array length = 500 m and subbottom model 1 (ref. Fig. 6)
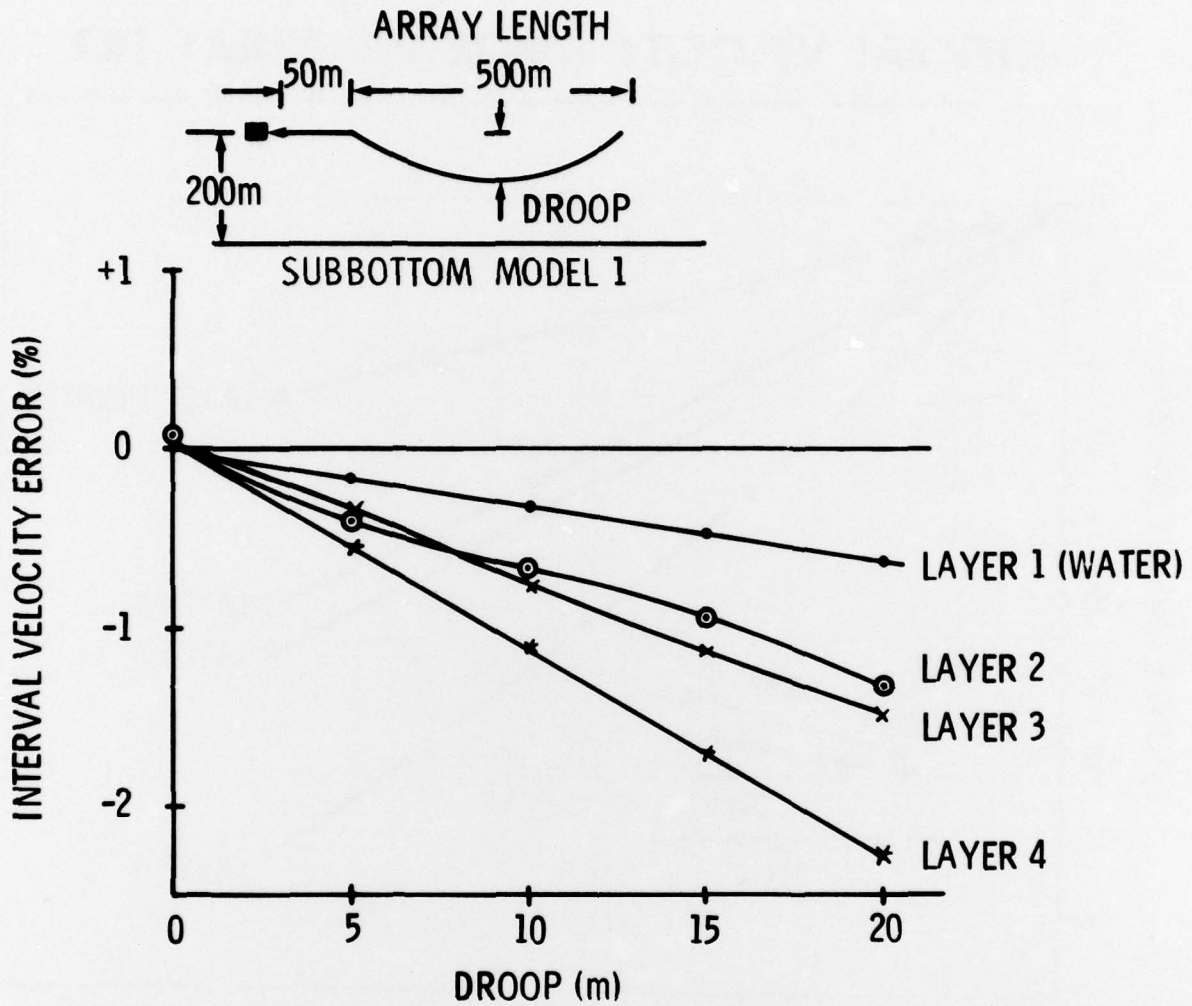
Figure 24. Interval velocity error as a function of array droop for array length = 500 m and subbottom model 1 (ref. Fig. 6)

Figure 25. Interval velocity error as a function of fixed picking error for array length = 500 m and subbottom model 1 (ref. Fig. 6)

57

500 METER ARRAY/12 PHONES EQUALLY SPACED
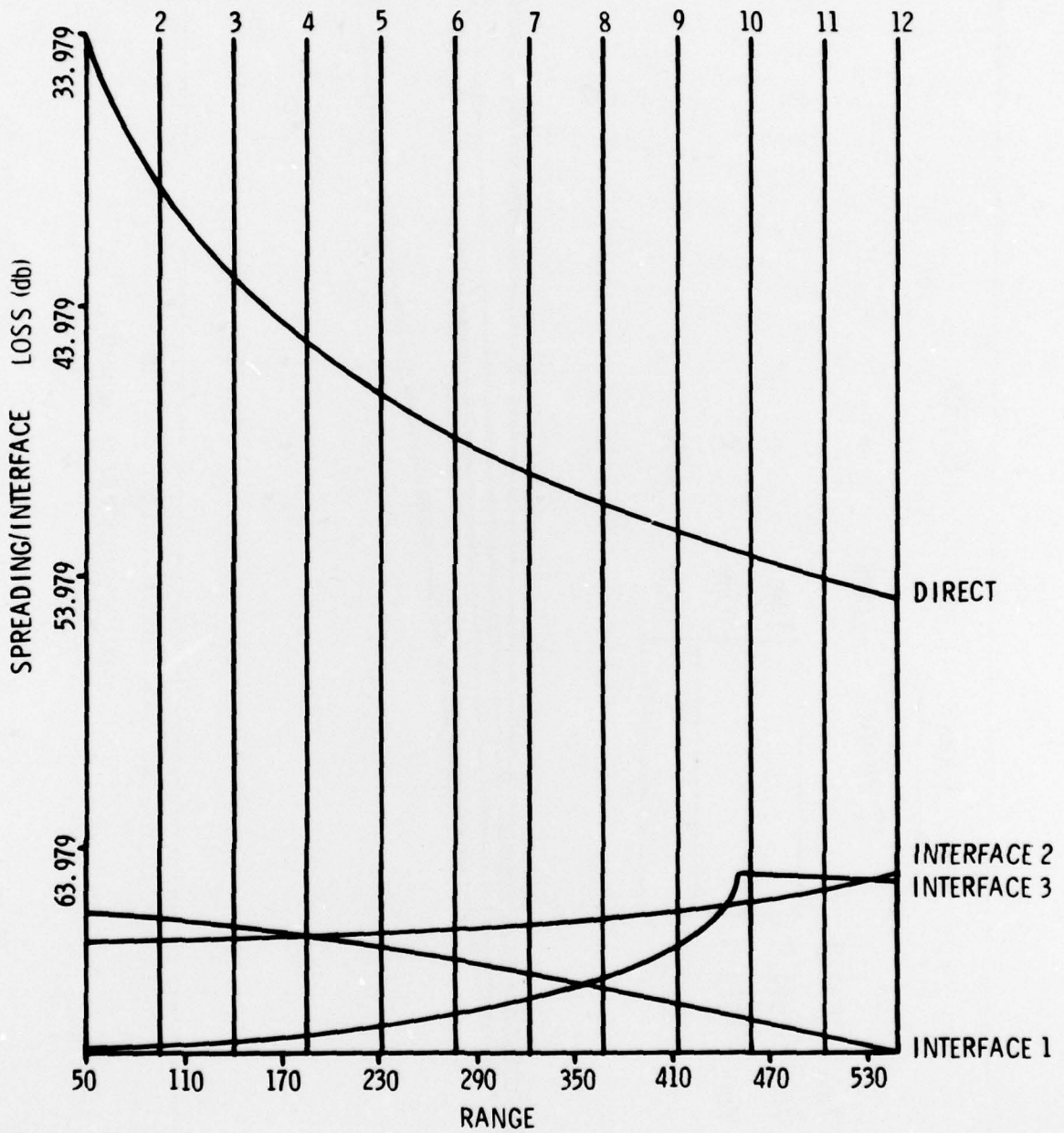# SUBBOTTOM MODEL B /200METER ALTITUDE

Figure 26. Spreading/interface loss plot for 500 m array and subbottom model B
(ref. Fig. 12)

SOURCE LEVEL
12 PHONES EQUALLY SPACED/SUBBOTTOM MODEL B

FREQUENCY   400 Hz

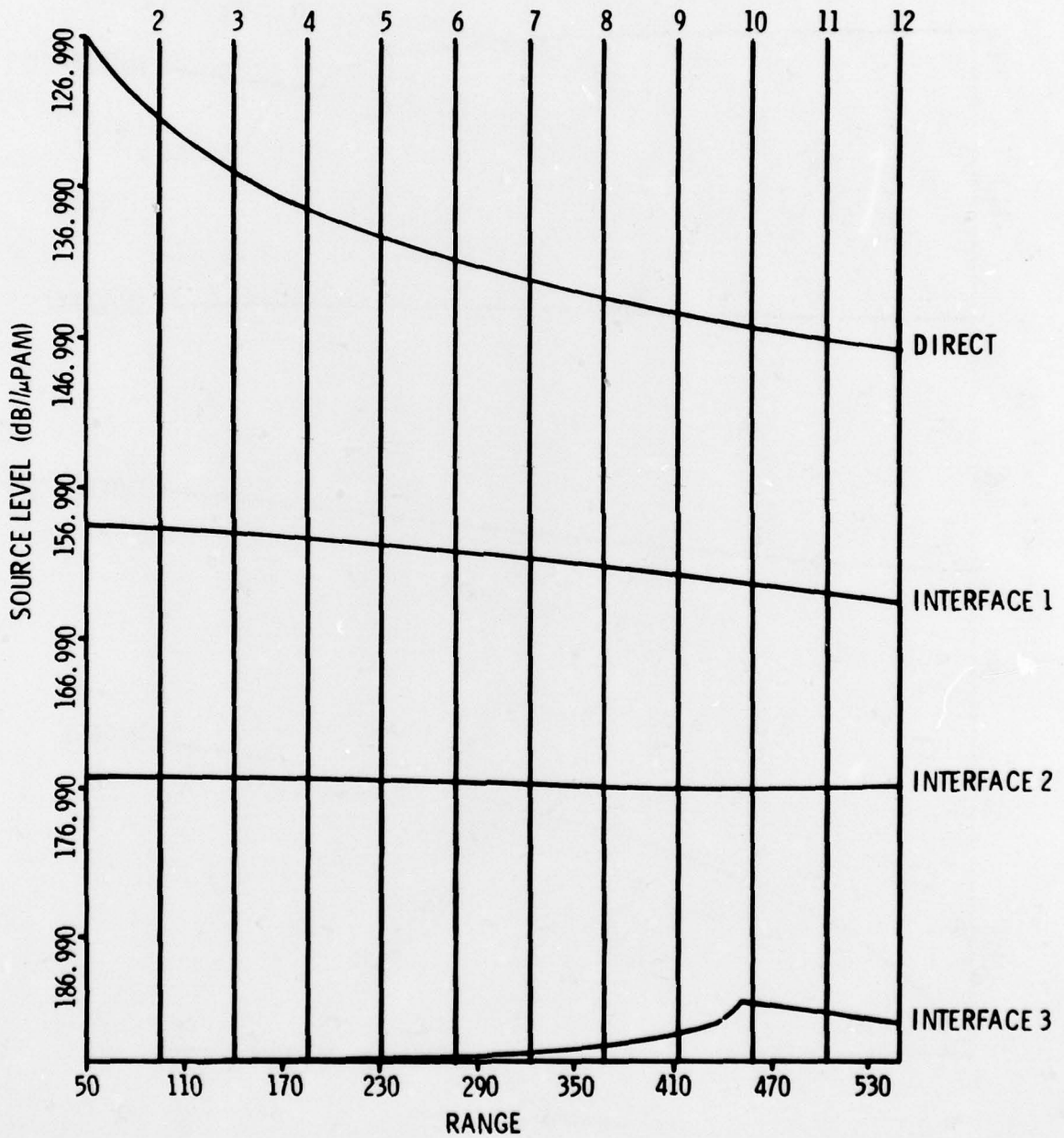DETECTION LEVEL   0 DB
ABSORPTION   0.033 dB/M

Figure 27. Source level required for 500 m array and subbottom model B (ref. Fig. 12)
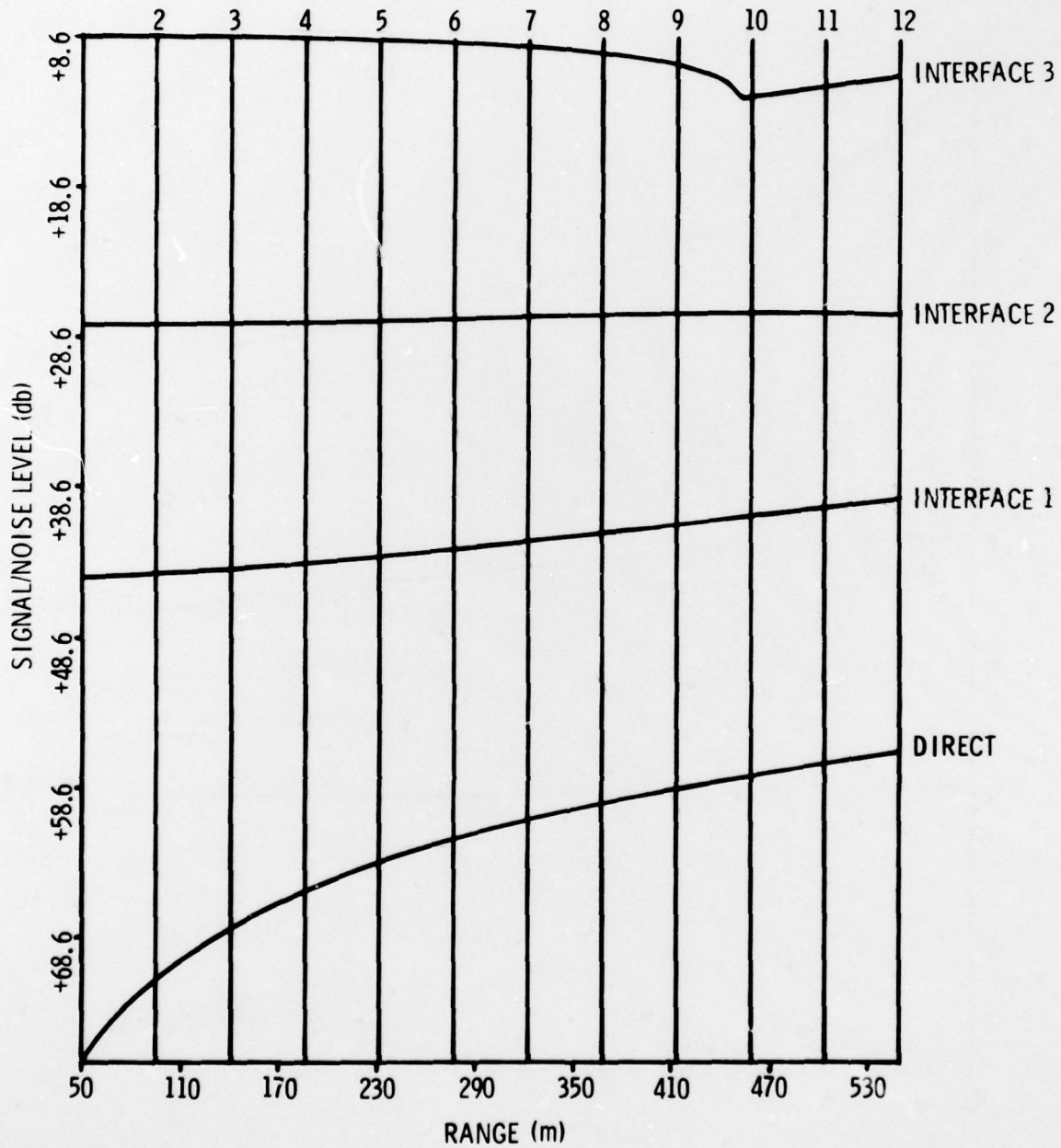
Figure 28. S/N level plot for 500 m array and deep-towed sound source for subbottom model B (ref. Fig. 12)

60

SOURCE LEVEL

12 PHONES EQUALLY SPACED/SUBBOTTOM MODEL 1

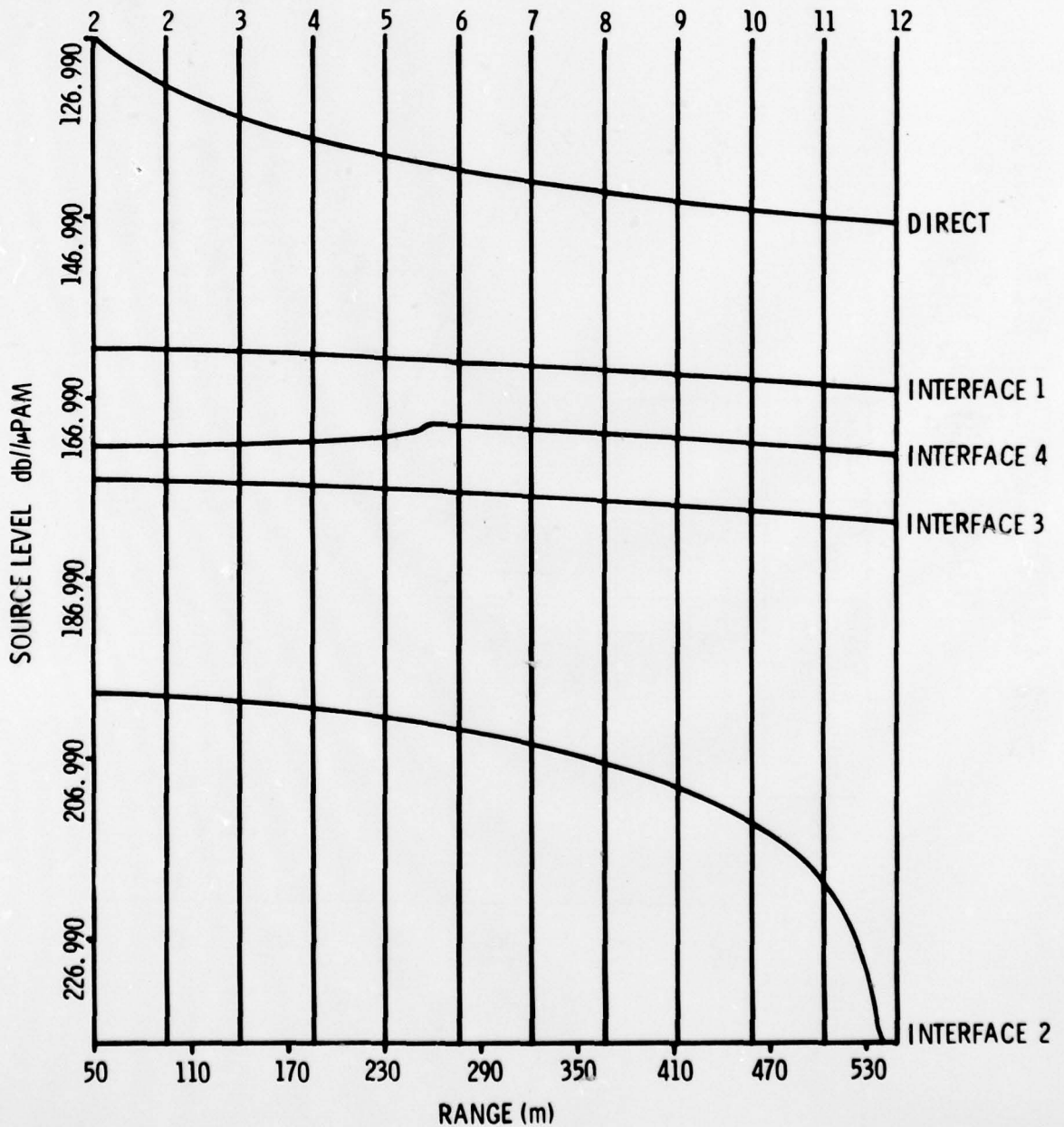|				
ARRAY LENGTH	500 m	DETECTION LEVEL	O db	
OFFSET	50 m	NOISE LEVEL	70 db //mPA/Hz	
ALTITUDE	200 m	FREQUENCY	400 Hz	
		BANDWIDTH	200 Hz	
		ABSORPTION	.033 db/m	

Figure 29. Source level required for 500 m array and subbottom model 1 (ref. Fig. 6)
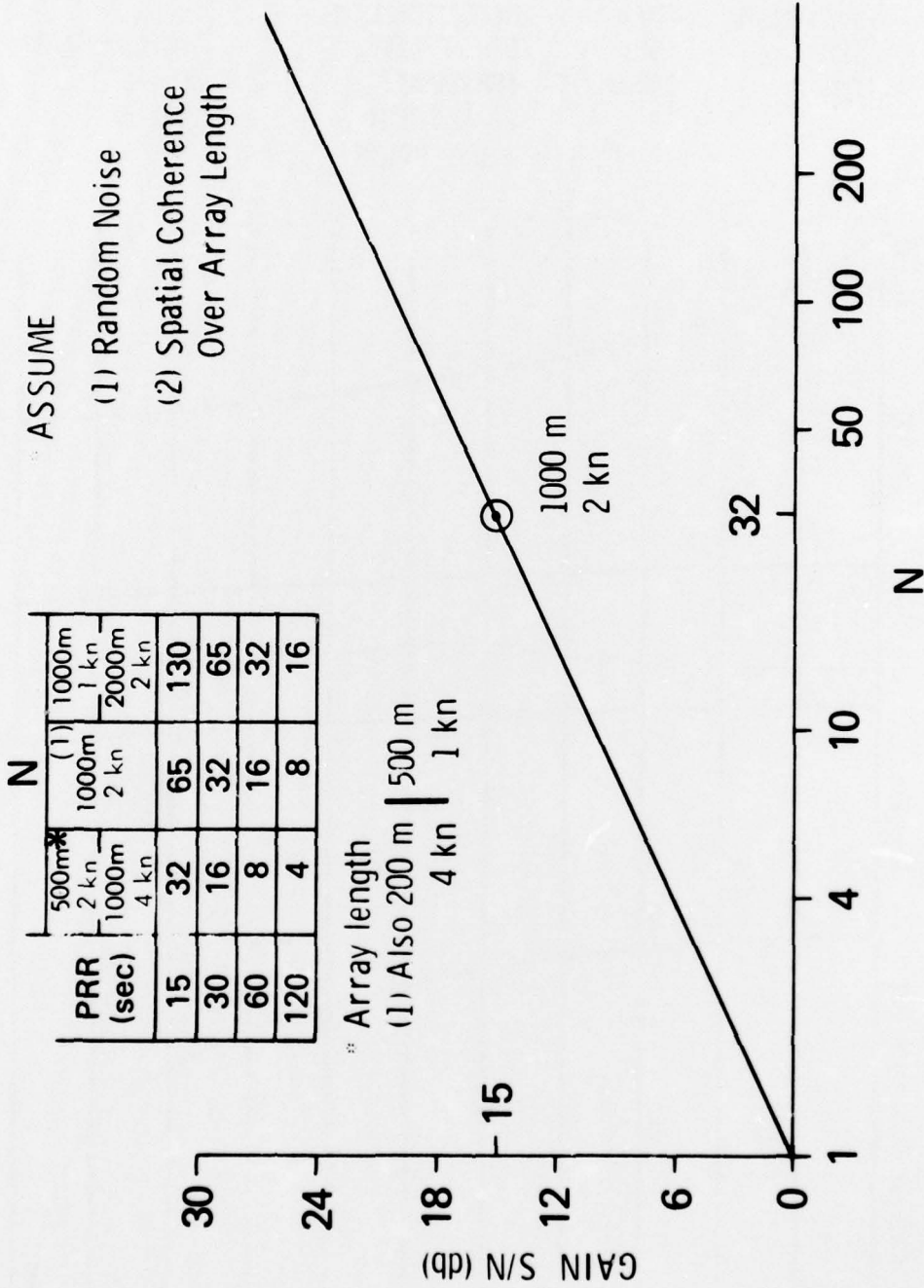
61

S/N IMPROVEMENT STACKING*
(GAIN = 20 log N½)

ASSUME

(1) Random Noise

(2) Spatial Coherence
Over Array Length

PRR (sec)	500m* 2 kn / 1000m 4 kn	N (1) 1000m 2 kn / 1000m 2 kn	1000m 1 kn / 2000m 2 kn
15	32	65	130
30	16	32	65
60	8	16	32
120	4	8	16

* Array length
(1) Also 200 m / 500 m
        4 kn   1 kn

1000 m
2 kn

GAIN S/N (db)

30 24 18 15 12 6 0

N

1 4 10 32 50 100 200

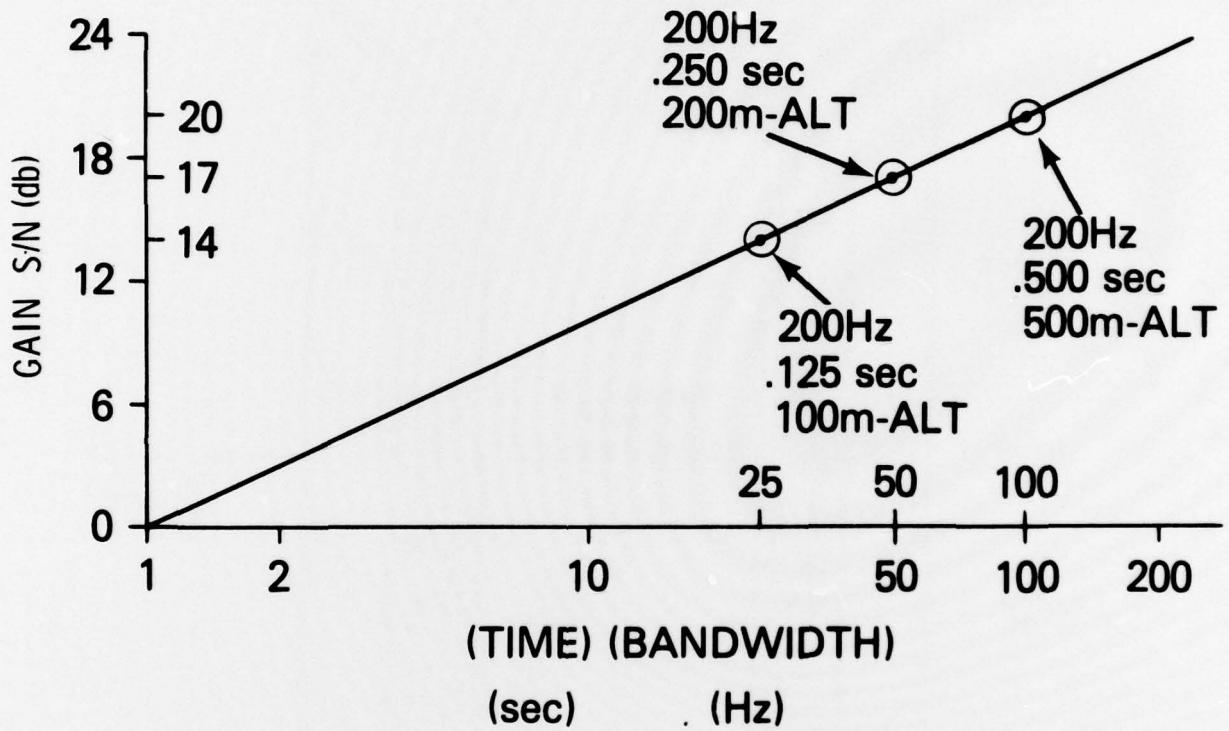Figure 30. S/N improvement resulting from vertical stack of N traces

62

Figure 31. S/N improvement resulting from increased time-bandwidth product
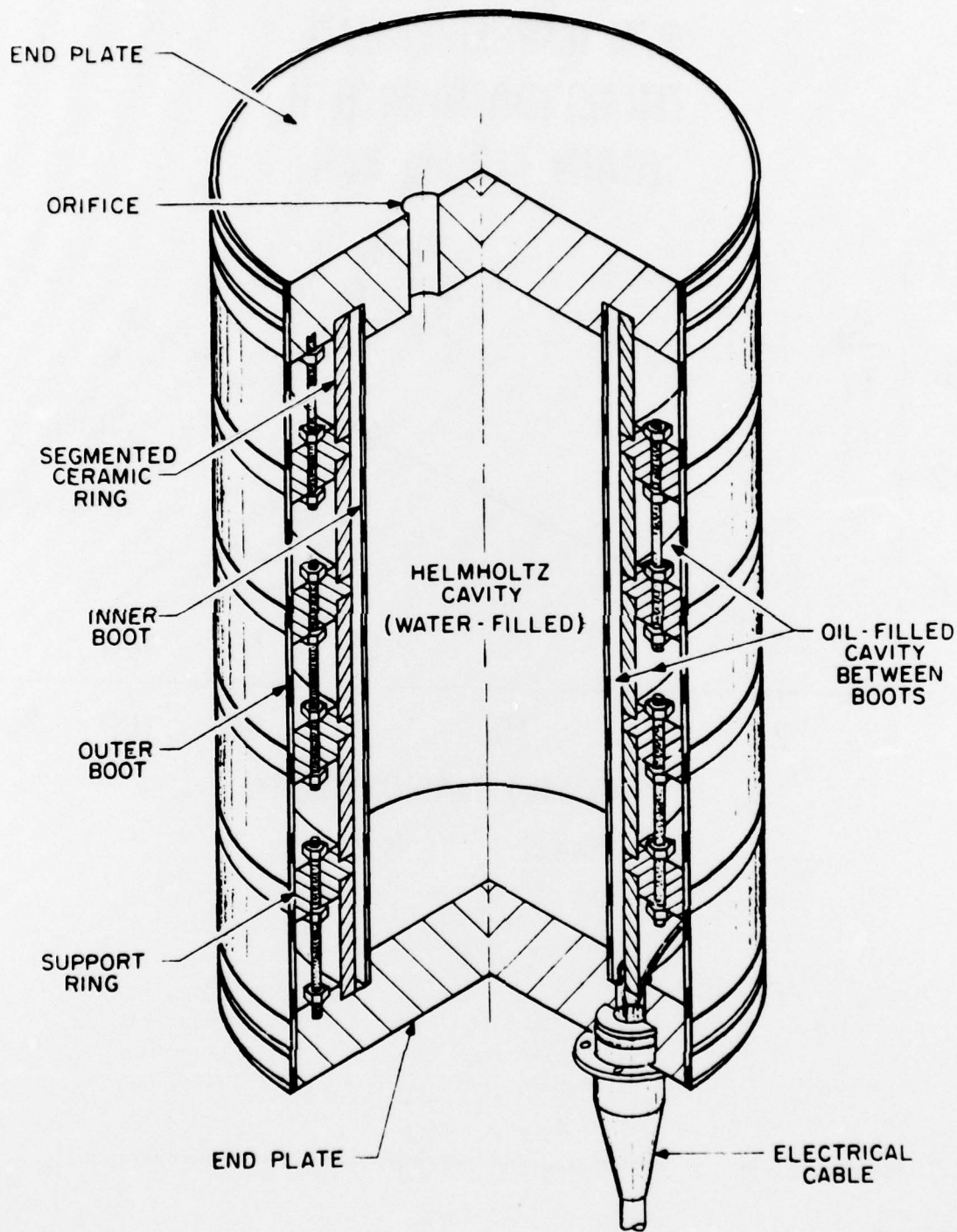
CONCEPTUAL DESIGN FOR LOW FREQUENCY DEEP TOW SOURCE

END PLATE

ORIFICE

SEGMENTED
CERAMIC
RING

INNER
BOOT

HELMHOLTZ
CAVITY
(WATER-FILLED)

OIL-FILLED
CAVITY
BETWEEN
BOOTS

OUTER
BOOT

SUPPORT
RING

END PLATE

ELECTRICAL
CABLE

Figure 32. Helmholtz resonator sound source — Cut-away view

64

TOW CABLE LENGTH VERSUS TOW SPEED
(FIXED TOW DEPTH)

STEEL TOW CABLE DIA. 17.5 MM (0.69 IN.)
BREAK STRENGTH 9300 kg (20400 LB.)

FISH WEIGHT, W_F = 545 kg (1200 LB.)

9.15 km (30,000 FT.)

TOW DEPTH, H = 6 km
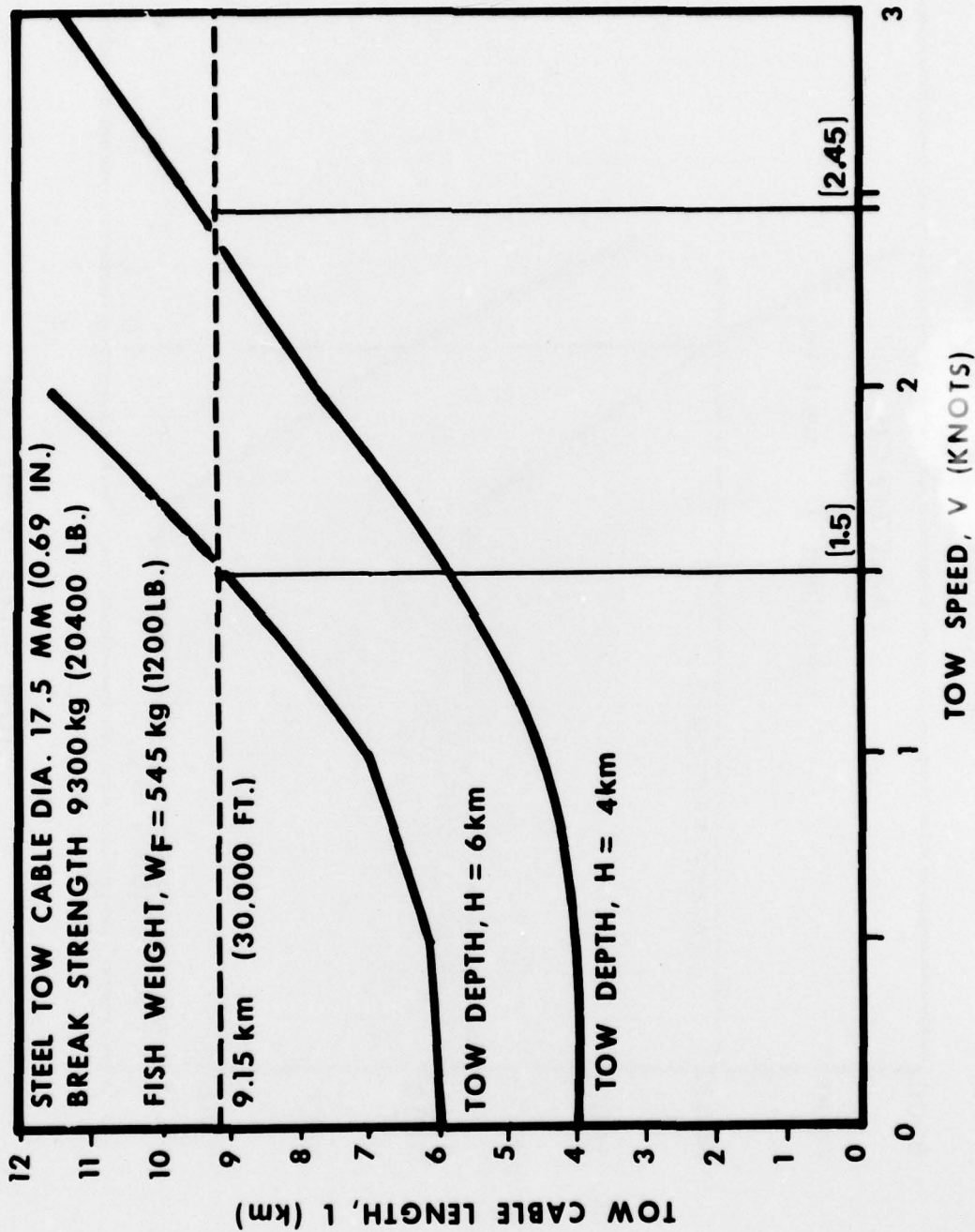
TOW DEPTH, H = 4km

[1.5]   [2.45]

TOW SPEED, V (KNOTS)

TOW CABLE LENGTH, L (km)

Figure 33. Static tow analysis of tow cable length as a function of tow speed for
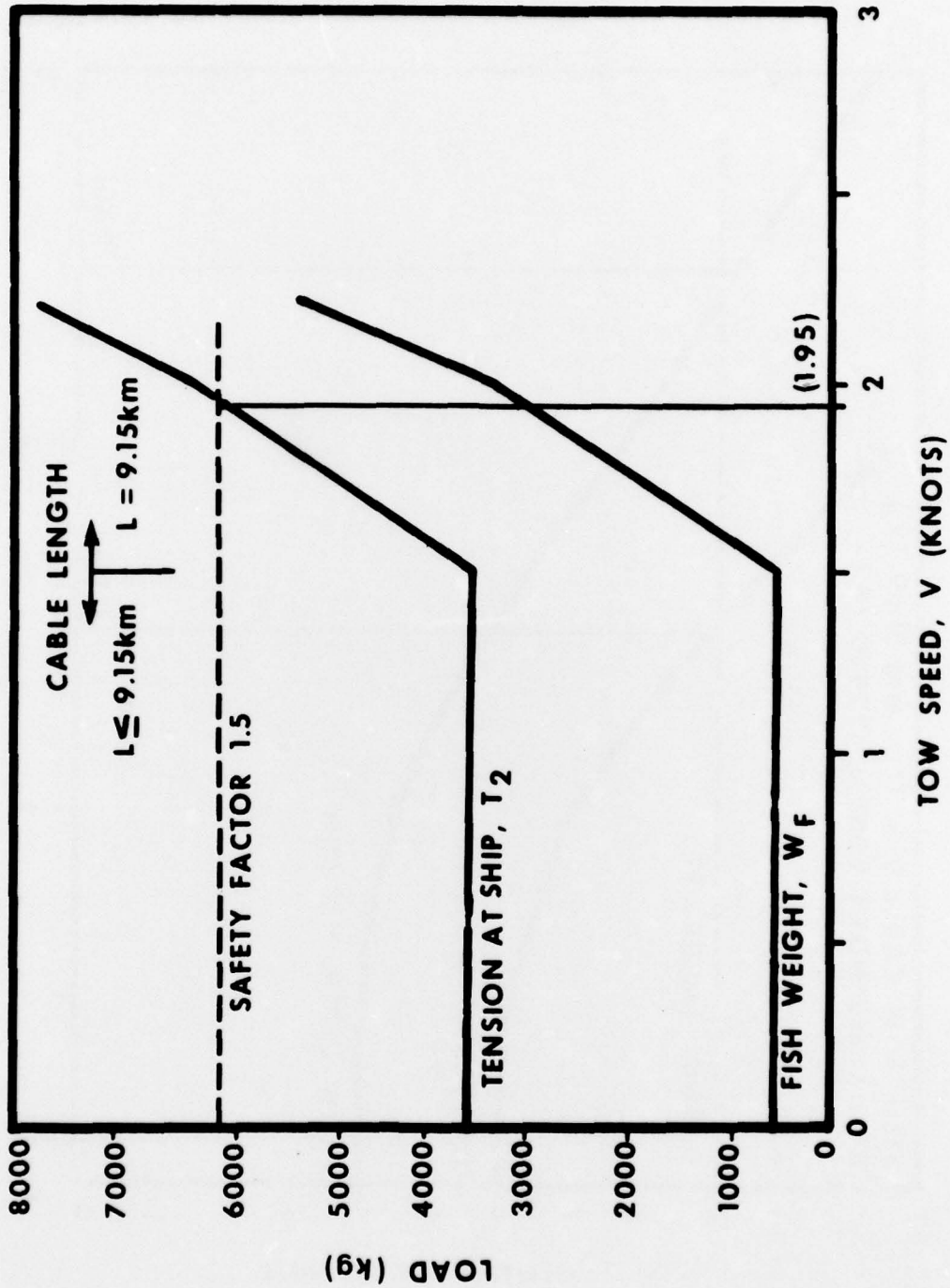fixed tow depths of 4 km and 6 km

65

Figure 34. Static tow analysis of increased fish weight as a function of tow speed for a fixed cable length of 9.15 km and tow depth of 6 km

REPORT DOCUMENTATION PAGE		READ INSTRUCTIONS BEFORE COMPLETING FORM
1. REPORT NUMBER NORDA Technical Note 41	2. GOVT ACCESSION NO.	3. RECIPIENT'S CATALOG NUMBER
4. TITLE (and Subtitle) Deep-towed Geophysical Array Development Program Progress Report (FY 1978)		5. TYPE OF REPORT & PERIOD COVERED
		6. PERFORMING ORG. REPORT NUMBER
7. AUTHOR(s) Martin G. Fagot Bruce E. Eckstein		8. CONTRACT OR GRANT NUMBER(s)
9. PERFORMING ORGANIZATION NAME AND ADDRESS Naval Ocean Research and Development Activity NSTL Station, Mississippi 39529		10. PROGRAM ELEMENT, PROJECT, TASK AREA & WORK UNIT NUMBERS
11. CONTROLLING OFFICE NAME AND ADDRESS Naval Ocean Research and Development Activity NSTL Station, Mississippi 39529		12. REPORT DATE February 1979
		13. NUMBER OF PAGES 74
14. MONITORING AGENCY NAME & ADDRESS(if different from Controlling Office)		15. SECURITY CLASS. (of this report) Unclassified
		15a. DECLASSIFICATION/DOWNGRADING SCHEDULE

16. DISTRIBUTION STATEMENT (of this Report)

Approved for public release; distribution unlimited.

17. DISTRIBUTION STATEMENT (of the abstract entered in Block 20, if different from Report)

18. SUPPLEMENTARY NOTES

19. KEY WORDS (Continue on reverse side if necessary and identify by block number)

Geophysical measurement, performance prediction model, subbottom model, ray trace model, reflection, refraction, sonar equation, spatial model, interval velocity.

20. ABSTRACT (Continue on reverse side if necessary and identify by block number)

A multi-channel array system towed near the bottom in the deep ocean provides the capability to determine detailed geophysical character of the subbottom structure. This report presents the progress during FY78 on the development of a deep-towed geophysical array system.

The identified system's design measurement goals are accurate sound speed determination (<1%), quantitative reflection strength measurements, high-resolution layer definitions (4 m), and subbottom penetration up to 500 m. The development approach

20.

employs a quantitative performance prediction model for a deep-towed source/multi-channel array configuration which includes: a subbottom multilayer acoustic model, a ray trace capability, and a sonar equation and spatial model. The status of the performance prediction model is reviewed, with the deficiencies noted and planned improvements identified.

The subbottom model input parameters include layer thickness, density, interval velocity, and velocity gradient. The performance prediction effort employed a subbottom model typical of the Venezuelan Basin. The ray trace capability focused primarily on a deep-towed, wide-angle reflection application. A refracted ray trace routine for head and diving waves has been initiated for future assessment of refraction spread requirements and reflection data processing complications arising from refracted arrivals. A sonar equation analysis provided an initial estimate for defining the basic sonar requirements of a deep-towed sound source. These analysis results were used to review the state-of-the-art in high power, low-frequency, deep-towed, acoustic sources. The review identified a candidate approach employing a Helmholtz resonator-type source with the following characteristics: source level, 204 dB/ pam; frequency, 400 Hz; bandwidth, 200 Hz; size, 0.5 m diameter X 0.9 m long; and weight (water), 380 kg. A static tow analysis established the initial tow system characteristics for placing the source/array system at a preselected depth. Tow speeds up to 3 kn at tow depths of 4 km are predicted for projected system component characteristics.

The sensitivity of system configuration parameters on extracting interval velocity has been initiated employing the Dix (1955) interval velocity equation. Plotted results are presented for varied critical parameters of array length, offset, and altitude. Within the constraints of noise-free data and the limits imposed by the Dix equation, the initially identified configuration parameters are array length = 500 m, offset = 50 m, and altitude = 200 m. A preliminary sensitivity analysis of array deformation on interval velocity accuracy measurement indicates that for a fixed 1° array tilt angle (kiting), errors can be in excess of 4%. Plans to identify implementation requirements and towing configurations to reduce this error are given.

A review of oil exploration industry techniques for extracting subbottom velocity information is presented. The review considered basic environmental and operational constraints; these were compared to the deep-towed configuration.